MOX-Report No. 67/2025

Structure-preserving local discontinuous Galerkin discretization of conformational conversion systems

Antonietti, P.F.; Corti, M.; Gómez S.; Perugia, I.

MOX, Dipartimento di Matematica
Politecnico di Milano, Via Bonardi 9 - 20133 Milano (Italy)

mox-dmat@polimi.it https://mox.polimi.it

Structure-preserving local discontinuous Galerkin discretization of conformational conversion systems

Paola F. Antonietti [*] Mattia Corti [*†] Sergio Gómez [‡§] Ilaria Perugia [†]

Abstract

We investigate a two-state conformational conversion system and introduce a novel structure-preserving numerical scheme that couples a local discontinuous Galerkin space discretization with the backward Euler time-integration method. The model is first reformulated in terms of auxiliary variables involving suitable nonlinear transformations, which allow us to enforce positivity and boundedness at the numerical level. Then, we prove a discrete entropy-stability inequality, which we use to show the existence of discrete solutions, as well as to establish the convergence of the scheme by means of some discrete compactness arguments. As a by-product of the theoretical analysis, we also prove the existence of global weak solutions satisfying the system's physical bounds. Numerical results validate the theoretical results and assess the capabilities of the proposed method in practice.

Keywords. Conformational conversion systems, semilinear reaction–diffusion system, structure-preserving discretizations, local discontinuous Galerkin method, molecule/particle dynamics.

Mathematics Subject Classification. 65M60, 65M12, 35K57, 35Q92

1 Introduction

Conformational conversion systems are a class of coupled (semilinear) reaction–diffusion systems of partial differential equations (PDEs) that describe how multiple conformational states of molecules or particles change over space and time, including their ability to interconvert and diffuse. The population associated with each conformation is represented by one variable governed by its own PDE, where the diffusion terms model the spatial spreading, and the reaction terms describe production, elimination, and interconversion between conformations. Conformational conversion systems take into account three main mechanisms: i) state transitions, representing chemical or physical changes; ii) spatial dynamics, describing diffusion of each state; and iii) external forces, accounting for external inputs. These systems are commonly used across numerous biological, chemical, and physical processes, where elements of a spatially distributed system can change their internal structure (i.e., their conformational state), while simultaneously undergoing diffusion through space. For instance, in cell biology, they are used to describe protein conformational changes and how these propagate within a cell. In neuroscience, they are used either to model the spread of misfolded proteins in neurodegenerative diseases [21, 29, 32]. In chemical kinetics, they appear as spatially extended catalytic reaction models, while in materials science, they are used to describe phase transitions in innovative materials. Similar formulations have also been proposed for ecosystem modeling, such as resource–consumer systems with negligible resource competition, known as "MacArthur-type" models [17, 28], or for plant–water interaction dynamics in soil models, where they appear as two-component reaction–diffusion systems [24].

Due to the nonlinear coupling between reaction kinetics, multiple interacting states, and diffusion occurring at different scales, the mathematical analysis of conformational conversion systems poses significant challenges. A key point is that, under suitable assumptions on the model's data, it is often possible to prove the positivity

[*]MOX-Dipartimento di Matematica, Politecnico di Milano, Piazza Leonardo da Vinci 32, Milan, 20133, Italy (paola.antonietti@polimi.it, mattia.corti@polimi.it)

[†]Faculty of Mathematics, University of Vienna, Oskar-Morgenstern-Platz 1, 1090 Vienna, Austria (mattia.corti@univie.ac.at, ilaria.perugia@univie.ac.at)

[‡]Department of Mathematics and Applications, University of Milano-Bicocca, 20125 Milan, Italy (sergio.gomezmacias@unimib.it)

[§]IMATI-CNR "E. Magenes", Via Ferrata 5, 27100 Pavia, Italy

and boundedness of solutions, which are essential for ensuring physical consistency. Approximating the solution to conformational conversion systems adds its own challenges, as it demands schemes that preserve, at the discrete level, the key structural properties of the corresponding continuous model. In particular, positivity preservation is not automatically ensured by standard numerical schemes, even when it holds for the continuous PDE system. Consequently, the development of structure-preserving numerical methods is an active area of research. Notable contributions in the framework of numerical discretization approaches that can preserve physical bounds at the discrete level, within a variational setting, are, e.g., the nodally bound-preserving finite element method [1,5], the proximal Galerkin method [25,26], and structure-preserving schemes for cross-diffusion [7,22] and (advection)–diffusion–reaction problems [4,6,16,27,30].

Novelty. In this paper, we consider a two-state conformational conversion system and propose a novel structure-preserving scheme based on a local discontinuous Galerkin (LDG) space discretization coupled with the backward Euler time-integration scheme. The key point is to reformulate (via a suitable change of variables involving non linear transformations) the model problem as a system in terms of entropy variables, thereby ensuring solution positivity, boundedness of one of the two components, and an entropy-stability inequality at the discrete level. The entropy densities underlying these changes of variables are related to Legendre functions in the framework of proximal Galerkin methods [26]. In the spirit of the LDG method for elliptic problems [10], the *numerical fluxes* do not involve differential operators, which allows us to avoid the presence of nonlinearities on interface terms. This property endows the method with an outstanding parallelizable structure. We establish convergence of the discrete scheme (up to subsequences) under minimal regularity assumptions. As a byproduct of our analysis, we also prove the existence of global weak solutions satisfying the physical bounds of the model. A distinctive novelty of this work, compared to the framework in [22] for cross-diffusion systems, is that we get a "degeneracy" in the entropy estimate, which provides a bound in the L^2 norm on $\nabla\sqrt{q}$, instead of ∇q, being q one of the conformational variables. The ideas used to address the theoretical challenges resulting from this "degeneracy" are key to extend the framework in [22] to a broader class of nonlinear models.

Structure of the manuscript. The remainder of the paper is organized as follows: Section 2 presents the model problem and the structure-preserving numerical method, and Sections 3 and 4 present its theoretical analysis. More precisely, in Section 2.1, we introduce the conformational conversion system under investigation, we reformulate it using a suitable change of variables in Section 2.2, and present its discretization using the proposed structure-preserving backward Euler-LDG method in Section 2.3. In Section 3.1, we prove an entropy stability bound of the system. Then, we derive a discrete analogue for our structure-preserving scheme in Section 3.2, and use it to prove the existence of discrete solutions in Section 3.3. Section 4 is devoted to establishing the convergence of the structure-preserving scheme. First, we prove that the scheme converges to a regularized semidiscrete-in-time formulation as the mesh size h goes to zero; then, we analyze the convergence of such a formulation as $(\varepsilon, \tau) \to (0,0)$, being ε and τ a suitable penalty term and the time integration step, respectively. Section 5 discusses numerical results aimed at validating the theoretical results and assessing the proposed structure-preserving method in practice. In Section 6, we draw some conclusions and discuss further developments. Finally, Appendix A presents a detailed derivation of the linear systems that arise from applying Newton's method to the backward Euler-LDG method.

2 Model problem and numerical approximation

In this section, we first introduce the model problem (Section 2.1) and then reformulate it in a convenient form (Section 2.2). Next, we define the structure-preserving backward Euler-LDG method to discretize it (Section 2.3), and conclude by presenting the matrix formulation of the fully discrete method (Section 2.4). An explicit derivation of the linear systems that arise from applying Newton's method is postponed to Appendix A. Here and in the following, we use standard notation for L^p, Sobolev, and Bochner spaces.

2.1 The conformational conversion system

We define the space–time cylinder $Q_T := \Omega \times (0,T)$, where $\Omega \subset \mathbb{R}^d$ $(d \in \{2,3\})$ is a polytopic domain with Lipschitz boundary $\Gamma := \partial\Omega$ and outward-pointing normal unit vector $\boldsymbol{n}_\Omega$, and $T > 0$ is some final time. We consider the following system: find $p : Q_T \to \mathbb{R}$ and $q : Q_T \to \mathbb{R}$ such that

$$\begin{aligned}
\partial_t p - \nabla\cdot(\boldsymbol{D}\nabla p) &= -p(\lambda_p + \mu_{pq} q) + \kappa_p \quad && \text{in } Q_T, && \text{(2.1a)}\\
\partial_t q - \nabla\cdot(\boldsymbol{D}\nabla q) &= -q(\lambda_q - \mu_{pq} p) && \text{in } Q_T, && \text{(2.1b)}\\
(\boldsymbol{D}\nabla p)\cdot\boldsymbol{n}_\Omega = 0 \ \text{ and } \ (\boldsymbol{D}\nabla q)\cdot\boldsymbol{n}_\Omega &= 0 && \text{on } \Gamma\times(0,T), && \text{(2.1c)}\\
p(\cdot,0) = p_0 \ \text{ and } \ q(\cdot,0) &= q_0 && \text{in } \Omega. && \text{(2.1d)}
\end{aligned}$$

The unknowns p and q represent the populations associated with the two conformations. As such, they must be nonnegative. We assume that the tensor $\boldsymbol{D} = \boldsymbol{D}(\boldsymbol{x}) \in \mathbb{R}^{d\times d}$, which characterizes the diffusion of both p and q, belongs to $L^\infty(\Omega)^{d\times d}$ and is uniformly positive definite in Ω: there exist $\mathrm{d_{upd}}, D_{\max} > 0$ such that

$$\|\boldsymbol{D}\|_{L^\infty(\Omega)^{d\times d}} = D_{\max} < \infty \qquad \text{and} \qquad \forall \boldsymbol{z}\in\mathbb{R}^d, \quad \boldsymbol{z}^\top\boldsymbol{D}\boldsymbol{z} \geq \mathrm{d_{upd}}|\boldsymbol{z}|^2 \quad \text{a.e. in } \Omega. \tag{2.2}$$

The parameter $\kappa_p > 0$ is the production rate of p, $\lambda_p > 0$ and $\lambda_q > 0$ are the clearance rates of p and q, respectively, and $\mu_{pq} > 0$ is the conversion rate from p to q. For convenience, we set

$$\Upsilon_{pq} := \kappa_p\mu_{pq} - \lambda_p\lambda_q, \qquad \mathcal{E}_p := \frac{\kappa_p}{\lambda_p}, \qquad \mathcal{E}_q := \frac{\Upsilon_{pq}}{\lambda_q\mu_{pq}}.$$

Traveling wave solutions exist under the assumption $\Upsilon_{pq} > 0$; [29, §2.2]. For the initial conditions, we assume that

$$0 \leq p_0 \leq \mathcal{E}_p \quad \text{a.e. in } \Omega, \qquad q_0 \in L^\infty(\Omega) \text{ and } q_0 \geq 0 \quad \text{a.e. in } \Omega, \tag{2.3}$$

so that

$$0 \leq p \leq \mathcal{E}_p \quad \text{and} \quad q \geq 0 \qquad \text{a.e. in } Q_T; \tag{2.4}$$

see [15, §2.1].

Remark 2.1 (Initial datum p_0)**.** *The assumption $p_0 \leq \mathcal{E}_p = \kappa_p/\lambda_p$ in Ω is motivated by the fact that, in this system, it is assumed to be the maximum of the population p (which is associated with the unstable equilibrium).* ∎

Remark 2.2 (The Fisher-Kolmogorov equation)**.** *For $p \gg q$, neglecting the time derivative and the diffusion of p, and using a Taylor approximation, system (2.1) reduces to the following Fisher-Kolmogorov equation in the rescaled variable $c := q/q_M$, with $q_M := \Upsilon_{pq}/(\mathcal{E}_p\mu_{pq}^2)$:*

$$\begin{aligned}
\partial_t c - \nabla\cdot(\boldsymbol{D}\nabla c) &= \alpha\, c(1-c) \quad && \textit{in } Q_T, && \text{(2.5a)}\\
(\boldsymbol{D}\nabla c)\cdot\boldsymbol{n}_\Omega &= \boldsymbol{0} && \textit{on } \Gamma\times(0,T), && \text{(2.5b)}\\
c(\cdot,0) &= c_0 && \textit{in } \Omega, && \text{(2.5c)}
\end{aligned}$$

with $\alpha := \Upsilon_{pq}/\lambda_p$ and $c_0 = q_0/q_M$; see [20, §2]. ∎

Remark 2.3 (The heterodimer model)**.** *An example of a system of the form (2.1) is the so-called heterodimer model, which describes the spatial and temporal dynamics of protein conformational changes. The heterodimer model is relevant in the modeling of neurodegenerative diseases, e.g. proteinopathies such as Alzheimer's, Parkinson's, and prion diseases [21, 29, 32]. In this context, the unknowns p and q represent the quantities of healthy and misfolded proteins, respectively.* ∎

2.2 Change of variables and reformulation

The following change of variables enforces the bounds in (2.4) on p and q:

$$p = u_p(w_p) := \mathcal{E}_p\left(\frac{e^{w_p}}{1+e^{w_p}}\right), \qquad q = u_q(w_q) := \mathcal{E}_q e^{w_q}, \qquad w_p, w_q : Q_T \mapsto \mathbb{R}, \tag{2.6}$$

In the boundedness-by-entropy setting of [23], this corresponds to writing $u_p = (s_p')^{-1}$, $u_q = (s_q')^{-1}$, with the *entropy density functions* s_p and s_q defined, respectively, by

$$s_p(p) := p\log p + (\mathcal{E}_p - p)\log(\mathcal{E}_p - p) + \max\{\mathcal{E}_p\log(2\mathcal{E}_p^{-1}), 0\} \geq 0, \qquad s_q(q) := q(\log(\mathcal{E}_q^{-1}q) - 1) + \mathcal{E}_q \geq 0, \tag{2.7}$$

where $\log = \log_e$, for which

$$s_p'(p) = \log p - \log(\mathcal{E}_p - p) = \log\left(\frac{p}{\mathcal{E}_p - p}\right), \qquad s_q'(q) = \log\frac{q}{\mathcal{E}_q},$$

and

$$s_p''(p) = \frac{1}{p(1-\mathcal{E}_p^{-1}p)}, \qquad s_q''(q) = \frac{1}{q}.$$

As $w_p = s_p'(p)$ and $w_q = s_q'(q)$, the chain rule gives

$$\nabla w_p = s_p''(p)\nabla p, \quad \nabla w_q = s_q''(q)\nabla q. \tag{2.8}$$

From assumption (2.3) on the initial data, it follows that the initial entropy is bounded, namely

$$\int_\Omega s_p(p_0)\,\mathrm{d}\boldsymbol{x} + \int_\Omega s_q(q_0)\,\mathrm{d}\boldsymbol{x} < +\infty. \tag{2.9}$$

We introduce the following auxiliary variables in Q_T, whose motivation is discussed in detail in Remark 2.5 below:

$$\begin{aligned}
(w_p, w_q) \text{ s.t. } (p,q) &= (u_p(w_p), u_q(w_q)), && (2.10a)\\
(\boldsymbol{z}_p, \boldsymbol{z}_q) &:= -(\nabla w_p, \nabla w_q), && (2.10b)\\
\boldsymbol{D}s_p''(p)\boldsymbol{\sigma}_p &:= -\boldsymbol{D}s_p''(p)\nabla p = \boldsymbol{D}\boldsymbol{z}_p, && (2.10c)\\
\boldsymbol{D}s_q''(q)\boldsymbol{\sigma}_q &:= -\boldsymbol{D}s_q''(q)\nabla q = \boldsymbol{D}\boldsymbol{z}_q, && (2.10d)\\
(\boldsymbol{r}_p, \boldsymbol{r}_q) &:= (\boldsymbol{D}\boldsymbol{\sigma}_p, \boldsymbol{D}\boldsymbol{\sigma}_q). && (2.10e)
\end{aligned}$$

As s_p'' is uniformly bounded away from zero by $4\mathcal{E}_p^{-1}$, $s_p''(p)\boldsymbol{D}$ is uniformly positive definite:

$$\boldsymbol{z}^\top \left(s_p''(p)\boldsymbol{D}\right)\boldsymbol{z} \geq \left(\inf_{(\boldsymbol{x},t)\in Q_T} s_p''(p(\boldsymbol{x},t))\right) \mathrm{d}_{\mathrm{upd}}|\boldsymbol{z}|^2 \geq 4\,\mathcal{E}_p^{-1}\mathrm{d}_{\mathrm{upd}}|\boldsymbol{z}|^2 \qquad \forall \boldsymbol{z}\in\mathbb{R}^d. \tag{2.11}$$

This is not the case for $s_q''(q)\boldsymbol{D}$, since s_q'' is not bounded away from zero. However, we have

$$(\nabla q)^\top \left(s_q''(q)\boldsymbol{D}\right)\nabla q = \frac{1}{q}(\nabla q)^\top \boldsymbol{D}\nabla q \geq \mathrm{d}_{\mathrm{upd}}\frac{|\nabla q|^2}{q} = 4\,\mathrm{d}_{\mathrm{upd}}|\nabla\sqrt{q}|^2, \tag{2.12}$$

where, in the last step, we have used the identity $|\nabla\sqrt{q}|^2 = \frac{1}{4}\frac{|\nabla q|^2}{q}$. A similar situation occurs for the Shigesada–Kawasaki–Teramoto (SKT) cross-diffusion system when the so-called *detailed-balance condition* does not hold; see, e.g., [13].

Remark 2.4 (Possible degeneracy)**.** *The first identities in equations (2.10c) and (2.10d) impose $\boldsymbol{\sigma}_p = -\nabla p$ and $\boldsymbol{\sigma}_q = -\nabla p$. This follows from the invertibility of $\boldsymbol{D}$ and the strict positivity of s_p'' and s_q''. However, while $s_p''(p)\boldsymbol{D}$ is uniformly positive definite, see (2.11), this is not true for $s_q''(q)\boldsymbol{D}$ and, for large values of $q = u_q(w_q)$, the equation in (2.10d) may degenerate. This further highlights that reformulating in terms of entropy variables leads to a different variational setting.* ∎

Remark 2.5 (Auxiliary variables)**.** *After the change of variables in (2.10a), the definition of the auxiliary variables follows the standard LDG approach, with an adjustment to prevent nonlinearities from appearing under differential operators. This is done by explicitly imposing the chain rule (2.8), so that it is preserved in a weak sense at the discrete level. More precisely, we define $\boldsymbol{r}_p := \boldsymbol{D}\boldsymbol{\sigma}_p = -\boldsymbol{D}\nabla p$ and $\boldsymbol{r}_q := \boldsymbol{D}\boldsymbol{\sigma}_q - \boldsymbol{D}\nabla q$ (equation (2.10e) and first identities in equations (2.10c) and (2.10d)). The second identities in equations (2.10c) and (2.10d), together with equation (2.10b), impose the chain rule (2.8), avoiding the appearance of $\nabla p = \nabla(u_p(w_p))$ and $\nabla q = \nabla(u_q(w_q))$ in the formulation.* ∎

With the variables defined in (2.10), and setting

$$f_p(p,q) := -p(\lambda_p + \mu_{pq}q) + \kappa_p, \qquad f_q(p,q) := -q(\lambda_q - \mu_{pq}p), \tag{2.13}$$

problem (2.1) can be rewritten as follows: find $w_p, w_q : Q_T \to \mathbb{R}$ and $\boldsymbol{r}_p, \boldsymbol{r}_q : Q_T \to \mathbb{R}^d$ such that

$$
\begin{aligned}
\partial_t p + \nabla \cdot \boldsymbol{r}_p &= f_p\,(p,q) && \text{in } Q_T, && \text{(2.14a)}\\
\partial_t q + \nabla \cdot \boldsymbol{r}_q &= f_q\,(p,q) && \text{in } Q_T, && \text{(2.14b)}\\
\boldsymbol{r}_p \cdot \boldsymbol{n}_\Omega = 0 \ \text{ and } \ &\boldsymbol{r}_q \cdot \boldsymbol{n}_\Omega = 0 && \text{on } \Gamma \times (0,T), && \text{(2.14c)}\\
p(\cdot,0) = p_0 \text{ and } &q(\cdot,0) = q_0 && \text{in } \Omega, && \text{(2.14d)}
\end{aligned}
$$

where, in $Q_T = \Omega \times (0,T)$, $p = u_p(w_p)$ and $q = u_q(w_q)$ are understood. The unknowns $\boldsymbol{r}_p$ and $\boldsymbol{r}_q$, which appear explicitly in formulation (2.14), are the fluxes of p and q, respectively; see Remark 2.5.

2.3 The structure-preserving backward Euler-LDG discretization

In this section, we introduce our structure-preserving discretization of system (2.1) based on the reformulation in (2.14) in terms of the auxiliary variables in (2.10).

Meshes. Let $\{\mathcal{T}_h\}_{h>0}$ be a family of conforming, locally quasi-uniform, simplicial partitions of the space domain Ω with shape-regular elements. For any element $K \in \mathcal{T}_h$, we denote by h_K its diameter and by $\boldsymbol{n}_K$ the unit normal d-dimensional vector to ∂K, pointing outward from K. Moreover, we denote by $(\partial K)^\circ$ the union of the facets of K that belong to $\mathcal{F}_h^{\mathcal{I}}$. The index h in $\mathcal{T}_h$ represents the mesh size defined as $h := \max_{K \in \mathcal{T}_h} h_K$. Let also $\mathcal{T}_\tau$ be a partition of the time interval $(0,T)$ of the form $0 := t_0 < t_1 < \ldots < t_{N_t} := T$. For $n = 1, \ldots, N_t$, we define the time interval $I_n := (t_{n-1}, t_n)$ and the time step $\tau_n := t_n - t_{n-1}$. The subscript τ in $\mathcal{T}_\tau$ represents the mesh size defined as $\tau := \max_{1 \le n \le N_t} \tau_n$.

Piecewise polynomial spaces. Given a degree of approximation in space $\ell \in \mathbb{N}$ with $\ell \geq 1$, we define the following (discontinuous) piecewise polynomial spaces of uniform degree:

$$
\mathcal{W}^\ell(\mathcal{T}_h) := \prod_{K \in \mathcal{T}_h} \mathbb{P}^\ell(K) \qquad \text{and} \qquad \boldsymbol{\mathcal{R}}^\ell(\mathcal{T}_h) := \prod_{K \in \mathcal{T}_h} \mathbb{P}^\ell(K)^d,
$$

where $\mathbb{P}^\ell(K)$ denotes the space of scalar-valued polynomials of degree at most ℓ defined on K. Moreover, we denote by $\Pi_{\mathcal{W}}$ and $\boldsymbol{\Pi}_{\boldsymbol{\mathcal{R}}}$ the $L^2(\Omega)$- and $L^2(\Omega)^d$-orthogonal projections in $\mathcal{W}^\ell(\mathcal{T}_h)$ and $\boldsymbol{\mathcal{R}}^\ell(\mathcal{T}_h)$, respectively.

Remark 2.6 (Space of d-vector-valued polynomials)**.** *In combination with $\mathcal{W}^\ell(\mathcal{T}_h)$, the space $\boldsymbol{\mathcal{R}}^{\ell-1}(\mathcal{T}_h)$ can be used in place of $\boldsymbol{\mathcal{R}}^\ell(\mathcal{T}_h)$, thereby reducing the number of degrees of freedom without compromising accuracy [11]. However, using the same polynomial basis for both spaces simplifies the computation of the discrete operators involved in the method. Moreover, some numerical studies suggest that both versions yield comparable efficiency (see, e.g., [14]).* ■

Mesh size function, stability parameters, jumps, and averages. We denote the set of all the mesh facets in $\mathcal{T}_h$ by $\mathcal{F}_h = \mathcal{F}_h^{\mathcal{I}} \cup \mathcal{F}_h^{\mathcal{N}}$, where $\mathcal{F}_h^{\mathcal{I}}$ and $\mathcal{F}_h^{\mathcal{N}}$ are the sets of internal and (Neumann) boundary facets, respectively. We define the mesh size function $\mathsf{h} \in L^\infty(\mathcal{F}_h^{\mathcal{I}})$ as

$$
\mathsf{h}(\boldsymbol{x}) := \min\{h_{K_1}, h_{K_2}\} \quad \text{if } \boldsymbol{x} \in F, \text{ and } F \in \mathcal{F}_h^{\mathcal{I}} \text{ is shared by } K_1, K_2 \in \mathcal{T}_h, \tag{2.15}
$$

and the stability parameters

$$
\eta_F := \eta_0 \ell^2 \frac{2(\boldsymbol{n}_{K_1}^T \mathbf{D}_{|K_1} \boldsymbol{n}_{K_1})(\boldsymbol{n}_{K_2}^T \mathbf{D}_{|K_2} \boldsymbol{n}_{K_2})}{\boldsymbol{n}_{K_1}^T \mathbf{D}_{|K_1} \boldsymbol{n}_{K_1} + \boldsymbol{n}_{K_2}^T \mathbf{D}_{|K_2} \boldsymbol{n}_{K_2}} > 0,
$$

where ℓ is the polynomial degree in the space discretization, and $\eta_0 > 0$ is a constant independent of the problem coefficients and discretization parameters (in practice, $\eta_0 = \mathcal{O}(1)$). For any piecewise smooth, scalar-valued function μ, and any d-vector-valued function $\boldsymbol{\mu}$, we define the normal jumps and weighted mean values as follows: on each facet $F \in \mathcal{F}_h^{\mathcal{I}}$ shared by $K_1, K_2 \in \mathcal{T}_h$,

$$
\begin{aligned}
[\![\mu]\!]_{\mathsf{N}} &:= \mu_{|K_1} \boldsymbol{n}_{K_1} + \mu_{|K_2} \boldsymbol{n}_{K_2}, & \{\!\!\{\mu\}\!\!\}_{\gamma_F} &:= (1-\gamma_F)\mu_{|K_1} + \gamma_F \mu_{|K_2},\\
[\![\boldsymbol{\mu}]\!]_{\mathsf{N}} &:= \boldsymbol{\mu}_{|K_1} \cdot \boldsymbol{n}_{K_1} + \boldsymbol{\mu}_{|K_2} \cdot \boldsymbol{n}_{K_2}, & \{\!\!\{\boldsymbol{\mu}\}\!\!\}_{1-\gamma_F} &:= \gamma_F \boldsymbol{\mu}_{|K_1} + (1-\gamma_F)\boldsymbol{\mu}_{|K_2},
\end{aligned}
$$

with $\gamma_F \in [0,1]$.

Discrete gradient and divergence operators in space. The discrete gradient operator $\nabla_{\mathrm{LDG}} : \mathcal{W}^{\ell}(\mathcal{T}_h) \to \boldsymbol{\mathcal{R}}^{\ell}(\mathcal{T}_h)$ is defined by

$$(\nabla_{\mathrm{LDG}} v_h, \boldsymbol{\phi}_h)_\Omega = (\nabla_h v_h - \mathcal{L}(v_h), \boldsymbol{\phi}_h)_\Omega \quad \forall \boldsymbol{\phi}_h \in \boldsymbol{\mathcal{R}}^{\ell}(\mathcal{T}_h), \tag{2.16}$$

where ∇_h denotes the piecewise gradient operator defined element-by-element, and the jump lifting operator $\mathcal{L} : \mathcal{W}^{\ell}(\mathcal{T}_h) \to \boldsymbol{\mathcal{R}}^{\ell}(\mathcal{T}_h)$ is given by

$$(\mathcal{L}(v_h), \boldsymbol{\phi}_h)_\Omega = \sum_{F \in \mathcal{F}_h^{\mathcal{I}}} (\llbracket v_h \rrbracket_{\mathsf{N}}, \{\!\!\{ \boldsymbol{\phi}_h \}\!\!\}_{1-\gamma_F})_F \quad \forall \boldsymbol{\phi}_h \in \boldsymbol{\mathcal{R}}^{\ell}(\mathcal{T}_h).$$

Accordingly, the discrete divergence operator $\mathrm{div}_{\mathrm{LDG}} : \boldsymbol{\mathcal{R}}^{\ell}(\mathcal{T}_h) \to \mathcal{W}^{\ell}(\mathcal{T}_h)$ is defined by

$$(\mathrm{div}_{\mathrm{LDG}} \boldsymbol{r}_h, \psi_h)_\Omega = -(\boldsymbol{r}_h, \nabla_{\mathrm{LDG}} \psi_h)_\Omega \quad \forall \psi_h \in \mathcal{W}^{\ell}(\mathcal{T}_h). \tag{2.17}$$

These definitions correspond to choosing the numerical fluxes in the LDG method using weighted averages, with weight γ_F for the scalar unknowns and $(1 - \gamma_F)$ for vector-valued unknowns, thus preserving the symmetry of the discretization of the second-order differential operator.

The backward Euler-LDG method. We fix a penalty parameter $\varepsilon > 0$, whose role in the method is described in Remark 2.7 below. The method is defined as follows: for $n = 0, \dots, N_t - 1$, find $w_{p,h}^{(n+1)}, w_{q,h}^{(n+1)} \in \mathcal{W}^{\ell}(\mathcal{T}_h)$ and $\boldsymbol{z}_{p,h}^{(n+1)}$, $\boldsymbol{z}_{q,h}^{(n+1)}$, $\boldsymbol{\sigma}_{p,h}^{(n+1)}$, $\boldsymbol{\sigma}_{q,h}^{(n+1)}$, $\boldsymbol{r}_{p,h}^{(n+1)}$, $\boldsymbol{r}_{q,h}^{(n+1)} \in \boldsymbol{\mathcal{R}}^{\ell}(\mathcal{T}_h)$ (where the dependence on ε has been omitted for brevity), such that, for $\star = p, q$,

$$\boldsymbol{z}_{\star,h}^{(n+1)} = -\nabla_{\mathrm{LDG}} w_{\star,h}^{(n+1)}, \tag{2.18a}$$

$$\Big(\boldsymbol{D} s_\star''(u_\star(w_{\star,h}^{(n+1)}))\boldsymbol{\sigma}_{\star,h}^{(n+1)}, \boldsymbol{\phi}_h\Big)_\Omega = \Big(\boldsymbol{D}\boldsymbol{z}_{\star,h}^{(n+1)}, \boldsymbol{\phi}_h\Big)_\Omega \qquad \forall \boldsymbol{\phi}_h \in \boldsymbol{\mathcal{R}}^{\ell}(\mathcal{T}_h), \tag{2.18b}$$

$$\boldsymbol{r}_{\star,h}^{(n+1)} = \boldsymbol{\Pi}_{\boldsymbol{\mathcal{R}}}\big(\boldsymbol{D}\boldsymbol{\sigma}_{\star,h}^{(n+1)}\big), \tag{2.18c}$$

$$\begin{aligned}\varepsilon \Big(w_{\star,h}^{(n+1)}, \psi_h\Big)_{\mathrm{LDG}} &+ \frac{1}{\tau_{n+1}}\big(u_\star(w_{\star,h}^{(n+1)}) - u_{\star,h}^{(n)}, \psi_h\big)_\Omega \\ &+ \Big(\mathrm{div}_{\mathrm{LDG}} \boldsymbol{r}_{\star,h}^{(n+1)}, \psi_h\Big)_\Omega + \sum_{F \in \mathcal{F}_h^{\mathcal{I}}} \big(\eta_F \mathsf{h}^{-1} \llbracket w_{\star,h}^{(n+1)} \rrbracket_{\mathsf{N}}, \llbracket \psi_h \rrbracket_{\mathsf{N}}\big)_F \\ &= \Big(f_\star\big(u_p(w_{p,h}^{(n+1)}), u_q(w_{q,h}^{(n+1)})\big), \psi_h\Big)_\Omega \qquad \forall \psi_h \in \mathcal{W}^{\ell}(\mathcal{T}_h).\end{aligned} \tag{2.18d}$$

In (2.18d), the quantities $u_{\star,h}^{(n)}$ transmitted from the previous time step are defined as follows:

$$u_{p,h}^{(n)} := \begin{cases} \Pi_{\mathcal{W}} p_0 & \text{if } n = 0, \\ \Pi_{\mathcal{W}} u_p(w_{p,h}^{(n)}) & \text{otherwise,} \end{cases} \quad \text{and} \quad u_{q,h}^{(n)} := \begin{cases} \Pi_{\mathcal{W}} q_0 & \text{if } n = 0, \\ \Pi_{\mathcal{W}} u_q(w_{q,h}^{(n)}) & \text{otherwise,} \end{cases}$$

namely, at the first time step, they are the $L^2(\Omega)$ projections of the initial conditions for the *original* variables p and q; at the subsequent time steps, they are the $L^2(\Omega)$ projections of the *transformed* variables computed at the previous time step. Additionally, $(\cdot, \cdot)_{\mathrm{LDG}}$ is an inner product that is coercive with respect to a norm $\|\cdot\|_{\mathrm{DG}}$ in the space $\mathcal{W}^{\ell}(\mathcal{T}_h)$, which satisfies the following discrete Sobolev embedding: there exists a positive constant C_{Sob} independent of the mesh size h such that

$$\|v_h\|_{L^\infty(\Omega)} \le C_{\mathrm{Sob}} \|v_h\|_{\mathrm{DG}} \qquad \forall v_h \in \mathcal{W}^{\ell}(\mathcal{T}_h). \tag{2.19}$$

A possible choice of such an inner product and DG norm is given in Section 4.1 below.

Remark 2.7 (Role of the penalty term)**.** *The penalty term with parameter $\varepsilon > 0$ in (2.18d) is introduced to prevent $u_p(w_p)$ from approaching the extreme values 0 and 1, and $u_q(w_q)$ from approaching 0. This is necessary because $s_p''(\cdot)$ and $s_q''(\cdot)$ in (2.18b) become singular at these limits. The penalty term thus plays a crucial role in the analysis of the method. From a numerical perspective, it enhances the stability and convergence of nonlinear solvers, such as the Newton method described in Appendix A below.* ■

Remark 2.8 (Equation (2.18b) uniquely determines $\boldsymbol{\sigma}_{\star,h}^{(n+1)}$). *As $s_p''(p)\boldsymbol{D}$ is uniformly positive definite, see (2.11), given $w_{p,h}^{(n+1)}$ and $\boldsymbol{z}_{p,h}^{(n+1)}$, equation (2.18b) with $\star = p$ determines $\boldsymbol{\sigma}_{p,h}^{(n+1)}$ in a unique way; see also Remark 2.4. Given $w_{q,h}^{(n+1)}$, and choosing $\boldsymbol{\phi}_{q,h} = \boldsymbol{\sigma}_{q,h}^{(n+1)}$ in the term on the left-hand side of (2.18b) with $\star = q$, we get*

$$\left(\boldsymbol{D}s_q''\big(u_q(w_{q,h}^{(n+1)})\big)\boldsymbol{\sigma}_{q,h}^{(n+1)}, \boldsymbol{\sigma}_{q,h}^{(n+1)}\right)_\Omega = \int_\Omega \frac{1}{u_q(w_{q,h}^{(n+1)})}\boldsymbol{D}\boldsymbol{\sigma}_{q,h}^{(n+1)} \cdot \boldsymbol{\sigma}_{q,h}^{(n+1)} \,\mathrm{d}\boldsymbol{x} \geq d_{\mathrm{upd}} \int_\Omega \frac{|\boldsymbol{\sigma}_{q,h}^{(n+1)}|^2}{u_q(w_{q,h}^{(n+1)})}\,\mathrm{d}\boldsymbol{x}. \quad (2.20)$$

Therefore, since $d_{\mathrm{upd}} > 0$ and $u_q(w_{q,h}^{(n+1)}) > 0$, if the right-hand side of (2.18b) with $\star = q$ is equal to zero, then $\boldsymbol{\sigma}_{q,h} = 0$, which implies that (2.18b) with $\star = q$ determines $\boldsymbol{\sigma}_{q,h}^{(n+1)}$ in a unique way. However, as observed in Remark 2.4, for large values of $u_q(w_{q,h}^{(n+1)})$, the linear system may degenerate. Such a degeneracy must be prevented using the penalty term $\varepsilon(\cdot,\cdot)_{\mathrm{LDG}}$; see Remark 2.7. ■

2.4 Matrix form

For $\star = p, q$, we define the following forms and functionals: for all $w_h, \psi_h \in \mathcal{W}^\ell(\mathcal{T}_h)$ and $\boldsymbol{z}_h, \boldsymbol{\sigma}_h, \boldsymbol{\phi}_h \in \boldsymbol{\mathcal{R}}^\ell(\mathcal{T}_h)$,

$$\begin{aligned}
\mathsf{m}_h(\boldsymbol{z}_h, \boldsymbol{\phi}_h) &:= (\boldsymbol{z}_h, \boldsymbol{\phi}_h)_\Omega\,, && (2.21a)\\
\mathsf{b}_h(w_h, \boldsymbol{\phi}_h) &:= (\nabla_h w_h, \boldsymbol{\phi}_h)_\Omega - \sum_{F\in\mathcal{F}_h^{\mathcal{I}}} (\llbracket w_h\rrbracket_{\mathsf{N}}, \{\!\{\boldsymbol{\phi}_h\}\!\}_{1-\gamma_F})_F\,, && (2.21b)\\
\mathsf{j}_h(w_h, \psi_h) &:= \sum_{F\in\mathcal{F}_h^{\mathcal{I}}} \big(\eta_F \mathsf{h}^{-1}\llbracket w_h\rrbracket_{\mathsf{N}}, \llbracket \psi_h\rrbracket_{\mathsf{N}}\big)_F, && (2.21c)\\
\mathsf{d}_h(w_h, \boldsymbol{\phi}_h) &:= \sum_{K\in\mathcal{T}_h} (\boldsymbol{D}\boldsymbol{z}_h, \boldsymbol{\phi}_h)_K\,, && (2.21d)\\
\mathsf{n}_{\star,h}(w_h; \boldsymbol{\sigma}_h, \boldsymbol{\phi}_h) &:= \sum_{K\in\mathcal{T}_h} (\boldsymbol{D}s_\star''(u_\star(w_h))\,\boldsymbol{\sigma}_h, \boldsymbol{\phi}_h)_K\,, && (2.21e)\\
\mathsf{u}_{\star,h}(w_h, \psi_h) &:= (u_\star(w_h), \psi_h)_\Omega\,, && (2.21f)\\
\mathsf{f}_{\star,h}(w_{p,h}, w_{q,h}; \psi_h) &:= (f_\star(u_p(w_{p,h}), u_q(w_{q,h})), \psi_h)_\Omega\,. && (2.21g)
\end{aligned}$$

We fix the bases of $\mathcal{W}^\ell(\mathcal{T}_h)$ and $\boldsymbol{\mathcal{R}}^\ell(\mathcal{T}_h)$. For $\star = p, q$, we denote by $\mathbf{W}_{\star,h}$, $\mathbf{Z}_{\star,h}$, $\boldsymbol{\Sigma}_{\star,h}$, and $\mathbf{R}_{\star,h}$ the vectors of expansion coefficients expressing $w_{\star,h}$, $\boldsymbol{z}_{\star,h}$, $\boldsymbol{\sigma}_{\star,h}$, $\boldsymbol{r}_{\star,h}$, respectively, in the chosen bases. Additionally, we denote by M_I, B, J, M_D, and A_{LDG} the matrices associated with the bilinear forms $\mathsf{m}_h(\cdot,\cdot)$, $\mathsf{b}_h(\cdot,\cdot)$, $\mathsf{j}_h(\cdot,\cdot)$, $\mathsf{d}_h(\cdot,\cdot)$, and $(\cdot,\cdot)_{\mathrm{LDG}}$, respectively, and by $\mathcal{N}_\star$, $\mathcal{U}_\star$, and $\mathcal{F}_\star$ the operators associated with the nonlinear functionals $\mathsf{n}_{\star,h}(\cdot\,;\cdot,\cdot)$, $\mathsf{u}_{\star,h}(\cdot,\cdot)$, and $\mathsf{f}_{\star,h}(\cdot,\cdot\,;\cdot)$, respectively. Since the nonlinear functional $\mathsf{n}_{\star,h}(\cdot\,;\cdot,\cdot)$ is linear with respect to its second argument, we write $\mathcal{N}_\star(\mathbf{W}_{\star,h}^{(n+1)})\boldsymbol{\Sigma}_{\star,h}^{(n+1)}$ instead of $\mathcal{N}_\star(\mathbf{W}_{\star,h}^{(n+1)}; \boldsymbol{\Sigma}_{\star,h}^{(n+1)})$.

With the above notation, the scheme in (2.18) can be written in matrix form as follows:

$$\begin{aligned}
M_I\mathbf{Z}_{\star,h}^{(n+1)} &= -B\mathbf{W}_{\star,h}^{(n+1)}, && (2.22a)\\
\mathcal{N}_\star(\mathbf{W}_{\star,h}^{(n+1)})\boldsymbol{\Sigma}_{\star,h}^{(n+1)} &= M_D\mathbf{Z}_{\star,h}^{(n+1)}, && (2.22b)\\
M_I\mathbf{R}_{\star,h}^{(n+1)} &= M_D\boldsymbol{\Sigma}_{\star,h}^{(n+1)}, && (2.22c)\\
\varepsilon A_{\mathrm{LDG}}\mathbf{W}_{\star,h}^{(n+1)} + \frac{1}{\tau_{n+1}}\mathcal{U}_\star(\mathbf{W}_{\star,h}^{(n+1)}) - B^T\mathbf{R}_{\star,h}^{(n+1)} + J\mathbf{W}_{\star,h}^{(n+1)} &= \mathcal{F}_\star(\mathbf{W}_{p,h}^{(n+1)}, \mathbf{W}_{q,h}^{(n+1)}) + \frac{1}{\tau_{n+1}}\mathcal{U}_{\star,h}^{(n)}, && (2.22d)
\end{aligned}$$

where, in (2.22d), for $\star = p, q$,

$$\mathcal{U}_{\star,h}^{(n)} \text{ is the coefficient vector of } \Pi_{\mathcal{W}}(\star)_0 \text{ if } n = 0, \text{ or the coefficient vector of } \Pi_{\mathcal{W}} u_\star(w_{\star,h}^{(n)}) \text{ if } n > 0.$$

Since the mass matrix M_I is symmetric, positive definite, and block diagonal, it is easy to invert. Therefore, representing $\mathbf{Z}_{\star,h}^{(n+1)}$ and $\mathbf{R}_{\star,h}^{(n+1)}$ as

$$\mathbf{Z}_{\star,h}^{(n+1)} = -M_I^{-1}B\mathbf{W}_{\star,h}^{(n+1)} \quad \text{and} \quad \mathbf{R}_{\star,h}^{(n+1)} = M_I^{-1}M_D\boldsymbol{\Sigma}_{\star,h}^{(n+1)},$$

system (2.22) becomes

$$\mathcal{N}_\star(\mathbf{W}_{\star,h}^{(n+1)})\mathbf{\Sigma}_{\star,h}^{(n+1)} = -M_D M_I^{-1} B \mathbf{W}_{\star,h}^{(n+1)}, \tag{2.23a}$$

$$\varepsilon A_{\mathrm{LDG}}\mathbf{W}_{\star,h}^{(n+1)} + \frac{1}{\tau_{n+1}}\mathcal{U}_\star(\mathbf{W}_{\star,h}^{(n+1)}) - B^T M_I^{-1} M_D \mathbf{\Sigma}_{\star,h}^{(n+1)} + J\mathbf{W}_{\star,h}^{(n+1)} = \mathcal{F}_\star(\mathbf{W}_{p,h}^{(n+1)}, \mathbf{W}_{q,h}^{(n+1)}) + \frac{1}{\tau_{n+1}}\mathcal{U}_{\star,h}^{(n)}. \tag{2.23b}$$

Remark 2.9 (Formulation in terms of the $\mathbf{W}$ unknowns only)**.** *Given $\mathbf{W}_{\star,h}^{(n+1)}$, equation (2.23a) determines $\mathbf{\Sigma}_{\star,h}^{(n+1)}$ in a unique way; see Remark 2.8. Then, using $\mathbf{\Sigma}_{\star,h}^{(n+1)} = -\big(\mathcal{N}_\star(\mathbf{W}_{\star,h}^{(n+1)})\big)^{-1} M_D M_I^{-1} B \mathbf{W}_{\star,h}^{(n+1)}$, system (2.23) can be reformulated in terms of the $\mathbf{W}_{\star,h}^{(n+1)}$ unknowns only as*

$$\varepsilon A_{\mathrm{LDG}}\mathbf{W}_{\star,h}^{(n+1)} + \frac{1}{\tau_{n+1}}\mathcal{U}_\star(\mathbf{W}_{\star,h}^{(n+1)}) + B^T M_I^{-1} M_D \big(\mathcal{N}_\star(\mathbf{W}_{\star,h}^{(n+1)})\big)^{-1} M_D M_I^{-1} B \mathbf{W}_{\star,h}^{(n+1)} + J\mathbf{W}_{\star,h}^{(n+1)} = \mathcal{F}_\star(\mathbf{W}_{p,h}^{(n+1)}, \mathbf{W}_{q,h}^{(n+1)}) + \frac{1}{\tau_{n+1}}\mathcal{U}_{\star,h}^{(n)}, \tag{2.24}$$

thus reducing the size of the global nonlinear system. ∎

3 Stability and existence of discrete solutions

In this section, we start by establishing a stability property of the system in (2.1) (Section 3.1). Then, we derive a discrete analogue of this stability property for the backward Euler-LDG method (Section 3.2), which we use to prove the existence of discrete solutions (Section 3.3).

3.1 Entropy stability of the continuous problem

We now derive an entropy stability estimate for problem (2.1). Before doing so, we prove the following bound for the reaction terms, which we write using the notation introduced in (2.13).

Proposition 3.1 (A bound for the reaction term)**.** *For all p, q satisfying (2.4) with strict inequalities, we have*

$$f_p(p,q)s_p'(p) + f_q(p,q)s_q'(q) \leq C_f\left(\mathcal{E}_q + s_q(q)\right), \tag{3.1}$$

with $C_f := \frac{1+\log 2}{\log 2}\,\mathcal{E}_p\left(\frac{\lambda_p}{\mathcal{E}_q} + 2\mu_{pq}\right)$.

Proof. We compute

$$\begin{aligned} f_p(p,q)s_p'(p) + f_q(p,q)s_q'(q) &= (-\lambda_p p + \kappa_p)\log\left(\frac{p}{\mathcal{E}_p - p}\right) - \mu_{pq}pq\log\left(\frac{p}{\mathcal{E}_p - p}\right) - q(\lambda_q - \mu_{pq}p)\log\frac{q}{\mathcal{E}_q} \\ &=: J_1 + J_2 + J_3, \end{aligned}$$

and proceed to estimate J_1, J_2, and J_3. Recalling that $0 < p < \mathcal{E}_p = \kappa_p/\lambda_p$, we have

$$J_1 = \lambda_p p\left(1 - \frac{\kappa_p}{\lambda_p p}\right)\log\left(\frac{\mathcal{E}_p - p}{p}\right) = -\lambda_p p\left(\frac{\mathcal{E}_p - p}{p}\right)\log\left(\frac{\mathcal{E}_p - p}{p}\right) \leq \frac{\lambda_p p}{e} < \frac{\kappa_p}{e},$$

where we have used the inequality $-\rho\log\rho \leq 1/e$ for all $\rho > 0$.

For J_2, using again that $0 < p < \mathcal{E}_p$ and $-\rho\log\rho \leq 1/e$ for all $\rho > 0$, and the inequality $\rho\log(1-\rho) \leq 0$ for all $0 < \rho < 1$, we get

$$\begin{aligned} J_2 = -\mu_{pq}pq\log\left(\frac{\mathcal{E}_p^{-1}p}{1 - \mathcal{E}_p^{-1}p}\right) &= \mu_{pq}q\mathcal{E}_p\Big[\mathcal{E}_p^{-1}p\log(1 - \mathcal{E}_p^{-1}p) - \mathcal{E}_p^{-1}p\log(\mathcal{E}_p^{-1}p)\Big] \\ &\leq \frac{\mathcal{E}_p\mu_{pq}}{e}q \leq \frac{\mathcal{E}_p\mu_{pq}}{e\log 2}\left(\mathcal{E}_q + s_q(q)\right), \end{aligned}$$

where, in the last inequality, we have used the bound $q \le (\mathcal{E}_q + s_q(q)) / \log 2$, which follows from $(x-1) \ge \log x$ for all $x > 0$.

Finally, for J_3, recalling the definition of $s_q(q)$ in (2.7), we have

$$\begin{aligned} J_3 = (\mu_{pq} p - \lambda_q)\big(s_q(q) + q - \mathcal{E}_q\big) &\le \frac{\Upsilon_{pq}}{\lambda_p}\left(s_q(q) + q\right) + \mathcal{E}_q\lambda_q - \mathcal{E}_q\mu_{pq}p \\ &\le \frac{1+\log 2}{\log 2}\,\frac{\Upsilon_{pq}}{\lambda_p}\left(\mathcal{E}_q + s_q(q)\right) + \mathcal{E}_q\lambda_q, \end{aligned}$$

where, in the last inequality, we have used again $q \le (\mathcal{E}_q + s_q(q)) / \log 2$. Collecting the previous estimates of J_1, J_2, and J_3 gives

$$\begin{aligned} f_p(p,q)s_p'(p) + f_q(p,q)s_q'(q) &\le \mathcal{E}_q\left(\frac{\kappa_p}{\mathcal{E}_q e} + \lambda_q\right) + \left(\frac{\mathcal{E}_p\mu_{pq}}{e\log 2} + \frac{1+\log 2}{\log 2}\,\frac{\Upsilon_{pq}}{\lambda_p}\right)\left(\mathcal{E}_q + s_q(q)\right) \\ &\le \left(\frac{\kappa_p}{\mathcal{E}_q e} + \lambda_q + \frac{\mathcal{E}_p\mu_{pq}}{e\log 2} + \frac{1+\log 2}{\log 2}\,\frac{\Upsilon_{pq}}{\lambda_p}\right)\left(\mathcal{E}_q + s_q(q)\right) \\ &\le \frac{1+\log 2}{\log 2}\left(\frac{\kappa_p}{\mathcal{E}_q} + \lambda_q + \mathcal{E}_p\mu_{pq} + \frac{\Upsilon_{pq}}{\lambda_p}\right)\left(\mathcal{E}_q + s_q(q)\right) \\ &= \frac{1+\log 2}{\log 2}\,\mathcal{E}_p\left(\frac{\lambda_p}{\mathcal{E}_q} + 2\mu_{pq}\right)\left(\mathcal{E}_q + s_q(q)\right) =: C_f\left(\mathcal{E}_q + s_q(q)\right), \end{aligned}$$

and the proof is complete. ☐

We prove the following *local* entropy-stability estimate.

Theorem 3.2 (Local entropy stability)**.** *Let $t \in [0,T]$ be such that $t < 1/C_f$, with C_f as in Proposition 3.1. Then, every solution (p,q) to (2.1) satisfies the following stability estimate:*

$$\begin{aligned} \int_\Omega \left(s_p\left(p(\cdot,t)\right) + s_q\left(q(\cdot,t)\right)\right) \mathrm{d}\boldsymbol{x} + 4d_{\mathrm{upd}}\left(\mathcal{E}_p^{-1}\int_0^t \|\nabla p(\cdot,\tau)\|^2_{L^2(\Omega)^d}\,\mathrm{d}\tau + \int_0^t \|\nabla\sqrt{q(\cdot,\tau)}\|^2_{L^2(\Omega)^d}\,\mathrm{d}\tau\right) \\ \le \left(\int_\Omega \left(s_p\left(p_0\right) + s_q\left(q_0\right)\right)\mathrm{d}\boldsymbol{x} + t\mathcal{E}_q C_f|\Omega|\right) e. \end{aligned} \tag{3.2}$$

Proof. By testing the first equation in (2.1) with $w_p\, e^{-\tau/t} = s_p'(p)\, e^{-\tau/t}$, and using the chain rule (2.8), we obtain

$$\begin{aligned} \int_0^t \int_\Omega f_p(p,q)\, s_p'(p)\, e^{-\tau/t}\,\mathrm{d}\boldsymbol{x}\,\mathrm{d}\tau &= \int_0^t \int_\Omega f_p(p,q)\, w_p\, e^{-\tau/t}\,\mathrm{d}\boldsymbol{x}\,\mathrm{d}\tau \\ &= \int_0^t \int_\Omega \partial_\tau p\, w_p\, e^{-\tau/t}\,\mathrm{d}\boldsymbol{x}\,\mathrm{d}\tau - \int_0^t \int_\Omega \nabla\cdot(\boldsymbol{D}\nabla p)\, w_p\, e^{-\tau/t}\,\mathrm{d}\boldsymbol{x}\,\mathrm{d}\tau \\ &= \int_0^t \int_\Omega \partial_\tau p\, s_p'(p)\, e^{-\tau/t}\,\mathrm{d}\boldsymbol{x}\,\mathrm{d}\tau + \int_0^t \int_\Omega (\boldsymbol{D}\nabla p)\cdot\nabla w_p\, e^{-\tau/t}\,\mathrm{d}\boldsymbol{x}\,\mathrm{d}\tau \\ &= \int_0^t \int_\Omega \partial_\tau\left(s_p(p)\, e^{-\tau/t}\right)\mathrm{d}\boldsymbol{x}\,\mathrm{d}\tau + \frac{1}{t}\int_0^t \int_\Omega s_p(p)\, e^{-\tau/t}\,\mathrm{d}\boldsymbol{x}\,\mathrm{d}\tau \\ &\quad + \int_0^t \int_\Omega \left(s_p''(p)\boldsymbol{D}\nabla p\right)\cdot\nabla p\, e^{-\tau/t}\,\mathrm{d}\boldsymbol{x}\,\mathrm{d}\tau \\ &= \frac{1}{e}\int_\Omega s_p\left(p(\cdot,t)\right)\mathrm{d}\boldsymbol{x} - \int_\Omega s_p\left(p_0\right)\mathrm{d}\boldsymbol{x} + \frac{1}{t}\int_0^t \int_\Omega s_p(p)\, e^{-\tau/t}\,\mathrm{d}\boldsymbol{x}\,\mathrm{d}\tau \\ &\quad + \int_0^t \int_\Omega \left(s_p''(p)\boldsymbol{D}\nabla p\right)\cdot\nabla p\, e^{-\tau/t}\,\mathrm{d}\boldsymbol{x}\,\mathrm{d}\tau. \end{aligned} \tag{3.3}$$

Similarly, from the second equation in (2.1) tested with $w_q\, e^{-\tau/t} = s_q'(q)\, e^{-\tau/t}$, we get

$$\begin{aligned} \int_0^t \int_\Omega f_q(p,q)\, s_q'(q)\, e^{-\tau/t}\,\mathrm{d}\boldsymbol{x}\,\mathrm{d}\tau &= \frac{1}{e}\int_\Omega s_q\left(q(\cdot,t)\right)\mathrm{d}\boldsymbol{x} - \int_\Omega s_q\left(q_0\right)\mathrm{d}\boldsymbol{x} + \frac{1}{t}\int_0^t \int_\Omega s_q(q)\, e^{-\tau/t}\,\mathrm{d}\boldsymbol{x}\,\mathrm{d}\tau \\ &\quad + \int_0^t \int_\Omega \left(s_q''(q)\boldsymbol{D}\nabla q\right)\cdot\nabla q\, e^{-\tau/t}\,\mathrm{d}\boldsymbol{x}\,\mathrm{d}\tau. \end{aligned} \tag{3.4}$$

Summing (3.3) and (3.4), and using the bound in (3.1), we obtain

$$\begin{aligned}
&\frac{1}{e}\int_\Omega \left(s_p\left(p(\cdot,t)\right)+s_q\left(q(\cdot,t)\right)\right)\mathrm{d}\boldsymbol{x}+\int_0^t\int_\Omega\left[\left(s_p''(p)\boldsymbol{D}\nabla p\right)\cdot\nabla p+\left(s_q''(q)\boldsymbol{D}\nabla q\right)\cdot\nabla q\right]e^{-\tau/t}\,\mathrm{d}\boldsymbol{x}\,\mathrm{d}\tau\\
&\quad+\frac{1}{t}\int_0^t\int_\Omega\left(s_p(p)+s_q(q)\right)e^{-\tau/t}\,\mathrm{d}\boldsymbol{x}\,\mathrm{d}\tau\\
&\qquad\leq\int_\Omega\left(s_p\left(p_0\right)+s_q\left(q_0\right)\right)\mathrm{d}\boldsymbol{x}+C_f\int_0^t\int_\Omega\left(\mathcal{E}_q+s_q\left(q\right)\right)e^{-\tau/t}\,\mathrm{d}\boldsymbol{x}\,\mathrm{d}\tau\\
&\qquad\leq\int_\Omega\left(s_p\left(p_0\right)+s_q\left(q_0\right)\right)\mathrm{d}\boldsymbol{x}+t\mathcal{E}_qC_f|\Omega|+C_f\int_0^t\int_\Omega\left(s_p\left(p\right)+s_q\left(q\right)\right)e^{-\tau/t}\,\mathrm{d}\boldsymbol{x}\,\mathrm{d}\tau.
\end{aligned}\tag{3.5}$$

Thus, estimate (3.2) is obtained by inserting (2.11) and (2.12) into (3.5), and using the inequalities $\frac{1}{t}-C_f>0$ and $e^{-\tau/t}\geq 1/e$ for all $\tau\in[0,t]$. □

3.2 Discrete entropy stability

For $\star=p,q$, recall that $\mathbf{W}_{\star,h}$, $\mathbf{Z}_{\star,h}$, $\mathbf{\Sigma}_{\star,h}$, and $\mathbf{R}_{\star,h}$ denote the coefficient vectors expressing $w_{\star,h}$, $\boldsymbol{z}_{\star,h}$, $\boldsymbol{\sigma}_{\star,h}$, $\boldsymbol{r}_{\star,h}$, respectively, in terms of fixed, given bases. Similar to [22, Thm. 3.1], we prove a discrete entropy stability estimate and existence of solutions to the discrete problem (2.23). Before doing so, we establish the following discrete Grönwall-type inequality.

Lemma 3.3 (A discrete Grönwall inequality)**.** *Assume that the time mesh $\mathcal{T}_\tau$ is quasi-uniform, i.e., there exists a constant $C_{\mathrm{qu}}>0$ such that $\tau\leq C_{\mathrm{qu}}\tau_{\min}$, and that its mesh size satisfies $\tau<1/(2C_f)$ for some positive constant C_f. Let $\{\alpha_n\}_{n=0}^{N_t}\subset\mathbb{R}^+$ and $\beta\in\mathbb{R}^+$ be such that*

$$(1-C_f\tau_{n+1})\alpha_{n+1}\leq\alpha_n+\beta C_f\tau_{n+1}\qquad \text{for } n=0,\ldots,N_t-1.\tag{3.6}$$

Then, the following bound holds for $n=0,\ldots,N_t-1$:

$$\alpha_{n+1}\leq\exp\left(\frac{3}{2}C_fC_{\mathrm{qu}}t_{n+1}\right)\left(\alpha_0+2\beta C_ft_{n+1}\right).\tag{3.7}$$

Proof. Let $n\in\{0,\ldots,N_t-1\}$. Since $1-C_f\tau_{n+1}\geq 1-C_f\tau>1/2$, we have

$$\alpha_{n+1}\leq\frac{1}{1-C_f\tau}\alpha_n+\frac{1}{1-C_f\tau}\beta C_f\tau_{n+1}\leq\frac{1}{1-C_f\tau}\alpha_n+2\beta C_f\tau_{n+1}.$$

This, together with $1/(1-C_f\tau)^\ell<1/(1-C_f\tau)^{n+1}$ for all $\ell\leq n$, implies

$$\alpha_{n+1}\leq\left(\frac{1}{1-C_f\tau}\right)^{n+1}\alpha_0+2\beta C_f\sum_{k=0}^n\left(\frac{1}{1-C_f\tau}\right)^k\tau_{n+1-k}\leq\left(\frac{1}{1-C_f\tau}\right)^{n+1}(\alpha_0+2\beta C_ft_{n+1}).\tag{3.8}$$

Moreover, the following inequality can be easily proven using Taylor expansions:

$$0<-\log(1-\delta)\leq\delta+\delta^2\qquad\text{for all } 0<\delta<\frac{1}{2},$$

which implies

$$1<\frac{1}{1-\delta}\leq\exp\left(\delta+\delta^2\right)\qquad\text{for all } 0<\delta<\frac{1}{2}.\tag{3.9}$$

Then, combining (3.9) for $\delta=C_f\tau$ with the inequalities $(n+1)\tau\leq C_{\mathrm{qu}}t_{n+1}$ and $C_f\tau<1/2$, we get

$$\left(\frac{1}{1-C_f\tau}\right)^{n+1}\leq\exp\Big(C_f(n+1)\tau\big(1+C_f\tau\big)\Big)\leq\exp\left(\frac{3}{2}C_fC_{\mathrm{qu}}t_{n+1}\right),$$

which, together with (3.8), leads to the desired result. □

The quasi-uniformity assumption on $\mathcal{T}_\tau$

$$\text{there exists a constant } C_{\text{qu}} > 0 \text{ such that } \tau \leq C_{\text{qu}}\tau_n, \quad n = 1, \ldots, N_t. \tag{3.10}$$

is used in the last step of the proof of Lemma 3.3, where it simplifies the argument and the expression of the final estimate. While not essential, such an assumption simplifies the notation and presentation, so we adopt it from here on.

Recalling from Section 2.3 that $\|\cdot\|_{\text{DG}}$ denotes a norm in $\mathcal{W}^\ell(\mathcal{T}_h)$, in which the inner product $(\cdot,\cdot)_{\text{LDG}}$ is coercive (see Section 4.1 below for details), we state the following theorem.

Theorem 3.4 (Discrete entropy stability)**.** *Assume that the time mesh $\mathcal{T}_\tau$ satisfies the quasi-uniformity assumption (3.10), and that its mesh size satisfies $\tau < 1/(2C_f)$, where C_f is the constant in Proposition 3.1. Then, any solution $\{(w_{p,h}^{(n)}, w_{q,h}^{(n)}, \boldsymbol{\sigma}_{p,h}^{(n)}, \boldsymbol{\sigma}_{q,h}^{(n)})\}_{n=1}^{N_t}$ to (2.18) (recall that $\boldsymbol{z}_{\star,h}^{(n)}$ and $\boldsymbol{r}_{\star,h}^{(n)}$ are defined in terms of $w_{\star,h}^{(n)}$ and $\boldsymbol{\sigma}_{\star,h}^{(n)}$, respectively) satisfies*

$$\begin{aligned}
\varepsilon\tau_{n+1}\sum_{\star=p,q}\|w_{\star,h}^{(n+1)}\|_{\text{DG}}^2 + \sum_{\star=p,q}\int_\Omega s_\star(u_\star(w_{\star,h}^{(n+1)}))\,\mathrm{d}\boldsymbol{x} + 4\,\mathcal{E}_p^{-1}d_{\text{upd}}\tau_{n+1}\|\boldsymbol{\sigma}_{p,h}^{(n+1)}\|_{L^2(\Omega)^d} \\
+\mathcal{E}_q^{-1}d_{\text{upd}}\tau_{n+1}\exp\big(-C/\sqrt{\varepsilon\tau_{n+1}}\big)\|\boldsymbol{\sigma}_{q,h}^{(n+1)}\|_{L^2(\Omega)^d}^2 + \tau_{n+1}\sum_{\star=p,q}\|\eta_F^{\frac{1}{2}}\mathsf{h}^{-1/2}[\![w_{\star,h}^{(n+1)}]\!]_{\mathsf{N}}\|_{L^2(\mathcal{F}_h^{\mathcal{I}})^d}^2 \\
\leq \sum_{\star=p,q}\int_\Omega s_\star(u_\star(w_{\star,h}^{(n)}))\,\mathrm{d}\boldsymbol{x} + C_f\tau_{n+1}\left(\mathcal{E}_q|\Omega| + C^*\right),
\end{aligned} \tag{3.11}$$

and

$$\begin{aligned}
\sum_{n=0}^{N_t-1}\tau_{n+1}\Bigg(\varepsilon\sum_{\star=p,q}\|w_{\star,h}^{(n+1)}\|_{\text{DG}}^2 + 4\,\mathcal{E}_p^{-1}d_{\text{upd}}\|\boldsymbol{\sigma}_{p,h}^{(n+1)}\|_{L^2(\Omega)^d}^2 \\
+\mathcal{E}_q^{-1}d_{\text{upd}}\exp\big(-C/\sqrt{\varepsilon\tau_{n+1}}\big)\|\boldsymbol{\sigma}_{q,h}^{(n+1)}\|_{L^2(\Omega)^d}^2 + \sum_{\star=p,q}\|\eta_F^{\frac{1}{2}}\mathsf{h}^{-\frac{1}{2}}[\![w_{\star,h}^{(n+1)}]\!]_{\mathsf{N}}\|_{L^2(\mathcal{F}_h^{\mathcal{I}})^d}^2\Bigg) \\
+\sum_{\star=p,q}\int_\Omega s_\star(u_\star(w_{\star,h}^{N_t}))\,\mathrm{d}\boldsymbol{x} \leq \int_\Omega s_p(p_0)\,\mathrm{d}\boldsymbol{x} + \int_\Omega s_q(q_0)\,\mathrm{d}\boldsymbol{x} + C_fT\left(\mathcal{E}_q|\Omega| + C^*\right),
\end{aligned} \tag{3.12}$$

where C is a positive constant independent of h, τ, and ε, and

$$C^* := \exp\Big(\frac{3}{2}C_fC_{\text{qu}}T\Big)\Big(\int_\Omega s_q(q_0)\,\mathrm{d}\boldsymbol{x} + 2\mathcal{E}_q|\Omega|C_fT\Big). \tag{3.13}$$

Proof. Multiplying (2.23b) by $\mathbf{W}_{\star,h}^{(n+1)}$, we obtain

$$\begin{aligned}
\tau_{n+1}\sum_{\star=p,q}\Big[\varepsilon\langle A_{\text{LDG}}\mathbf{W}_{\star,h}^{(n+1)}, \mathbf{W}_{\star,h}^{(n+1)}\rangle + \frac{1}{\tau_{n+1}}\langle\mathcal{U}_\star(\mathbf{W}_{\star,h}^{(n+1)}) - \mathcal{U}_{\star,h}^{(n)}, \mathbf{W}_{\star,h}^{(n+1)}\rangle \\
-\langle B^TM_I^{-1}M_D\boldsymbol{\Sigma}_{\star,h}^{(n+1)}, \mathbf{W}_{\star,h}^{(n+1)}\rangle + \langle J\mathbf{W}_{\star,h}^{(n+1)}, \mathbf{W}_{\star,h}^{(n+1)}\rangle\Big] \\
= \tau_{n+1}\sum_{\star=p,q}\langle\mathcal{F}_\star(\mathbf{W}_{p,h}^{(n+1)}, \mathbf{W}_{q,h}^{(n+1)}), \mathbf{W}_{\star,h}^{(n+1)}\rangle,
\end{aligned} \tag{3.14}$$

Step 1. We start by establishing bounds for all terms in (3.14). For the first two terms in the sum on the left-hand side, using that $u_\star = (s_\star')^{-1}$, for $n = 1, \ldots, N_t - 1$, we obtain

$$\begin{aligned}
\varepsilon\tau_{n+1}\langle A_{\text{LDG}}\mathbf{W}_{\star,h}^{(n+1)}, \mathbf{W}_{\star,h}^{(n+1)}\rangle + \langle\mathcal{U}_\star(\mathbf{W}_{\star,h}^{(n+1)}) - \mathcal{U}_{\star,h}^{(n)}, \mathbf{W}_{\star,h}^{(n+1)}\rangle \\
\geq \varepsilon\tau_{n+1}\|w_{\star,h}^{(n+1)}\|_{\text{DG}}^2 + \int_\Omega\Big(u_\star(w_{\star,h}^{(n+1)}) - u_{\star,h}^{(n)}\Big)\,w_{\star,h}^{(n+1)}\,\mathrm{d}\boldsymbol{x} \\
= \varepsilon\tau_{n+1}\|w_{\star,h}^{(n+1)}\|_{\text{DG}}^2 + \int_\Omega\Big(u_\star(w_{\star,h}^{(n+1)}) - u_\star(w_{\star,h}^{(n)})\Big)\,w_{\star,h}^{(n+1)}\,\mathrm{d}\boldsymbol{x} \\
\geq \varepsilon\tau_{n+1}\|w_{\star,h}^{(n+1)}\|_{\text{DG}}^2 + \int_\Omega\Big(s_\star(u_\star(w_{\star,h}^{(n+1)})) - s_\star(u_\star(w_{\star,h}^{(n)}))\Big)\,\mathrm{d}\boldsymbol{x},
\end{aligned} \tag{3.15}$$

where, in the last step, we used the convexity of $s_\star$. For $n = 0$, the term $u_\star(w_{\star,h}^{(n)})$ in (3.15) is replaced by p_0 (resp. q_0) for $\star = p$ (resp. $\star = q$). In what follows, we focus on the case $n > 0$, while the case $n = 0$ can be treated similarly.
For the third term, we have

$$
\begin{aligned}
-\tau_{n+1}\langle B^T M_I^{-1} M_D \mathbf{\Sigma}_{\star,h}^{(n+1)}, \mathbf{W}_{\star,h}^{(n+1)}\rangle &= -\tau_{n+1}\langle M_I^{-1} M_D \mathbf{\Sigma}_{\star,h}^{(n+1)}, B\mathbf{W}_{\star,h}^{(n+1)}\rangle \\
&= -\tau_{n+1}\int_\Omega \boldsymbol{D}\boldsymbol{\sigma}_{\star,h}^{(n+1)} \cdot \nabla_{\mathrm{LDG}} w_{\star,h}^{(n+1)}\,\mathrm{d}\boldsymbol{x} \\
&= \tau_{n+1}\int_\Omega \boldsymbol{D}\boldsymbol{\sigma}_{\star,h}^{(n+1)} \cdot \boldsymbol{z}_{\star,h}^{(n+1)}\,\mathrm{d}\boldsymbol{x} = \tau_{n+1}\int_\Omega \boldsymbol{\sigma}_{\star,h}^{(n+1)} \cdot \boldsymbol{D}\boldsymbol{z}_{\star,h}^{(n+1)}\,\mathrm{d}\boldsymbol{x} \\
&= \tau_{n+1}\int_\Omega \boldsymbol{\sigma}_{\star,h}^{(n+1)} \cdot \boldsymbol{D}s_\star''(u_\star(w_{\star,h}^{(n+1)}))\boldsymbol{\sigma}_{\star,h}^{(n+1)}\,\mathrm{d}\boldsymbol{x}.
\end{aligned}
$$

Then, for $\star = p$, using (2.11), we obtain

$$
-\tau_{n+1}\langle B^T M_I^{-1} M_D \mathbf{\Sigma}_{p,h}^{(n+1)}, \mathbf{W}_{p,h}^{(n+1)}\rangle \geq 4\,\mathcal{E}_p^{-1}\mathrm{d}_{\mathrm{upd}}\tau_{n+1}\|\boldsymbol{\sigma}_{p,h}^{(n+1)}\|_{L^2(\Omega)^d}^2. \tag{3.16}
$$

For $\star = q$, using (2.20), we derive

$$
\begin{aligned}
-\tau_{n+1}\langle B^T M_I^{-1} M_D \mathbf{\Sigma}_{q,h}^{(n+1)}, \mathbf{W}_{q,h}^{(n+1)}\rangle &\geq \mathrm{d}_{\mathrm{upd}}\tau_{n+1}\int_\Omega \frac{|\boldsymbol{\sigma}_{q,h}^{(n+1)}|^2}{u_q(w_{q,h}^{(n+1)})}\,\mathrm{d}\boldsymbol{x} = \mathcal{E}_q^{-1}\mathrm{d}_{\mathrm{upd}}\tau_{n+1}\int_\Omega \frac{|\boldsymbol{\sigma}_{q,h}^{(n+1)}|^2}{e^{w_{q,h}^{(n+1)}}}\,\mathrm{d}\boldsymbol{x} \\
&\geq \mathcal{E}_q^{-1}\mathrm{d}_{\mathrm{upd}}\tau_{n+1}\exp(-\|w_{q,h}^{(n+1)}\|_{L^\infty(\Omega)})\|\boldsymbol{\sigma}_{q,h}^{(n+1)}\|_{L^2(\Omega)^d}^2.
\end{aligned} \tag{3.17}
$$

For the fourth term, by definition, we have the identity

$$
\tau_{n+1}\langle J\mathbf{W}_{\star,h}^{(n+1)}, \mathbf{W}_{\star,h}^{(n+1)}\rangle = \tau_{n+1}\|\eta_F^{\frac{1}{2}}\mathsf{h}^{-\frac{1}{2}}[\![w_{\star,h}^{(n+1)}]\!]_{\mathsf{N}}\|_{L^2(\mathcal{F}_h^{\mathcal{I}})^d}^2. \tag{3.18}
$$

Finally, for the term on the right-hand side, we have

$$
\begin{aligned}
&\tau_{n+1}\sum_{\star=p,q}\langle \mathcal{F}_\star(\mathbf{W}_{p,h}^{(n+1)}, \mathbf{W}_{q,h}^{(n+1)}), \mathbf{W}_{\star,h}^{(n+1)}\rangle \\
&\quad= \tau_{n+1}\sum_{\star=p,q}\int_\Omega f_\star\left(u_p(w_{p,h}^{(n+1)}), u_q(w_{q,h}^{(n+1)})\right) w_{\star,h}^{(n+1)}\,\mathrm{d}\boldsymbol{x} \\
&\quad= \tau_{n+1}\sum_{\star=p,q}\int_\Omega f_\star\left(u_p(w_{p,h}^{(n+1)}), u_q(w_{q,h}^{(n+1)})\right) s_\star'(u_\star(w_{\star,h}^{(n+1)}))\,\mathrm{d}\boldsymbol{x} \\
&\quad\leq C_f\mathcal{E}_q\tau_{n+1}|\Omega| + C_f\tau_{n+1}\int_\Omega s_q(u_q(w_{q,h}^{(n+1)}))dx,
\end{aligned} \tag{3.19}
$$

where, in the last step, we used Proposition 3.1.

Step 2. We proceed by proving the following bound: for $n = 1, \ldots, N_t$,

$$
\int_\Omega s_q(u_q(w_{q,h}^{(n)}))\,\mathrm{d}\boldsymbol{x} \leq \exp\left(\frac{3}{2}C_f C_{\mathrm{qu}} T\right)\left(\int_\Omega s_q(q_0)\,\mathrm{d}\boldsymbol{x} + 2\mathcal{E}_q|\Omega|C_f T\right) =: C^*. \tag{3.20}
$$

We emphasize that the constant C^* is independent of h, τ, and n. Using (3.15) with $\star = q$, (3.19), and the fact that the right-hand sides of (3.17) and (3.18) are nonnegative, from (2.23b) with $\star = q$ multiplied by $\mathbf{W}_{q,h}^{(n+1)}$, we get

$$
\varepsilon\tau_{n+1}\|w_{q,h}^{(n+1)}\|_{\mathrm{DG}}^2 + (1 - C_f\tau_{n+1})\int_\Omega s_q(u_q(w_{q,h}^{(n+1)}))\,\mathrm{d}\boldsymbol{x} \leq \int_\Omega s_q(u_q(w_{q,h}^{(n)}))\,\mathrm{d}\boldsymbol{x} + C_f\mathcal{E}_q\tau_{n+1}|\Omega|,
$$

which implies

$$
(1 - C_f\tau_{n+1})\int_\Omega s_q(u_q(w_{q,h}^{(n+1)}))\,\mathrm{d}\boldsymbol{x} \leq \int_\Omega s_q(u_q(w_{q,h}^{(n)}))\,\mathrm{d}\boldsymbol{x} + C_f\mathcal{E}_q\tau_{n+1}|\Omega|.
$$

We apply Lemma 3.3 with $\beta = \mathcal{E}_q|\Omega|$ and

$$\alpha_n := \begin{cases} \displaystyle\int_\Omega s_q(q_0)\,\mathrm{d}\boldsymbol{x} & \text{if } n = 0, \\ \displaystyle\int_\Omega s_q(u_q(w_{q,h}^{(n)}))\,\mathrm{d}\boldsymbol{x} & \text{if } n > 0 \end{cases}$$

to obtain, for $n = 1, \ldots, N_t$,

$$\int_\Omega s_q(u_q(w_{q,h}^{(n)}))\,\mathrm{d}\boldsymbol{x} \le \exp\Big(\frac{3}{2}C_f C_{\mathrm{qu}} t_n\Big)\Big(\int_\Omega s_q(q_0)\,\mathrm{d}\boldsymbol{x} + 2\mathcal{E}_q|\Omega|C_f t_n\Big),$$

which directly yields (3.20).

Step 3. We use the bounds in **Step 1** and **Step 2** to prove a weaker version of (3.11). Inserting (3.15)–(3.19) into (3.14) gives

$$\begin{aligned} &\varepsilon\tau_{n+1}\sum_{\star=p,q}\|w_{\star,h}^{(n+1)}\|_{\mathrm{DG}}^2 + \sum_{\star=p,q}\int_\Omega s_\star(u_\star(w_{\star,h}^{(n+1)}))\,\mathrm{d}\boldsymbol{x} \\ &\qquad + 4\,\mathcal{E}_p^{-1}\mathrm{d}_{\mathrm{upd}}\tau_{n+1}\|\boldsymbol{\sigma}_{p,h}^{(n+1)}\|_{L^2(\Omega)^d}^2 + \tau_{n+1}\sum_{\star=p,q}\|\eta_F^{\frac{1}{2}}\mathsf{h}^{-\frac{1}{2}}[\![w_{\star,h}^{(n+1)}]\!]_{\mathsf{N}}\|_{L^2(\mathcal{F}_h^{\mathcal{I}})^d}^2 \\ &\qquad \le \sum_{\star=p,q}\int_\Omega s_\star(u_\star(w_{\star,h}^{(n)}))\,\mathrm{d}\boldsymbol{x} + C_f\mathcal{E}_q\tau_{n+1}|\Omega| + C_f\tau_{n+1}\int_\Omega s_q(u_q(w_{q,h}^{(n+1)}))\,\mathrm{d}\boldsymbol{x}. \end{aligned}$$

This, together with (3.20), implies

$$\begin{aligned} &\varepsilon\tau_{n+1}\sum_{\star=p,q}\|w_{\star,h}^{(n+1)}\|_{\mathrm{DG}}^2 + \sum_{\star=p,q}\int_\Omega s_\star(u_\star(w_{\star,h}^{(n+1)}))\,\mathrm{d}\boldsymbol{x} \\ &\qquad + 4\,\mathcal{E}_p^{-1}\mathrm{d}_{\mathrm{upd}}\tau_{n+1}\|\boldsymbol{\sigma}_{p,h}^{(n+1)}\|_{L^2(\Omega)^d}^2 + \tau_{n+1}\sum_{\star=p,q}\|\eta_F^{\frac{1}{2}}\mathsf{h}^{-\frac{1}{2}}[\![w_{\star,h}^{(n+1)}]\!]_{\mathsf{N}}\|_{L^2(\mathcal{F}_h^{\mathcal{I}})^d}^2 \\ &\qquad \le \sum_{\star=p,q}\int_\Omega s_\star(u_\star(w_{\star,h}^{(n)}))\,\mathrm{d}\boldsymbol{x} + C_f\tau_{n+1}\left(\mathcal{E}_q|\Omega| + C^*\right). \end{aligned} \tag{3.21}$$

We emphasize that, at this point, there is no term containing $\boldsymbol{\sigma}_{q,h}$ on the left-hand side of estimate (3.21).

Step 4. Estimate (3.21) implies that the term $\varepsilon\tau_{n+1}\|w_{q,h}^{(n+1)}\|_{\mathrm{DG}}^2$, and consequently $\varepsilon\tau_{n+1}\|w_{q,h}^{(n+1)}\|_{L^\infty(\Omega)}^2$ (see the discrete Sobolev inequality (2.19)), is uniformly bounded, which yields the lower bound $\exp(-\|w_{q,h}^{(n+1)}\|_{L^\infty(\Omega)}) \ge \exp(-C/\sqrt{\varepsilon\tau_{n+1}})$, with a constant $C > 0$ independent of h, τ, n, and ε. Inserting this into (3.17) and proceeding as in **Step 3** give (3.11). Finally, summing (3.11) over n gives (3.12). □

Remark 3.5 (Bound on $\|\boldsymbol{\sigma}_{q,h}^{(n+1)}\|_{L^2(\Omega)^d}$). *In the estimates of Theorem 3.4, the bound on the terms $\boldsymbol{\sigma}_{q,h}^{(n+1)}$ is weaker than that of $\boldsymbol{\sigma}_{p,h}^{(n+1)}$. This is a consequence of the fact that s_q'' is not bounded away from zero, which requires a modification in the derivation and leads to the appearance of the additional factor* $\exp(-C/(\varepsilon\tau_{n+1}))$ *in front of $\|\boldsymbol{\sigma}_{q,h}^{(n+1)}\|_{L^2(\Omega)^d}^2$. This issue is related to the absence of a bound on ∇q at the continuous level (see (2.12)).* ■

3.3 Existence of discrete solutions

In the following theorem, we establish the existence of discrete solutions. The proof follows the lines of [22, Thm. 3.2], adapted to our setting. The main modifications concern the terms related to the q variable.

Theorem 3.6 (Existence of discrete solutions). *For each time step $n = 0, \ldots, N_t - 1$, problem (2.23) admits a solution $(\mathbf{W}_{p,h}^{(n+1)}, \mathbf{W}_{q,h}^{(n+1)}, \boldsymbol{\Sigma}_{p,h}^{(n+1)}, \boldsymbol{\Sigma}_{q,h}^{(n+1)})$.*

Proof. We apply the Leray-Schauder theorem. Set $N_h := \dim(\mathcal{W}^\ell(\mathcal{T}_h))$ and begin with the case $n = 0$.

Case $n = 0$. Define the operator $\Phi : \mathbb{R}^{2N_h} \to \mathbb{R}^{2N_h}$ that maps $(\mathbf{V}_{p,h}, \mathbf{V}_{q,h}) \in \mathbb{R}^{2N_h}$ to the unique solution $(\mathbf{W}_{p,h}, \mathbf{W}_{q,h}) \in \mathbb{R}^{2N_h}$ to the following problem: for $\star = p, q$,

$$\varepsilon A_{\mathrm{LDG}} \mathbf{W}_{\star,h} = -\frac{1}{\tau_1}\mathcal{U}_\star(\mathbf{V}_{\star,h}) + \frac{1}{\tau_1}\mathcal{U}^{(0)}_{\star,h} + B^T M_I^{-1} M_D \mathbf{\Sigma}_{\star,h} - J\mathbf{V}_{\star,h} + \mathcal{F}_\star\big(\mathbf{V}_{p,h}, \mathbf{V}_{q,h}\big), \tag{3.22}$$

where $\mathbf{\Sigma}_{\star,h} = \mathbf{\Sigma}_{\star,h}(\mathbf{V}_{\star,h})$ is the unique solution to

$$\mathcal{N}_\star\big(\mathbf{V}_{\star,h}\big)\mathbf{\Sigma}_{\star,h} = -M_D M_I^{-1} B \mathbf{V}_{\star,h}, \tag{3.23}$$

see Remarks 2.9 and 2.8, and $\mathcal{U}^{(0)}_{\star,h}$ is the coefficient vector of $\Pi_{\mathcal{W}} p_0$ or $\Pi_{\mathcal{W}} q_0$ accordingly. Denoting by $w_{\star,h} \in \mathcal{W}^\ell(\mathcal{T}_h)$, $\boldsymbol{\sigma}_{\star,h} \in \boldsymbol{\mathcal{R}}^\ell(\mathcal{T}_h)$, and $v_{\star,h} \in \mathcal{W}^\ell(\mathcal{T}_h)$ the functions whose coefficient vectors are, respectively, $\mathbf{W}_{\star,h}$, $\mathbf{\Sigma}_{\star,h}$, and $\mathbf{V}_{\star,h}$, the map Φ can be defined equivalently as the operator

$$\Phi : (\mathcal{W}^\ell(\mathcal{T}_h))^2 \to (\mathcal{W}^\ell(\mathcal{T}_h))^2, \qquad (v_{p,h}, v_{q,h}) \mapsto (w_{p,h}, w_{q,h}).$$

Well-definedness of Φ. The well-posedness of the linear system (3.22) follows from the positive-definiteness of A_{LDG}, while that of (3.23) is discussed in Remark 2.8.

Continuity of Φ. As for the continuity of Φ, we aim to prove that, for any sequence $\{(v^r_{p,h}, v^r_{q,h})\}_{r\in\mathbb{N}} \subset (\mathcal{W}^\ell(\mathcal{T}_h))^2$ converging to some $(v^\diamond_{p,h}, v^\diamond_{q,h}) \in (\mathcal{W}^\ell(\mathcal{T}_h))^2$, the sequence $\{\Phi(v^r_{p,h}, v^r_{q,h})\}_{r\in\mathbb{N}}$ converges to $\Phi(v^\diamond_{p,h}, v^\diamond_{q,h})$. Since the space $\mathcal{W}^\ell(\mathcal{T}_h)$ is finite dimensional, the sequence $(v^r_{p,h}, v^r_{q,h})$ converges pointwise to $(v^\diamond_{p,h}, v^\diamond_{q,h})$, and it is bounded uniformly in Ω (recall that h, τ, and ε are fixed). We show that the relation (3.23) leads to

$$\mathbf{\Sigma}_{\star,h}(\mathbf{V}^r_{\star,h}) \to \mathbf{\Sigma}_{\star,h}(\mathbf{V}^\diamond_{\star,h}). \tag{3.24}$$

Since the sequence $(v^r_{p,h}, v^r_{q,h})$ is bounded uniformly in Ω, and both $u_p(\cdot)$ and $u_q(\cdot)$ are continuous in $\mathbb{R}^d$, then the sequences $(u_p(v^r_{p,h}))$ and $(u_q(v^r_{q,h}))$ take values in compact sets $\mathcal{K}_p \subset (0, \mathcal{E}_p)$ and $\mathcal{K}_q \subset (0, \infty)$, respectively. Moreover, $s''_\star(\cdot)$ is continuous on $\mathcal{K}_\star$, which implies the uniform boundedness in Ω of the sequence $s''_\star(u_\star(v^r_{\star,h}))$ for $\star = p, q$, i.e., there exist positive constants $C^{\min}_{s,\star}$ and $C^{\max}_{s,\star}$ independent of r such that

$$0 < C^{\min}_{s,\star} \le s''_\star(u_\star(v^r_{\star,h})) \le C^{\max}_{s,\star}. \tag{3.25}$$

We emphasize that, for s''_p, we actually have $s''_p \ge 4\mathcal{E}_p^{-1}$ (see the text above (2.11)), so that $C^{\min}_{s,p} = 4\mathcal{E}_p^{-1}$.

Additionally, since $s''_\star(u_\star(\cdot))$ is locally Lipschitz for both $\star = p, q$ [1], and both $v^r_{\star,h}$ and $v^\diamond_{\star,h}$ are bounded in $L^\infty(\Omega)$, we have

$$\lim_{r\to\infty} \|s''_\star(u_\star(v^r_{\star,h})) - s''_\star(u_\star(v^\diamond_{\star,h}))\|_{L^\infty(\Omega)} \le \lim_{r\to\infty} C\|v^r_{\star,h} - v^\diamond_{\star,h}\|_{L^\infty(\Omega)} = 0, \qquad \star = p, q. \tag{3.26}$$

From the definition of $\boldsymbol{\sigma}_{\star,h}(v^r_{\star,h})$ and $\boldsymbol{\sigma}_{\star,h}(v^\diamond_{\star,h})$ in (3.24), we deduce the following identity:

$$\begin{aligned}\big(\boldsymbol{D} s''_\star(u_\star(v^r_{\star,h}))(\boldsymbol{\sigma}_{\star,h}(v^r_{\star,h}) - \boldsymbol{\sigma}_{\star,h}(v^\diamond_{\star,h})), \boldsymbol{\phi}_h\big)_\Omega &= \Big(\boldsymbol{D}\big(s''_\star(u_\star(v^r_{\star,h})) - s''_\star(u_\star(v^\diamond_{\star,h}))\big)\boldsymbol{\sigma}_{\star,h}(v^\diamond_{\star,h}), \boldsymbol{\phi}_h\Big)_\Omega \\ &\quad - \Big(\boldsymbol{D}\nabla_{\mathrm{LDG}}\big(v^r_{\star,h} - v^\diamond_{\star,h}\big), \boldsymbol{\phi}_h\Big)_\Omega\end{aligned} \tag{3.27}$$

for all $\boldsymbol{\phi}_h \in \boldsymbol{\mathcal{R}}^\ell(\mathcal{T}_h)$. Taking $\boldsymbol{\phi}_h = \boldsymbol{\sigma}_{\star,h}(v^r_{\star,h}) - \boldsymbol{\sigma}_{\star,h}(v^\diamond_{\star,h})$ in (3.27) and using the properties of $\boldsymbol{D}$ in (2.2), the bound in (3.25), and the Cauchy–Schwarz inequality, we obtain

$$\begin{aligned}&\mathrm{d}_{\mathrm{upd}} C^{\min}_{s,\star}\|\boldsymbol{\sigma}_{\star,h}(v^r_{\star,h}) - \boldsymbol{\sigma}_{\star,h}(v^\diamond_{\star,h})\|^2_{L^2(\Omega)^d} \\ &\quad \le D_{\max}\Big(\|s''_\star(u_\star(v^r_{\star,h})) - s''_\star(u_\star(v^\diamond_{\star,h}))\|_{L^\infty(\Omega)^d}\|\boldsymbol{\sigma}_{\star,h}(v^\diamond_{\star,h})\|_{L^2(\Omega)^d} + \|\nabla_{\mathrm{LDG}}(v^r_{\star,h} - v^\diamond_{\star,h})\|_{L^2(\Omega)^d}\Big) \\ &\quad\quad \times \|\boldsymbol{\sigma}_{\star,h}(v^r_{\star,h}) - \boldsymbol{\sigma}_{\star,h}(v^\diamond_{\star,h})\|_{L^2(\Omega)^d}.\end{aligned}$$

This bound, together with (3.26) and the convergence of $\|\nabla_{\mathrm{LDG}}(v^r_{\star,h} - v^\diamond_{\star,h})\|_{L^2(\Omega)^d}$ due to the norm equivalence in finite dimensions, implies

$$\lim_{r\to\infty} \|\boldsymbol{\sigma}_{\star,h}(v^r_{\star,h}) - \boldsymbol{\sigma}_{\star,h}(v^\diamond_{\star,h})\|_{L^2(\Omega)^d} = 0,$$

[1] For $\star = p$, $s''_p(u_p(\cdot)) = (1 + \exp(\cdot))^2/\mathcal{E}_p \exp(\cdot)$ and, for $\star = q$, $s''_q(u_q(\cdot)) = 1/\mathcal{E}_q \exp(\cdot)$.

which completes the proof of (3.24).

The continuity property in (3.24), together with the continuity of $u_\star(\cdot)$ and $f_\star(\cdot,\cdot)$, and the linearity and boundedness of the remaining terms, implies the continuity of the right-hand side of (3.22) with respect to $\mathbf{V}_{\star,h}$. Passing to the limit in (3.22) for the sequence $\{(\mathbf{V}^r_{p,h}, \mathbf{V}^r_{q,h})\}_{r\in\mathbb{N}}$, the following equations are obtained: for $\star = p, q$,

$$\varepsilon A_{\mathrm{LDG}} \mathbf{W}^\diamond_{\star,h} = -\frac{1}{\tau_1}\mathcal{U}_\star(\mathbf{V}^\diamond_{\star,h}) + \frac{1}{\tau_1}\mathcal{U}^{(0)}_{\star,h} + B^T M_I^{-1} M_D \mathbf{\Sigma}_{\star,h}(\mathbf{V}^\diamond_{\star,h}) - J\mathbf{V}^\diamond_{\star,h} + \mathcal{F}_\star\big(\mathbf{V}^\diamond_{p,h}, \mathbf{V}^\diamond_{q,h}\big).$$

The uniqueness of the solution to this linear system, guaranteed by the positive-definiteness of A_{LDG}, implies that $(w^\diamond_{p,h}, w^\diamond_{q,h}) = \Phi(v^\diamond_{p,h}, v^\diamond_{q,h})$, which completes the proof of the continuity of the map Φ.

Compactness of Φ. The compactness is automatic in finite dimensions.

Boundedness of scaled fixed points. It only remains to prove that

$$\text{all solutions to } (\mathbf{W}^\lambda_{p,h}, \mathbf{W}^\lambda_{q,h}) = \lambda\Phi((\mathbf{W}^\lambda_{p,h}, \mathbf{W}^\lambda_{q,h})) \text{ with } \lambda\in[0,1] \text{ satisfy } \|(\mathbf{W}^\lambda_{p,h}, \mathbf{W}^\lambda_{q,h})\|_{\mathbb{R}^{2N_h}} \le R, \tag{3.28}$$

with a constant $R > 0$ independent of λ. Then, the Leray-Schauder theorem implies that Φ has a fixed point, which gives the existence of a solution to (2.23) for $n = 0$.

Let $(\mathbf{W}^\lambda_{p,h}, \mathbf{W}^\lambda_{q,h}) \neq (\mathbf{0}, \mathbf{0})$ be such that $(\mathbf{W}^\lambda_{p,h}, \mathbf{W}^\lambda_{q,h}) = \lambda\Phi((\mathbf{W}^\lambda_{p,h}, \mathbf{W}^\lambda_{q,h}))$ with $\lambda\in[0,1]$. Then, necessarily, $\lambda\in(0,1]$ and

$$\frac{\varepsilon}{\lambda} A_{\mathrm{LDG}} \mathbf{W}^\lambda_{\star,h} + \frac{1}{\tau_1}\mathcal{U}_\star(\mathbf{W}^\lambda_{\star,h}) - \frac{1}{\tau_1}\mathcal{U}^{(0)}_{\star,h} - B^T M_I^{-1} M_D \mathbf{\Sigma}^\lambda_{\star,h} + J\mathbf{W}^\lambda_{\star,h} = \mathcal{F}_\star\big(\mathbf{W}^\lambda_{p,h}, \mathbf{W}^\lambda_{q,h}\big).$$

Multiplying by $\mathbf{W}^\lambda_{\star,h}$ and proceeding as in the proof of Theorem 3.4, we obtain, in terms of the finite element functions,

$$\frac{\varepsilon}{\lambda}\tau_1 \sum_{\star=p,q} \|w^\lambda_{\star,h}\|^2_{\mathrm{DG}} + \sum_{\star=p,q}\int_\Omega s_\star(u_\star(w^\lambda_{\star,h}))\,\mathrm{d}\boldsymbol{x} \le \int_\Omega s_p(p_0)\,\mathrm{d}\boldsymbol{x} + \int_\Omega s_q(q_0)\,\mathrm{d}\boldsymbol{x} + C_f\tau_1\left(\mathcal{E}_q|\Omega| + C^*\right), \tag{3.29}$$

with C^* as in Theorem 3.4. Using (2.9), we have that, for $\star = p, q$, $\|w^\lambda_{\star,h}\|_{\mathrm{DG}}$ is uniformly bounded with respect to λ, which implies (3.28). This concludes the proof of the existence of solutions to the system at the first time step. Additionally, from (3.29), for any of such solutions, we also have that

$$\sum_{\star=p,q}\int_\Omega s_\star(u_\star(w^{(1)}_{\star,h}))\,\mathrm{d}\boldsymbol{x} \le \int_\Omega s_p(p_0)\,\mathrm{d}\boldsymbol{x} + \int_\Omega s_q(q_0)\,\mathrm{d}\boldsymbol{x} + C_f\tau_1\left(\mathcal{E}_q|\Omega| + C^*\right).$$

Case $n \ge 1$. For $n \ge 1$, we proceed by induction and assume existence of solutions at time step $n-1$ as well as, for any of such solutions, the boundedness of $\sum_{\star=p,q}\int_\Omega s_\star(u_\star(w^{(n)}_{\star,h}))\,\mathrm{d}\boldsymbol{x}$. Proceeding as above for the linearized problem

$$\varepsilon A_{\mathrm{LDG}} \mathbf{W}_{\star,h} = -\frac{1}{\tau_{n+1}}\mathcal{U}_\star(\mathbf{V}_{\star,h}) + \frac{1}{\tau_{n+1}}\mathcal{U}^{(n)}_{\star,h} + B^T M_I^{-1} M_D \mathbf{\Sigma}_{\star,h} - J\mathbf{W}_{\star,h} + \mathcal{F}_\star\big(\mathbf{V}_{p,h}, \mathbf{V}_{q,h}\big),$$

where $\mathcal{U}^{(n)}_{\star,h} = \mathcal{U}_\star\big(\mathbf{W}^{(n)}_{\star,h}\big)$, we obtain

$$\frac{\varepsilon}{\lambda}\tau_{n+1} \sum_{\star=p,q} \|w^\lambda_{\star,h}\|^2_{\mathrm{DG}} + \sum_{\star=p,q}\int_\Omega s_\star(u_\star(w^\lambda_{\star,h}))\,\mathrm{d}\boldsymbol{x} \le \sum_{\star=p,q}\int_\Omega s_\star(u_\star(w^{(n)}_{\star,h}))\,\mathrm{d}\boldsymbol{x} + C_f\tau_{n+1}\left(\mathcal{E}_q|\Omega| + C^*\right). \tag{3.30}$$

The boundedness of $\sum_{\star=p,q}\int_\Omega s_\star(u_\star(w^{(n)}_{\star,h}))\,\mathrm{d}\boldsymbol{x}$ implies that, for $\star = p, q$, $\|w^\lambda_{\star,h}\|_{\mathrm{DG}}$ is uniformly bounded with respect to λ, and thus existence of solutions to (2.23) at the time step n. Additionally, from (3.30), for any of such solutions, we also have that

$$\sum_{\star=p,q}\int_\Omega s_\star(u_\star(w^{(n+1)}_{\star,h}))\,\mathrm{d}\boldsymbol{x} \le \sum_{\star=p,q}\int_\Omega s_\star(u_\star(w^{(n)}_{\star,h}))\,\mathrm{d}\boldsymbol{x} + C_f\tau_1\left(\mathcal{E}_q|\Omega| + C^*\right),$$

which completes the proof. $\square$

4 Convergence of the scheme

We now study the convergence of the scheme to a weak solution to the system (2.1) that satisfies the physical bounds in (2.4). To do so, we proceed in two steps: first, we prove that, as $h \to 0$, the scheme converges to a semidiscrete-in-time formulation (Section 4.1); then, we analyze the convergence of this formulation as $(\varepsilon, \tau) \to (0, 0)$ (Section 4.2). Henceforth, we assume that the degree of approximation in space satisfies $\ell \geq 2$, and set the weight parameter $\gamma_F = 1/2$ for all facets $F \in \mathcal{F}_h^{\mathcal{I}}$.

We introduce the auxiliary piecewise polynomial space

$$\boldsymbol{\mathcal{Z}}^\ell(\mathcal{T}_h) := \prod_{K \in \mathcal{T}_h} \mathbb{P}^\ell(K)^{d \times d}.$$

Then, the discrete LDG Hessian operator $\mathcal{H}_{\mathrm{LDG}} : \mathcal{W}^\ell(\mathcal{T}_h) \to \boldsymbol{\mathcal{Z}}^\ell(\mathcal{T}_h)$ is defined as follows:

$$\mathcal{H}_{\mathrm{LDG}} \lambda_h := \mathcal{H}_h \lambda_h - \mathcal{G}_h(\lambda_h) + \mathcal{B}_h(\lambda_h),$$

where $\mathcal{H}_h$ denotes the piecewise Hessian operator defined element-by-element, and the lifting operators $\mathcal{G}_h : \mathcal{W}^\ell(\mathcal{T}_h) \to \boldsymbol{\mathcal{Z}}^\ell(\mathcal{T}_h)$ and $\mathcal{B}_h : \mathcal{W}^\ell(\mathcal{T}_h) \to \boldsymbol{\mathcal{Z}}^\ell(\mathcal{T}_h)$ are given, respectively, by

$$(\mathcal{G}_h \lambda_h, \Theta_h)_\Omega = \sum_{K \in \mathcal{T}_h} (\nabla \lambda_h, \{\!\!\{\Theta_h\}\!\!\}_{\frac{1}{2}} \boldsymbol{n}_K)_{(\partial K)^\circ} \qquad \forall \Theta_h \in \boldsymbol{\mathcal{Z}}^\ell(\mathcal{T}_h), \tag{4.1a}$$

$$(\mathcal{B}_h \lambda_h, \Theta_h)_\Omega = ([\![\lambda_h]\!]_{\mathsf{N}}, \{\!\!\{\nabla_h \cdot \Theta_h\}\!\!\}_{\frac{1}{2}})_{\mathcal{F}_h^{\mathcal{I}}} \qquad \forall \Theta_h \in \boldsymbol{\mathcal{Z}}^\ell(\mathcal{T}_h). \tag{4.1b}$$

We define the inner product $(\cdot, \cdot)_{\mathrm{LDG}}$ as

$$\begin{aligned}(w_h, \lambda_h)_{\mathrm{LDG}} :=& (w_h, \lambda_h)_\Omega + (\nabla_{\mathrm{LDG}} w_h, \nabla_{\mathrm{LDG}} \lambda_h)_\Omega + (\mathcal{H}_{\mathrm{LDG}} w_h, \mathcal{H}_{\mathrm{LDG}} \lambda_h)_\Omega \\ &+ (\mathsf{h}^{-1} [\![\nabla_h w_h]\!], [\![\nabla_h \lambda_h]\!])_{\mathcal{F}_h^{\mathcal{I}}} + (\mathsf{h}^{-3} [\![w_h]\!]_{\mathsf{N}}, [\![\lambda_h]\!]_{\mathsf{N}})_{\mathcal{F}_h^{\mathcal{I}}},\end{aligned} \tag{4.2}$$

where $[\![\cdot]\!]$ denotes the standard (vector-valued) total jump on each facet $F \in \mathcal{F}_h^{\mathcal{I}}$. Finally, we define the discrete norm:

$$\|w_h\|_{\mathrm{DG}}^2 := \|w_h\|_{L^2(\Omega)}^2 + \|\nabla_h w_h\|_{L^2(\Omega)^d}^2 + \|\mathcal{H}_h w_h\|_{L^2(\Omega)^{d \times d}}^2 + \|\mathsf{h}^{-\frac{1}{2}} [\![\nabla_h w_h]\!]\|_{L^2(\mathcal{F}_h^{\mathcal{I}})^d}^2 + \|h^{-\frac{3}{2}} [\![w_h]\!]_{\mathsf{N}}\|_{L(\mathcal{F}_h^{\mathcal{I}})^d}^2. \tag{4.3}$$

We emphasize that $\|\cdot\|_{\mathrm{DG}}$ is *not* the norm associated with $(\cdot, \cdot)_{\mathrm{LDG}}$.

4.1 Convergence as $h \to 0$

In this section, we fix the penalty parameter $\varepsilon > 0$ and the partition $\mathcal{T}_\tau$ of the time interval $(0, T)$ with $\tau < 1/(2C_f)$. We consider a sequence of space meshes $\{\mathcal{T}_{h_m}\}_m$ with decreasing maximum mesh sizes $\{h_m\}_m$ such that $h_m \to 0$ as $m \to \infty$. For the sake of clarity, we henceforth write the superscript ε to highlight the dependence of the discrete solution to (2.18) on the penalty parameter ε.

Next lemma summarizes some properties of the inner product $(\cdot, \cdot)_{\mathrm{LDG}}$ that are instrumental in our convergence analysis; see [22, §4.2].

Lemma 4.1 (Properties of $(\cdot, \cdot)_{\mathrm{LDG}}$). *Let the inner product $(\cdot, \cdot)_{\mathrm{LDG}}$ be defined as in (4.2). Then, the following properties are satisfied:*

i) The inner product $(\cdot, \cdot)_{\mathrm{LDG}}$ is coercive in $\mathcal{W}^\ell(\mathcal{T}_{h_m})$ with respect to the norm $\|\cdot\|_{\mathrm{DG}}$ defined in (4.3), i.e., there exists a positive constant C_{coer} independent of h_m such that

$$(\psi_{h_m}, \psi_{h_m})_{\mathrm{LDG}} \geq C_{\mathrm{coer}} \|\psi_{h_m}\|_{\mathrm{DG}}^2 \qquad \forall \psi_{h_m} \in \mathcal{W}^\ell(\mathcal{T}_{h_m}).$$

ii) If $d = 2$, the following discrete Sobolev embedding holds: there exists a positive constant C_{Sob} independent of h_m such that

$$\|\psi_{h_m}\|_{L^\infty(\Omega)} \leq C_{\mathrm{Sob}} \|\psi_{h_m}\|_{\mathrm{DG}} \qquad \forall \psi_{h_m} \in \mathcal{W}^\ell(\mathcal{T}_{h_m}).$$

iii) *For any sequence* $\{w_m\}_{m\in\mathbb{N}}$ *with* $w_m \in \mathcal{W}^\ell(\mathcal{T}_{h_m})$ *that is uniformly bounded in the DG norm* (4.3)*, there exists a subsequence, that we still denote by* $\{w_m\}_{m\in\mathbb{N}}$*, and a function* $w \in H^2(\Omega)$ *such that, as* $m \to \infty$*,*

$$\begin{aligned} \nabla_{\mathrm{LDG}} w_m &\rightharpoonup \nabla w && \text{weakly in } L^2(\Omega)^d, \\ w_m &\to w && \text{strongly in } L^q(\Omega), \end{aligned}$$

with $1 \le q < \infty$ *(if* $d = 2$*) or* $1 \le q < 6$ *(if* $d = 3$*). Moreover, for any* $\psi \in H^2(\Omega)$*, there exists a sequence* $\{\psi_m\}_{m\in\mathbb{N}}$ *with* $\psi \in \mathcal{W}^2(\mathcal{T}_{h_m}) \cap H^1(\Omega)$ *such that, as* $m \to 0$*, such a sequence converges strongly in* $H^1(\Omega)$ *to* ψ *and*

$$(w_m, \psi_m)_{\mathrm{LDG}} \to (w, \psi)_\Omega + (\nabla w, \nabla \psi)_\Omega + (\mathcal{H} w, \mathcal{H}\psi)_\Omega.$$

Property *ii)* has been proven in [22, §4.2] for $d = 2$. Although the argument there does not extend to $d = 3$, we believe the property remains valid in that case. However, in the absence of a proof, we proceed by making the following abstract assumption, which is obviously satisfied for $d = 2$, as detailed above.

Assumption 4.1. *There exists an inner product* $(\cdot,\cdot)_{\mathrm{LDG}}$ *and a norm* $\|\cdot\|_{\mathrm{DG}}$ *such that* i)*,* ii)*, and* iii) *in Lemma 4.1 are satisfied.*

Theorem 4.2 (h-convergence)**.** *Let the penalty parameter* $\varepsilon > 0$ *and the time partition* $\mathcal{T}_\tau$ *be fixed, and assume that* $\mathcal{T}_\tau$ *satisfies the quasi-uniformity condition* (3.10) *with* $\tau < 1/(2C_f)$*. Let also the initial conditions* p_0 *and* q_0 *satisfy* (2.3)*, and the degree of approximation in space* $\ell \ge 2$*. For* $n = 1, \dots, N_t$*, there exist* $w_p^{\varepsilon,(n)}, w_q^{\varepsilon,(n)} \in H^2(\Omega)$ *and a subsequence of* $\{\mathcal{T}_{h_m}\}_{m\in\mathbb{N}}$ *still denoted by* $\{\mathcal{T}_{h_m}\}_{m\in\mathbb{N}}$ *such that, as* $m \to \infty$*,*

$$p_m^{\varepsilon,(n)} := u_p(w_{p,m}^{\varepsilon,(n)}) \to p^{\varepsilon,(n)} := u_p(w_p^{\varepsilon,(n)}) \qquad \text{strongly in } L^r \text{ for all } r \in [1,\infty), \tag{4.4a}$$
$$q_m^{\varepsilon,(n)} := u_q(w_{q,m}^{\varepsilon,(n)}) \to q^{\varepsilon,(n)} := u_q(w_q^{\varepsilon,(n)}) \qquad \text{strongly in } L^r \text{ for all } r \in [1,\infty). \tag{4.4b}$$

Moreover, for $n = 0, \dots, N_t - 1$*, the pair* $(w_p^{\varepsilon,(n+1)}, w_q^{\varepsilon,(n+1)})$ *solves the following semidiscrete-in-time variational formulation: for* $\star = p, q$*,*

$$\begin{aligned} \varepsilon\Big[\Big(w_\star^{\varepsilon,(n+1)}, \psi\Big)_\Omega + \Big(\nabla w_\star^{\varepsilon,(n+1)}, \nabla\psi\Big)_\Omega + \Big(\mathcal{H} w_\star^{\varepsilon,(n+1)}, \mathcal{H}\psi\Big)_\Omega \Big] + \frac{1}{\tau_{n+1}} \Big(u_\star(w_\star^{\varepsilon,(n+1)}) - (\star)^{\varepsilon,(n)}, \psi\Big)_\Omega \\ + \Big(\boldsymbol{D}\nabla u_\star(w_\star^{\varepsilon,(n+1)}), \nabla\psi\Big)_\Omega = \Big(f_\star(u_p(w_p^{\varepsilon,(n+1)}), u_q(w_q^{\varepsilon,(n+1)})), \psi\Big)_\Omega \qquad \forall \psi \in H^2(\Omega), \end{aligned} \tag{4.5}$$

where $(\star)^{\varepsilon,(0)} := (\star)_0$*, and* $\mathcal{H} : H^2(\Omega) \to L^2(\Omega)^{d\times d}$ *denotes the global Hessian operator.*

Finally, the following entropy stability estimate for the limit functions holds for $n = 1, \dots, N_t$*:*

$$\begin{aligned} \sum_{k=0}^{n-1} \tau_{k+1} \Bigg(\varepsilon \sum_{\star=p,q} \|w_\star^{\varepsilon,(k+1)}\|_{H^2(\Omega)}^2 + 4\,\mathcal{E}_p^{-1} d_{\mathrm{upd}} \|\nabla p^{\varepsilon,(k+1)}\|_{L^2(\Omega)^d}^2 + 4\mathcal{E}_q^{-1} d_{\mathrm{upd}} \|\nabla \sqrt{q^{\varepsilon,(k+1)}}\|_{L^2(\Omega)^d}^2 \Bigg) \\ + \int_\Omega s_p(p^{\varepsilon,n})\,\mathrm{d}\boldsymbol{x} + \int_\Omega s_q(q^{\varepsilon,n})\,\mathrm{d}\boldsymbol{x} \le \int_\Omega s_p(p_0)\,\mathrm{d}\boldsymbol{x} + \int_\Omega s_q(q_0)\,\mathrm{d}\boldsymbol{x} + C_f T\left(\mathcal{E}_q|\Omega| + C^*\right), \end{aligned} \tag{4.6}$$

where C^* *is the constant defined in* (3.13)*.*

Proof. We prove the result using an induction argument on the time steps.

Approximation of the initial conditions. Set $(p_m^{\varepsilon,0}, q_m^{\varepsilon,0}) := (\Pi_{\mathcal{W}} p_0, \Pi_{\mathcal{W}} q_0) \in \mathcal{W}^\ell(\mathcal{T}_{h_m}) \times \mathcal{W}^\ell(\mathcal{T}_{h_m})$. Using the orthogonality and approximation properties of $\Pi_{\mathcal{W}}$, for all $\psi \in H^2(\Omega)$, we have

$$(p_0 - p_m^{\varepsilon,0}, \psi)_\Omega = (p_0, \psi - \Pi_{\mathcal{W}}\psi)_\Omega \le C h_m^2 \|p_0\|_{L^2(\Omega)} |\psi|_{H^2(\Omega)},$$

for some positive constant C independent of h_m and ψ. An analogous estimate can be obtained for $q_0 - q_m^{\varepsilon,0}$. Therefore, as $m \to 0$, we get

$$\begin{aligned} (p_m^{\varepsilon,0}, \psi) &\to (p_0, \psi) && \forall \psi \in H^2(\Omega), \\ (q_m^{\varepsilon,0}, \psi) &\to (q_0, \psi) && \forall \psi \in H^2(\Omega). \end{aligned}$$

Convergence of $w_{\star,m}^{\varepsilon,(n)}$. The discrete entropy stability estimate (3.12) implies that, for $n = 1, \ldots, N_t$ and $\star = p, q$, the sequence $\{w_{\star,m}^{\varepsilon,(n)}\}_{m\in\mathbb{N}}$ is bounded in the DG norm uniformly with respect to h_m. Moreover, due to Lemma 4.1, *ii)*, it is also bounded in the $L^\infty(\Omega)$ norm uniformly with respect to h_m. Then, we apply Lemma 4.1, part *iii)* and obtain the existence of some functions $w_p^{\varepsilon,(n)}$, $w_q^{\varepsilon,(n)} \in H^2(\Omega)$ such that, up to subsequences that we still denote by $\{w_{\star,m}^{\varepsilon,(n)}\}_{m\in\mathbb{N}}$, it holds

$$\nabla_{\text{LDG}} w_{\star,m}^{\varepsilon,(n)} \rightharpoonup \nabla w_\star^{\varepsilon,(n)} \qquad \text{weakly in } L^2(\Omega)^d, \tag{4.7a}$$

$$w_{\star,m}^{\varepsilon,(n)} \to w_\star^{\varepsilon,(n)} \qquad \text{strongly in } L^q(\Omega), \tag{4.7b}$$

with $1 \le q < \infty$ (if $d = 2$) or $1 \le q < 6$ (if $d = 3$). Moreover, by [9, Thm. 4.9 in §4.2], we can extract from $\{w_{\star,m}^{\varepsilon,(n)}\}_{m\in\mathbb{N}}$ another subsequence that converges to $w_\star^{\varepsilon,(n)}$ almost everywhere in Ω.

Convergence of $u_\star(w_{\star,m}^{\varepsilon,(n)})$. Let $\{w_{\star,m}^{\varepsilon,(n)}\}_{m\in\mathbb{N}}$ be the subsequence extracted in the previous step. Since $u_p : \mathbb{R}^d \to (0, \mathcal{E}_p)$ is continuous, the sequence $\{u_p(w_{p,m}^{\varepsilon,(n)})\}_{m\in\mathbb{N}}$ converges almost everywhere in Ω to $u_p(w^{\varepsilon,(n)})$, and is uniformly bounded in the $L^\infty(\Omega)$ norm by $\mathcal{E}_p$. Thus, the convergence in (4.4a) is a consequence of the dominated convergence theorem (see, e.g., [9, Thm. 4.2 in §4.1]).

The proof of (4.4b) is less immediate as u_q is not uniformly bounded. In this case, we first use the discrete entropy stability estimates in Theorem 3.4 and the discrete compact embedding in Lemma 4.1, part *ii)*, to conclude that $\{w_{q,m}^{\varepsilon,(n)}\}_{m\in\mathbb{N}}$ is uniformly bounded in $L^\infty(\Omega)$ with respect to h_m (recall that ε and $\mathcal{T}_\tau$ are fixed). This implies that $w_{q,m}^{\varepsilon,(n)}(\boldsymbol{x}) \in \mathcal{K}_q$ almost everywhere in Ω, for some compact set $\mathcal{K}_q \subset \mathbb{R}$ independent of m. Consequently, since u_q is continuous on $\mathbb{R}$, $u_q(w_{q,m}^{\varepsilon,(n)})(\boldsymbol{x})$ belongs to the compact set $u_q(\mathcal{K}_q)$ for almost all $\boldsymbol{x} \in \Omega$. The convergence in (4.4b) then follows analogously to that in (4.4a).

In a similar way, it can be proven that, for $\star = p, q$,

$$f_\star(u_p(w_{p,m}^{\varepsilon,(n+1)}), u_q(w_{q,m}^{\varepsilon,(n+1)})) \to f_\star(u_p(w_p^{\varepsilon,(n+1)}), u_q(w_q^{\varepsilon,(n+1)})) \quad \text{strongly in } L^r(\Omega) \text{ for all } r \in [1,\infty). \tag{4.8}$$

Semidiscrete-in-time limit problem. In order to prove the last part of the theorem, we first rewrite the fully discrete scheme (2.23) in the following variational form: for $\star = p, q$,

$$\Big(\boldsymbol{D} s_\star''(u_\star(w_{\star,m}^{\varepsilon,(n+1)}))\boldsymbol{\sigma}_{\star,m}^{\varepsilon,(n+1)}, \boldsymbol{\phi}_m\Big)_\Omega = -\Big(\boldsymbol{D}\nabla_{\text{LDG}} w_{\star,m}^{\varepsilon,(n+1)}, \boldsymbol{\phi}_m\Big)_\Omega \qquad \forall \boldsymbol{\phi}_m \in \boldsymbol{\mathcal{R}}^\ell(\mathcal{T}_{h_m}), \tag{4.9}$$

$$\begin{aligned}\varepsilon\Big(w_{\star,m}^{\varepsilon,(n+1)}, \psi_m\Big)_{\text{LDG}} &+ \frac{1}{\tau_{n+1}}\Big(u_\star(w_{\star,m}^{\varepsilon,(n+1)}) - u_{\star,m}^{\varepsilon,(n)}, \psi_m\Big)_\Omega \\ - \Big(\boldsymbol{D}\boldsymbol{\sigma}_{\star,m}^{\varepsilon,(n+1)}, \nabla_{\text{LDG}}\psi_m\Big)_\Omega &+ \sum_{F\in\mathcal{F}_{h_m}^{\mathcal{I}}} \Big(\eta_F \mathsf{h}^{-1}[\![w_{\star,m}^{\varepsilon,(n+1)}]\!]_{\mathsf{N}}, [\![\psi_m]\!]_{\mathsf{N}}\Big)_F \\ &= \Big(f_\star(u_p(w_{p,m}^{\varepsilon,(n+1)}), u_q(w_{q,m}^{\varepsilon,(n+1)}), \psi_m\Big)_\Omega \qquad \forall \psi_m \in \mathcal{W}^\ell(\mathcal{T}_{h_m}).\end{aligned} \tag{4.10}$$

We aim to pass to the limit in each term in (4.10).

Since $\boldsymbol{\phi} \mapsto D\boldsymbol{\phi}$ defines a continuous linear operator, using the uniform boundedness of $\boldsymbol{D}$ and the weak convergence in (4.7a) of $\nabla_{\text{LDG}} w_{\star,m}^{\varepsilon,(n+1)}$, we can deduce (see [9, Thm. 3.10 in §3.3])

$$\boldsymbol{D}\nabla_{\text{LDG}} w_{\star,m}^{\varepsilon,(n+1)} \rightharpoonup \boldsymbol{D}\nabla w_\star^{\varepsilon,(n+1)} \quad \text{weakly in } L^2(\Omega)^d. \tag{4.11}$$

Moreover, the discrete entropy stability estimate (3.12) implies that $\{\boldsymbol{\sigma}_{\star,m}^{\varepsilon,(n+1)}\}_{m\in\mathbb{N}}$ is uniformly bounded in $L^2(\Omega)^d$ with respect to h_m (recall again that ε and $\mathcal{T}_\tau$ are fixed). Since $L^2(\Omega)^d$ is (trivially) reflexive, we can extract a subsequence, still denoted by $\{\boldsymbol{\sigma}_{\star,m}^{\varepsilon,(n+1)}\}_{m\in\mathbb{N}}$, such that (see [9, Thm. 3.18 in §3.5])

$$\boldsymbol{\sigma}_{\star,m}^{\varepsilon,(n+1)} \rightharpoonup \boldsymbol{\sigma}_\star^{\varepsilon,(n+1)} \quad \text{weakly in } L^2(\Omega)^d,$$

for some $\boldsymbol{\sigma}_\star^{\varepsilon,(n+1)} \in L^2(\Omega)^d$. Using the continuity and uniform boundedness of $\boldsymbol{D}$, $s_p''(\cdot)$, and $s_q''(\cdot)$ on $\mathbb{R}$, $u_p(\mathcal{K}_p)$, and $u_q(\mathcal{K}_q)$, respectively, we have

$$\boldsymbol{D}\boldsymbol{\sigma}_{\star,m}^{\varepsilon,(n+1)} \rightharpoonup \boldsymbol{D}\boldsymbol{\sigma}_\star^{\varepsilon,(n+1)} \qquad \text{weakly in } L^2(\Omega)^d, \tag{4.12a}$$

$$\boldsymbol{D} s_\star''(u_\star(w_{\star,m}^{\varepsilon,(n+1)}))\boldsymbol{\sigma}_{\star,m}^{\varepsilon,(n+1)} \rightharpoonup \boldsymbol{D} s_\star''(u_\star(w_\star^{\varepsilon,(n+1)}))\boldsymbol{\sigma}_\star^{\varepsilon,(n+1)} \qquad \text{weakly in } L^2(\Omega)^d. \tag{4.12b}$$

It only remains to prove that $\boldsymbol{\sigma}_\star^{\varepsilon,(n+1)} = -\nabla u_\star(w_\star^{\varepsilon,(n+1)})$ almost everywhere in Ω. The density of $H^1(\Omega)$ in $L^2(\Omega)$, and the approximation properties of $\boldsymbol{\mathcal{R}}^\ell(\mathcal{T}_{h_m})$ (see [8, Thm. 4.4.20 in §4.4]) imply that, for any $\boldsymbol{\phi} \in L^2(\Omega)^d$, there is a sequence $\{\boldsymbol{\phi}_m\}_{m\in\mathbb{N}}$ that converges strongly to $\boldsymbol{\phi}$ in $L^2(\Omega)^d$. This, combined with equation (4.9), the convergences in (4.11) and (4.12b), and the chain rule $\nabla w = \nabla s_\star'(u_\star(w)) = s_\star''(u_\star(w))\nabla u_\star(w)$, implies

$$\left(\boldsymbol{D}s_\star''(u_\star(w_\star^{\varepsilon,(n+1)}))\boldsymbol{\sigma}_\star^{\varepsilon,(n+1)}, \boldsymbol{\phi}\right)_\Omega = -\left(\boldsymbol{D}s_\star''(u_\star(w_\star^{\varepsilon,(n+1)}))\nabla u_\star(w_\star^{\varepsilon,(n+1)}), \boldsymbol{\phi}\right)_\Omega \qquad \forall \boldsymbol{\phi} \in L^2(\Omega)^d. \tag{4.13}$$

Taking $\boldsymbol{\phi} = \boldsymbol{\sigma}_\star^{\varepsilon,(n+1)} + \nabla u_\star(w_\star^{\varepsilon,(n+1)})$ in (4.13) and using that $\boldsymbol{D}$ is uniformly positive definite with constant larger than or equal to $\mathrm{d}_{\mathrm{upd}}$, we obtain

$$\mathrm{d}_{\mathrm{upd}} \operatorname*{ess\,inf}_{\boldsymbol{x}\in\Omega} s_\star''(u_\star(w_\star^{\varepsilon,(n+1)}(\boldsymbol{x}))) \|\boldsymbol{\sigma}_\star^{\varepsilon,(n+1)} + \nabla u_\star(w_\star^{\varepsilon,(n+1)})\|_{L^2(\Omega)^d}^2 = 0.$$

Recalling that $\operatorname{ess\,inf}_{\boldsymbol{x}\in\Omega} s_p''(u_p(w_p^{\varepsilon,(n+1)}(\boldsymbol{x}))) \geq 4\mathcal{E}_p^{-1}$ and $\operatorname{ess\,inf}_{\boldsymbol{x}\in\Omega} s_q''(u_q(w_q^{\varepsilon,(n+1)}(\boldsymbol{x}))) = \operatorname{ess\,inf}_{\boldsymbol{y}\in\mathcal{K}_q} s_q''(u_q(\boldsymbol{y})) > 0$, we deduce that $\boldsymbol{\sigma}_\star^{\varepsilon,(n+1)} = -\nabla u_\star(w_\star^{\varepsilon,(n+1)})$ almost everywhere in Ω, as desired.

For any $\psi \in H^2(\Omega)$, let $\{\psi_m\}_{m\in\mathbb{N}}$ be a sequence such that $\psi_m \in \mathcal{W}^2(\mathcal{T}_{h_m}) \cap H^1(\Omega)$ for $m \in \mathbb{N}$, and $\psi_m \to \psi$ strongly in $H^1(\Omega)$. Then, combining Lemma 4.1, part *iii)* with the convergences in (4.4), (4.12a), and (4.8), as well as the fact that $[\![\psi_m]\!]_{\mathsf{N}} = 0$, we obtain that the pair $(w_p^{\varepsilon,(n+1)}, w_q^{\varepsilon,(n+1)})$ solves the semidiscrete-in-time formulation (4.5).

Entropy stability. The entropy stability estimate in (4.6) can be proven analogously to that in Theorem 3.4, also using (2.12). □

4.2 Convergence to a weak solution of the continuous problem

We now consider the semidiscrete-in-time limit problem (4.5), which admits a solution $(w_p^{\varepsilon,(n+1)}, w_q^{\varepsilon,(n+1)})$; see Theorem 4.4. For the sake of simplicity, we assume that $\mathcal{T}_\tau$ is a uniform partition of $(0,T)$ and that $\varepsilon \leq 1$. We prove that, as $(\varepsilon,\tau) \to (0,0)$, any sequence $\{(w_p^{\varepsilon,(n+1)}, w_q^{\varepsilon,(n+1)})\}_{(\varepsilon,\tau)}$ of such solutions converges (up to a subsequence) to a weak solution of (2.1) satisfying the physical bounds (2.4). The precise notion of weak solution is specified in Theorem 4.3 below.

Based on the sequence of functions $\{(w_p^{\varepsilon,(n+1)}, w_q^{\varepsilon,(n+1)})\}_{(\varepsilon,\tau)}$ at the discrete times $\{t_n\}_{n=0}^{N_t}$, we conveniently introduce the piecewise constant functions in time $w_p^{\varepsilon,(\tau)} : Q_T \to \mathbb{R}$ and $w_q^{\varepsilon,(\tau)} : Q_T \to \mathbb{R}$, defined on the whole space–time domain Q_T, as follows:

$$\begin{aligned} w_p^{\varepsilon,(\tau)}(\cdot,t) &= w_p^{\varepsilon,(n)}(\cdot) && \text{for all } t \in (t_{n-1}, t_n] \text{ with } n \in \{1,\ldots,N_t\}, \\ w_q^{\varepsilon,(\tau)}(\cdot,t) &= w_q^{\varepsilon,(n)}(\cdot) && \text{for all } t \in (t_{n-1}, t_n] \text{ with } n \in \{1,\ldots,N_t\} \end{aligned}$$

We further use the notation $p^{\varepsilon,(\tau)} = u_p(w_p^{\varepsilon,(\tau)}) : Q_T \to (0,\mathcal{E}_p)$ and $q^{\varepsilon,(\tau)} = u_q(w_q^{\varepsilon,(\tau)}) : Q_T \to (0,\infty)$, and define the discrete derivatives

$$\begin{aligned} \partial_\tau p^{\varepsilon,(\tau)}(\cdot,t) &= \frac{1}{\tau}\big(p^{\varepsilon,(n)}(\cdot) - p^{\varepsilon,(n-1)}(\cdot)\big) && \text{for all } t \in (t_{n-1}, t_n] \text{ with } n \in \{1,\ldots,N_t\}, \\ \partial_\tau q^{\varepsilon,(\tau)}(\cdot,t) &= \frac{1}{\tau}\big(q^{\varepsilon,(n)}(\cdot) - q^{\varepsilon,(n-1)}(\cdot)\big) && \text{for all } t \in (t_{n-1}, t_n] \text{ with } n \in \{1,\ldots,N_t\}, \end{aligned}$$

where $p^{\varepsilon,(0)} := p_0$ and $q^{\varepsilon,(0)} := q_0$.

Theorem 4.3 (Convergence as $(\varepsilon,\tau) \to (0,0)$)**.** *Assume that $\tau < 1/(2C_f)$, and that the initial conditions p_0 and q_0 satisfy (2.3). Let $r = 2 + 4/d$, $\mu = (d+2)/(d+1)$, and $\mu' = \mu/(\mu-1)$. Then, there exists a pair (p,q), with*

$$\begin{aligned} p &\in H^1(0,T;H^2(\Omega)') \cap L^2(0,T;H^1(\Omega)) \cap L^\nu(Q_T) && \textit{for all } \nu \in [1,\infty), \\ q &\in W^{1,\mu}(0,T;W^{2,\mu'}(\Omega)') \cap L^\mu(0,T;W^{1,\mu}(\Omega)) \cap L^\omega(Q_T) && \textit{for all } \omega \in [1,r/2), \end{aligned}$$

such that, as $(\varepsilon,\tau)\to(0,0)$, up to subsequences that are not relabeled, the sequence $\{(w_p^{\varepsilon,(\tau)}, w_q^{\varepsilon,(\tau)})\}_{(\varepsilon,\tau)}$ of space–time reconstructions of any sequence of solutions $\{(w_p^{\varepsilon,(n+1)}, w_q^{\varepsilon,(n+1)})\}_{(\varepsilon,\tau)}$ to the semidiscrete-in-time formulation (4.5) *satisfies*

$$
\begin{aligned}
\sqrt{\varepsilon} w_\star^{\varepsilon,(\tau)} &\rightharpoonup 0 && \textit{weakly in } L^2(Q_T) \textit{ for } \star = p,q, && \text{(4.14a)}\\
\sqrt{\varepsilon}\nabla w_\star^{\varepsilon,(\tau)} &\rightharpoonup 0 && \textit{weakly in } L^2(Q_T)^d \textit{ for } \star = p,q, && \text{(4.14b)}\\
\sqrt{\varepsilon}\mathcal{H} w_\star^{\varepsilon,(\tau)} &\rightharpoonup 0 && \textit{weakly in } L^2(Q_T)^{d\times d} \textit{ for } \star = p,q, && \text{(4.14c)}\\
p^{\varepsilon,(\tau)} &\to p && \textit{strongly in } L^\nu(Q_T) \textit{ for all } \nu\in[1,\infty) \textit{ and a.e. in } Q_T, && \text{(4.14d)}\\
\boldsymbol{D}\nabla p^{\varepsilon,(\tau)} &\rightharpoonup \boldsymbol{D}\nabla p && \textit{weakly in } L^2(Q_T)^d, && \text{(4.14e)}\\
\partial_\tau p^{\varepsilon,(\tau)} &\rightharpoonup \partial_t p && \textit{weakly in } L^2(0,T;H^2(\Omega)'), && \text{(4.14f)}\\
q^{\varepsilon,(\tau)} &\to q && \textit{strongly in } L^\omega(Q_T) \textit{ for all } \omega\in[1,r/2) \textit{ and a.e. in } Q_T, && \text{(4.14g)}\\
\boldsymbol{D}\nabla q^{\varepsilon,(\tau)} &\rightharpoonup \boldsymbol{D}\nabla q && \textit{weakly in } L^\mu(Q_T)^d, && \text{(4.14h)}\\
\partial_\tau q &\rightharpoonup \partial_t q && \textit{weakly in } L^\mu(0,T;W^{2,\mu'}(\Omega)'), && \text{(4.14i)}\\
f_\star(p^{\varepsilon,(\tau)}, q^{\varepsilon,(\tau)}) &\rightharpoonup f_\star(p,q) && \textit{weakly in } L^{r/2}(Q_T) \textit{ for } \star = p,q. && \text{(4.14j)}
\end{aligned}
$$

Moreover, the pair (p,q) solves

$$
\begin{aligned}
\int_0^T \langle \partial_t p, \psi_p\rangle_{H^2(\Omega)'\times H^2(\Omega)}\,\mathrm{d}t + \int_0^T\int_\Omega \boldsymbol{D}\nabla p\cdot\nabla\psi_p\,\mathrm{d}\boldsymbol{x}\,\mathrm{d}t \\
= \int_0^T\int_\Omega f_p(p,q)\psi_p\,\mathrm{d}\boldsymbol{x}\,\mathrm{d}t \qquad \forall \psi_p\in L^2(0,T;H^2(\Omega)), \quad \text{(4.15a)}\\
\int_0^T \langle \partial_t q, \psi_q\rangle_{W^{2,\mu'}(\Omega)'\times W^{2,\mu'}(\Omega)}\,\mathrm{d}t + \int_0^T\int_\Omega \boldsymbol{D}\nabla q\cdot\nabla\psi_q\,\mathrm{d}\boldsymbol{x}\,\mathrm{d}t \\
= \int_0^T\int_\Omega f_q(p,q)\psi_q\,\mathrm{d}\boldsymbol{x}\,\mathrm{d}t \qquad \forall \psi_q\in L^{\mu'}(0,T;W^{2,\mu'}(\Omega)). \quad \text{(4.15b)}
\end{aligned}
$$

Proof. We first observe that, from the entropy stability estimate (4.6) , it follows that, for any $t\in(0,T]$,

$$
\begin{aligned}
\varepsilon\sum_{\star=p,q}\|w_\star^{\varepsilon,(\tau)}\|^2_{L^2(0,t;H^2(\Omega))} + 4\mathcal{E}_p^{-1}\mathrm{d}_{\mathrm{upd}}\|\nabla p^{\varepsilon,(\tau)}\|^2_{L^2(0,t;L^2(\Omega)^d)} + 4\mathcal{E}_q^{-1}\mathrm{d}_{\mathrm{upd}}\|\nabla\sqrt{q^{\varepsilon,(\tau)}}\|^2_{L^2(0,t;L^2(\Omega)^d)} \\
+ \int_\Omega s_p(p^{\varepsilon,(\tau)}(\cdot,t))\,\mathrm{d}\boldsymbol{x} + \int_\Omega s_q(q^{\varepsilon,(\tau)}(\cdot,t))\,\mathrm{d}\boldsymbol{x} \le \int_\Omega s_p(p_0)\,\mathrm{d}\boldsymbol{x} + \int_\Omega s_q(q_0)\,\mathrm{d}\boldsymbol{x} + C_f T\left(\mathcal{E}_q|\Omega| + C^*\right). \quad \text{(4.16)}
\end{aligned}
$$

We point out that the norm in $L^2(0,t;H^2(\Omega))$ appearing in (4.16) is defined as

$$
\|w\|^2_{L^2(0,t;H^2(\Omega))} = \|w\|^2_{L^2(0,t;L^2(\Omega))} + \|\nabla w\|^2_{L^2(0,t;L^2(\Omega)^d)} + \|\mathcal{H}w\|^2_{L^2(0,t;L^2(\Omega)^{d\times d})}.
$$

For $\star = p,q$, estimate (4.16) implies that

$$
\sqrt{\varepsilon}\|w_\star^{\varepsilon,(\tau)}\|_{L^2(0,T;H^2(\Omega))} \text{ is uniformly bounded with respect to } \tau \text{ and } \varepsilon, \tag{4.17}
$$

which leads to (4.14a), (4.14b), and (4.14c).

For the proofs of the limits involving $p^{\varepsilon,(\tau)}$, we proceed along the lines of [23, Thm. 2]. The definition of $p^{\varepsilon,(\tau)}$ as $p^{\varepsilon,(\tau)} = u_p(w_p^{\varepsilon,(\tau)})$, and the entropy stability estimate (4.16) imply that

$$
\|p^{\varepsilon,(\tau)}\|_{L^\infty(Q_T)},\ \|\nabla p^{\varepsilon,(\tau)}\|_{L^2(Q_T)^d}, \text{ and } \|\nabla\sqrt{q^{\varepsilon,(\tau)}}\|_{L^2(Q_T)^d} \text{ are uniformly bounded with respect to } \tau \text{ and } \varepsilon. \tag{4.18}
$$

As for $q^{\varepsilon,(\tau)}$, we use the inequality $s_q(q)\ge q - 2\mathcal{E}_q$ for all $q>0$ to obtain

$$
\int_\Omega q^{\varepsilon,(\tau)}(\cdot,t)\,\mathrm{d}\boldsymbol{x} \le \int_\Omega s_q(q^{\varepsilon,(\tau)}(\cdot,t)) + 2\mathcal{E}_q|\Omega| \qquad \forall t\in(0,T], \tag{4.19}
$$

which implies that

$$\|q^{\varepsilon,(\tau)}\|_{L^\infty(0,T;L^1(\Omega))} \text{ is uniformly bounded with respect to } \varepsilon \text{ and } \tau. \tag{4.20}$$

Denote by $\Pi^{(\tau)}$ the $L^2(0,T)$-orthogonal projection into $\mathbb{P}^0(\mathcal{T}_\tau)$. From the semidiscrete-in-time formulation (4.5) with $\star = p$ and the Hölder inequality, for all $\psi \in L^2(0,T;H^2(\Omega))$, we have

$$\begin{aligned}
\int_0^T \int_\Omega \partial_\tau p^{\varepsilon,(\tau)} \psi \, \mathrm{d}\boldsymbol{x} \, \mathrm{d}t &= \int_0^T \int_\Omega \partial_\tau p^{\varepsilon,(\tau)} \Pi^{(\tau)} \psi \, \mathrm{d}\boldsymbol{x} \, \mathrm{d}t \\
&\leq \varepsilon \|w_p^{\varepsilon,(\tau)}\|_{L^2(0,T;H^2(\Omega))} \|\Pi^{(\tau)}\psi\|_{L^2(0,T;H^2(\Omega))} \\
&\quad + \|\boldsymbol{D}\|_{L^\infty(\Omega)^{d\times d}} \|\nabla p^{\varepsilon,(\tau)}\|_{L^2(Q_T)^d} \|\Pi^{(\tau)} \nabla \psi\|_{L^2(Q_T)^d} \\
&\quad + \int_0^T \int_\Omega |f_p(p^{\varepsilon,(\tau)}, q^{\varepsilon,(\tau)})| \, |\Pi^{(\tau)}\psi| \, \mathrm{d}\boldsymbol{x} \, \mathrm{d}t.
\end{aligned} \tag{4.21}$$

The last term on the right-hand side of (4.21) can be estimated as follows:

$$\begin{aligned}
\int_0^T \int_\Omega |f_p(p^{\varepsilon,(\tau)}, q^{\varepsilon,(\tau)})| |\Pi^{(\tau)}\psi| \, \mathrm{d}\boldsymbol{x} \, \mathrm{d}t &\leq (\mathcal{E}_p \lambda_p + \kappa_p) \|\Pi^{(\tau)}\psi\|_{L^1(Q_T)} + \mathcal{E}_p \mu_{pq} \|q\|_{L^\infty(0,T;L^1(\Omega))} \|\Pi^{(\tau)}\psi\|_{L^1(0,T;L^\infty(\Omega))} \\
&\lesssim (\mathcal{E}_p \lambda_p + \kappa_p) \|\psi\|_{L^1(Q_T)} + \mathcal{E}_p \mu_{pq} \|q\|_{L^\infty(0,T;L^1(\Omega))} \|\psi\|_{L^1(0,T;L^\infty(\Omega))} \\
&\lesssim \|\psi\|_{L^2(0,T;H^2(\Omega))},
\end{aligned} \tag{4.22}$$

where the hidden constants are independent of ε, τ, and ψ, and, in the second step, we have used the stability properties of $\Pi^{(\tau)}$ (see [19, Thm. 18.16(ii)]). Combining (4.22) with (4.21), taking into account that $\varepsilon \|w_p^{\varepsilon,(\tau)}\|_{L^2(0,T;H^2(\Omega))}$ and $\|\nabla p^{\varepsilon,(\tau)}\|_{L^2(Q_T)^d}$ are uniformly bounded with respect to τ and ε, see (4.17) and (4.18), we deduce that

$$\|\partial_\tau p^{\varepsilon,(\tau)}\|_{L^2(0,T;H^2(\Omega)')} \text{ is uniformly bounded with respect to } \tau \text{ and } \varepsilon.$$

We can then apply the Aubin lemma in the version in [18, Thm. 1] with $p = 2$, $r = 1$, $X = H^1(\Omega)$, $B = L^2(\Omega)$, and $Y = H^2(\Omega)'$ (in the notation of [18, Thm. 1]). Consequently, as in the proof of [23, Thm. 2], up to a subsequence that is not relabeled, we obtain (4.14d), (4.14e), and (4.14f).

We now turn to the limits involving $q^{\varepsilon,(\tau)}$. Let $r = 2 + 4/d$ and $\theta r = 2$. Using the Gagliardo–Nirenberg inequality (see the version in [31, Thm. 1.24]) and the Hölder inequality, we get

$$\begin{aligned}
\|\sqrt{q^{\varepsilon,(\tau)}}\|_{L^r(Q_T)}^r &\leq C_{\mathrm{GN}} \int_0^T \|\sqrt{q^{\varepsilon,(\tau)}}\|_{L^2(\Omega)}^{r(1-\theta)} \|\sqrt{q^{\varepsilon,(\tau)}}\|_{H^1(\Omega)}^{r\theta} \, \mathrm{d}t \\
&\leq C_{\mathrm{GN}} \|\sqrt{q^{\varepsilon,(\tau)}}\|_{L^\infty(0,T;L^2(\Omega))}^{4/d} \|\sqrt{q^{\varepsilon,(\tau)}}\|_{L^2(0,T;H^1(\Omega))}^2.
\end{aligned}$$

Therefore, owing to (4.20) and (4.18), for $r = 4$ if $d = 2$, and $r = 10/3$ if $d = 3$,

$$\|\sqrt{q^{\varepsilon,(\tau)}}\|_{L^r(Q_T)} \text{ and } \|q^{\varepsilon,(\tau)}\|_{L^{r/2}(Q_T)} \text{ are uniformly bounded with respect to } \varepsilon \text{ and } \tau. \tag{4.23}$$

Moreover, we define $\mu := (d+2)/(d+1)$. Using the identity $\nabla q = 2\sqrt{q}\,\nabla\sqrt{q}$ and the Hölder inequality[2], we obtain

$$\begin{aligned}
\|\nabla q^{\varepsilon,(\tau)}\|_{L^\mu(Q_T)^d}^\mu = 2^\mu \|\sqrt{q^{\varepsilon,(\tau)}}\,\nabla\sqrt{q^{\varepsilon,(\tau)}}\|_{L^\mu(Q_T)^d}^\mu &\leq 2^\mu \int_{Q_T} \big(q^{\varepsilon,(\tau)}\big)^{\mu/2} |\nabla \sqrt{q^{\varepsilon,(\tau)}}|^\mu \, \mathrm{d}V \\
&\leq 2^\mu \Big(\int_{Q_T} \big(q^{\varepsilon,(\tau)}\big)^{r/2} \, \mathrm{d}V \Big)^{\mu/r} \Big(\int_{Q_T} |\nabla\sqrt{q^{\varepsilon,(\tau)}}|^2 \, \mathrm{d}V \Big)^{\frac{r-\mu}{r}} \\
&= 2^\mu \|q^{\varepsilon,(\tau)}\|_{L^{r/2}(Q_T)}^{\mu/2} \|\nabla\sqrt{q^{\varepsilon,(\tau)}}\|_{L^2(Q_T)^d}^{\frac{2(r-\mu)}{r}},
\end{aligned}$$

which implies that

$$\|\nabla q^{\varepsilon,(\tau)}\|_{L^\mu(Q_T)^d} \text{ is uniformly bounded with respect to } \tau \text{ and } \varepsilon, \tag{4.24}$$

[2] $\|fg\|_1 \leq \|f\|_p \|g\|_q$ with $p = r/\mu$, $q = r/(r-\mu)$, noting that $(r-\mu) = \frac{(d+2)^2}{d(d+1)} > 0$.

with $\mu = 4/3$ for $d = 2$, and $\mu = 5/4$ for $d = 3$.

Proceeding similarly as for (4.21), for all $\psi \in L^{\mu'}(0,T; W^{2,\mu'}(\Omega))$, we have

$$\begin{aligned}\int_0^T \int_\Omega \partial_\tau q^{\varepsilon,(\tau)} \psi \,\mathrm{d}\boldsymbol{x}\,\mathrm{d}t &= \int_0^T \int_\Omega \partial_\tau q^{\varepsilon,(\tau)} \Pi^{(\tau)} \psi \,\mathrm{d}\boldsymbol{x}\,\mathrm{d}t \\ &\lesssim \varepsilon \|w_q^{\varepsilon,(\tau)}\|_{L^2(0,T;H^2(\Omega))} \|\psi\|_{L^2(0,T;H^2(\Omega))} \\ &\quad + \|\boldsymbol{D}\|_{L^\infty(\Omega)^{d\times d}} \|\nabla q^{\varepsilon,(\tau)}\|_{L^\mu(Q_T)^d} \|\nabla\psi\|_{L^{\mu'}(Q_T)^d} \\ &\quad + \|f_q(p^{\varepsilon,(\tau)}, q^{\varepsilon,(\tau)})\|_{L^{r/2}(Q_T)} \|\psi\|_{L^{r/(r-2)}(Q_T)},\end{aligned} \tag{4.25}$$

where $\mu' = \mu/(\mu - 1) \geq 2$ (namely, $\mu' = 4$ if $d = 2$, and $\mu' = 5$ if $d = 3$) and $r/(r-2) \leq \mu'$. Since $\|p^{\varepsilon,(\tau)}\|_{L^\infty(Q_T)}$ is bounded uniformly with respect to ε and τ (see (4.18)), and the nonlinear terms $f_p(p,q)$ and $f_q(p,q)$ depend linearly on q, we also have that

$$\|f_p(p^{\varepsilon,(\tau)}, q^{\varepsilon,(\tau)})\|_{L^{r/2}(Q_T)} \text{ and } \|f_q(p^{\varepsilon,(\tau)}, q^{\varepsilon,(\tau)})\|_{L^{r/2}(Q_T)} \text{ are uniformly bounded with respect to } \varepsilon \text{ and } \tau. \tag{4.26}$$

Then, from (4.25), together with (4.17), (4.24), and (4.26), we conclude that

$$\|\partial_\tau q^{\varepsilon,(\tau)}\|_{L^\mu(0,T;W^{2,\mu'}(\Omega)')} \text{ is uniformly bounded with respect to } \varepsilon \text{ and } \tau. \tag{4.27}$$

By the Rellich–Kondrachov theorem, the space $W^{1,\mu}(\Omega)$ is compactly embedded in $L^\mu(\Omega)$. Since $L^\mu(\Omega)$ is continuously embedded in $W^{2,\mu'}(\Omega)'$, we can use again the Aubin lemma in the version in [18, Thm. 1] now with $p = \mu$, $r = 1$, $X = W^{1,\mu}(\Omega)$, $B = L^\mu(\Omega)$, and $Y = W^{2,\mu'}(\Omega)'$ (in the notation of [18, Thm. 1]), to conclude that there exists $q \in L^\mu(Q_T)$ such that, as $(\varepsilon, \tau) \to (0,0)$,

$$q^{\varepsilon,(\tau)} \to q \quad \text{strongly in } L^\mu(Q_T),$$

and, due to [9, Thm. 4.9], up to a subsequence that is not relabeled, it also converges a.e. in Q_T. This, together with the uniform bound in (4.23) and [12, Lemma 5], leads to (4.14g). Furthermore, by weak compactness, the uniform bounds in (4.24) and (4.27) imply (4.14h) and (4.14i). The uniform boundedness in (4.26), the continuity of $f_p(\cdot,\cdot)$ and $f_q(\cdot,\cdot)$, and the fact that, up to subsequences, $p^{\varepsilon,(\tau)} \to p$ and $q^{\varepsilon,(\tau)} \to q$ a.e. in Q_T give (4.14j). This completes the proof of (4.14a)–(4.14j).

Finally, the fact that (p,q) solves (4.15) follows by taking suitable test functions and passing to the limit on each term of (4.5), and the proof is complete. □

Remark 4.4. *As a byproduct of Theorem 4.3, we have that problem* (2.1) *admits a weak solution* (p,q) *in the sense of* (4.15). ■

5 Numerical results

In this section, we present some numerical tests on two-dimensional space domains to assess the accuracy of the proposed structure-preserving LDG method. In Section 5.1, we discuss the convergence properties in space for a smooth exact solution that is linear in time. Then, in Section 5.2, we study the accuracy of the method in simulating a traveling-wave solution.

All numerical simulations in this section are performed with the `lymph` library [2], implementing DG methods. We employ structured simplicial meshes with element diameter h for the space domain, and uniform time steps τ. Moreover, the weight parameter γ_F is set to $1/2$ for all internal facets. For the Newton iterations, given a small tolerance $\mathsf{tol} > 0$, we adopt the following stopping criterion:

$$\min\left\{\sqrt{\|w_{p,h}^{k+1} - w_{p,h}^k\|_{L^2(\Omega)}^2 + \|w_{q,h}^{k+1} - w_{q,h}^k\|_{L^2(\Omega)}^2},\ |\mathsf{res}_{k+1}^p + \mathsf{res}_{k+1}^q|\right\} \leq \mathsf{tol}, \tag{5.1}$$

where $\mathsf{res}_{k+1}^\star$ (with $\star = p, q$) is the residual of the algebraic system (2.24) for the approximation of $(w_{p,h}^{(n+1)}, w_{q,h}^{(n+1)})$ at the $(k+1)$th Newton's iteration. In the convergence tests reported below, we measure the following $L^2(\Omega)$ errors at the final time for the concentrations and the fluxes, respectively, of the two variables of the system:

$$E_\star := \|\star(\cdot,T) - u(w_{\star,h}^{(N)})\|_{L^2(\Omega)} \quad \text{and} \quad E_{\boldsymbol{\sigma}_\star} := \|\nabla\star(\cdot,T) + \boldsymbol{\sigma}_{\star,h}^{(N)}\|_{L^2(\Omega)^d} \quad \text{with } \star = p, q.$$

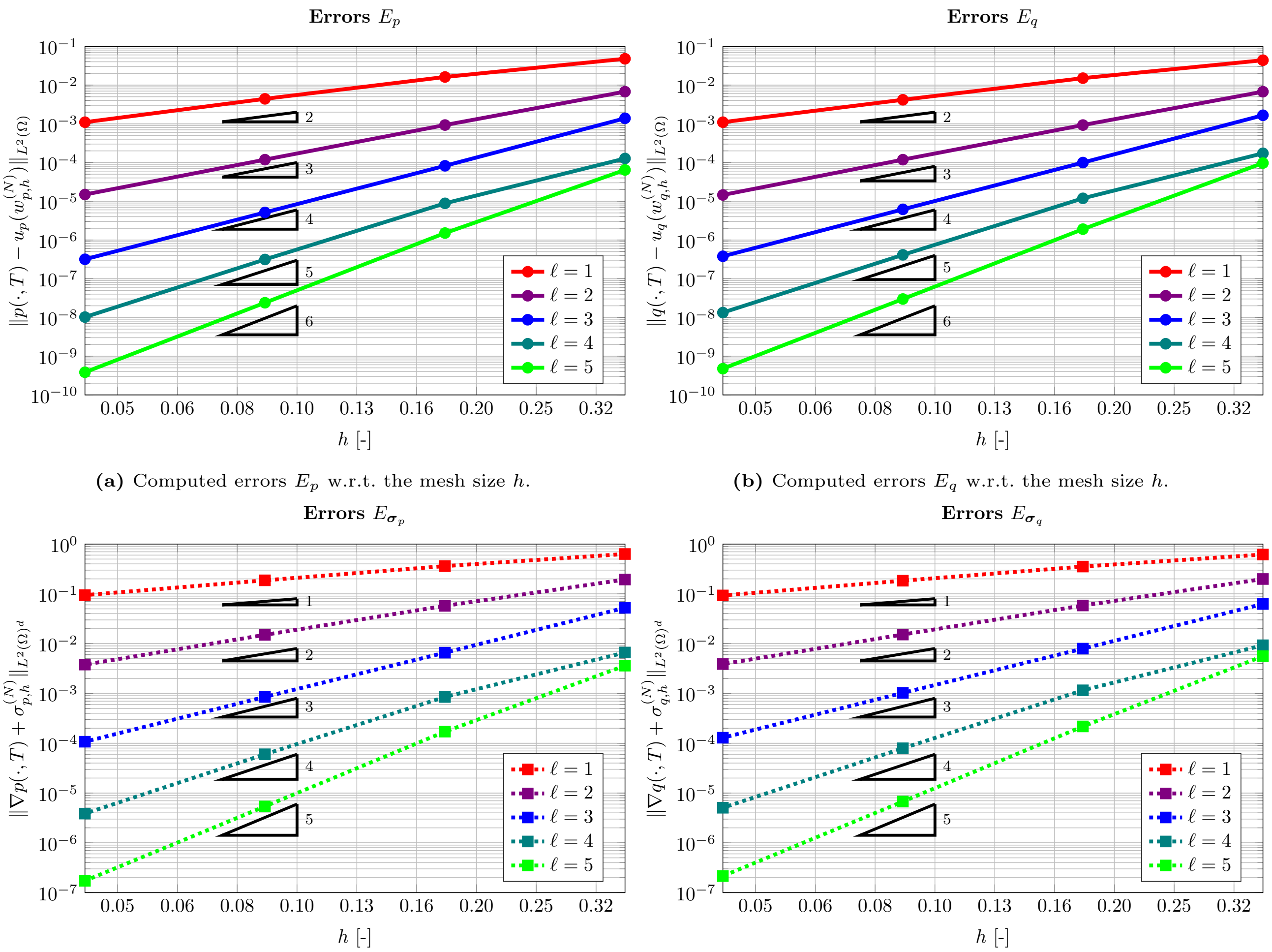

(a) Computed errors E_p w.r.t. the mesh size h.

(b) Computed errors E_q w.r.t. the mesh size h.

(c) Computed errors $E_{\boldsymbol{\sigma}_p}$ w.r.t. the mesh size h.

(d) Computed errors $E_{\boldsymbol{\sigma}_q}$ w.r.t. the mesh size h.

Figure 1: Test case 1: computed errors and convergence rates w.r.t. the mesh size h.

5.1 Test case 1: Convergence analysis

For the numerical tests in this section, we consider the space domain $\Omega = (0,1)^2$ and homogeneous Neumann boundary conditions on the boundary $\Gamma \times (0,T)$. For the nonlinear Newton solver, we adopt the stopping criterion (5.1) with $\mathsf{tol} = 10^{-10}$. The penalty parameter ε is set to 0 (see Remark 2.7). For both species, we select the diffusion tensor $\mathbf{D} = \mathbb{I}_2$, where $\mathbb{I}_2$ represents the identity matrix of size 2. Concerning the reaction coefficients, we fix $\lambda_p = \lambda_q = 1$ and the conversion term $\mu_{pq} = 0.5$.

For this test case, instead of using a constant production rate κ_p for p, we allow nonconstant source terms in both equations of (2.1) in order to construct a manufactured solution that is linear in time. This choice allows us to highlight the properties of the space discretization, neglecting the error due to the time integration scheme. Then, we set $\mathcal{E}_p = \mathcal{E}_q = 1$ in the change of variables (2.6), independently of the other parameters, since the choice of nonconstant functions on the right-hand side of both equations breaks the equilibrium structure of system (2.1). Thus, we consider system (2.1) with initial conditions and additional source terms on the two right-hand sides chosen so that the problem admits the following exact solution:

$$p(x,y,t) = q(x,y,t) = \frac{1}{4}\left(\cos(2\pi x)\cos(2\pi y) + 2\right)(1-t).$$

Choosing the same expression for p and q is useful for assessing the impact of the two different changes of variables, which take values over different ranges.

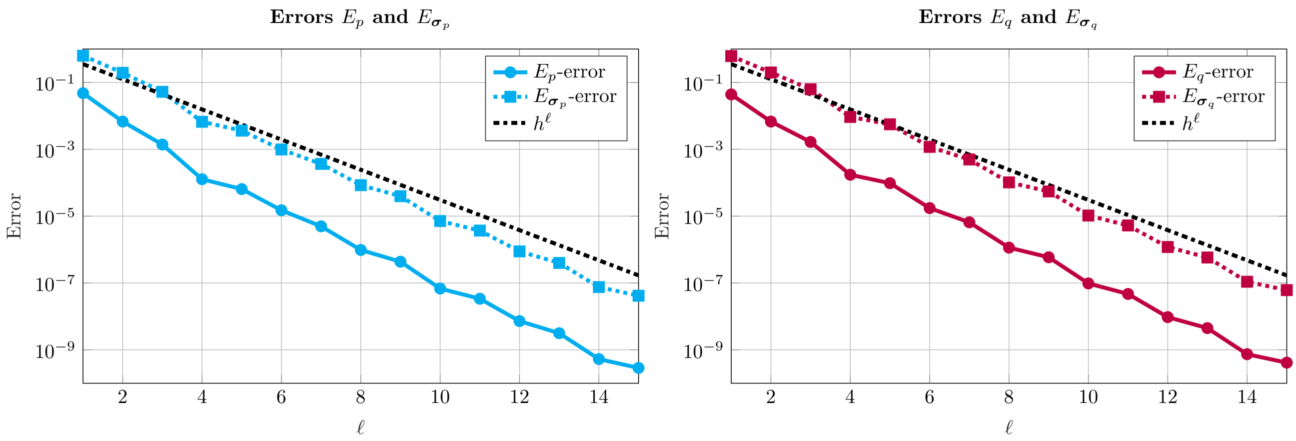

(a) Computed errors E_p and $E_{\boldsymbol{\sigma}_p}$ w.r.t. the polynomial degree ℓ.

(b) Computed errors E_q and $E_{\boldsymbol{\sigma}_q}$ w.r.t. the polynomial degree ℓ.

Figure 2: Test case 1: computed errors and convergence rates w.r.t. the polynomial degree ℓ.

Convergence with respect to the mesh size

We perform a convergence test keeping fixed the polynomial degree of the space approximation $\ell = 1, 2, 3, 4, 5$ and using, for each degree, different mesh refinements with number of elements $N_{\text{el}} = 32$, 128, 512, 2048. Concerning the time discretization, we take $\tau = 10^{-3}$ and a final time $T = 5 \times 10^{-2}$. In Figures 1a and 1b, we report the computed errors E_p and E_q for the primal variables p and q, respectively. Moreover, in Figures 1c and 1d, we report the computed errors $E_{\boldsymbol{\sigma}_p}$ and $E_{\boldsymbol{\sigma}_q}$ for the approximations of ∇p and ∇q, respectively. In all cases, the errors decrease with optimal convergence rates, namely, of order $\mathcal{O}(h^{\ell+1})$ for $E_\star$, and of order $\mathcal{O}(h^\ell)$ for $E_{\boldsymbol{\sigma}_\star}$.

Convergence with respect to the polynomial degree

Then, we develop a convergence analysis with respect to the polynomial degree ℓ. To do so, we consider the coarsest triangular mesh in space with 32 elements. The errors E_p and $E_{\boldsymbol{\sigma}_p}$ are reported in Figure 2a, and the errors E_q and $E_{\boldsymbol{\sigma}_q}$ are reported in Figure 2b. In all plots, we observe spectral convergence with respect to the polynomial degree ℓ, as expected since the solution is analytic.

5.2 Test case 2: Traveling-wave solution

In this section, we analyze the capabilities of our method for accurately simulating a traveling-wave solution, while respecting the physical bounds pointwise. For a positive constant d, we fix a constant, isotropic diffusion tensor $\boldsymbol{D} = \mathrm{d}\,\mathbb{I}_2$, as well as constant coefficients λ_p, λ_q, μ_{pq}, κ_p in the reaction terms. Then, we consider a solution to the equations of system (2.1) of the form

$$
\begin{aligned}
p(x, y, t) =& \psi_p(x - vt) = \psi_p(\xi), \\
q(x, y, t) =& \psi_q(x - vt) = \psi_q(\xi),
\end{aligned}
$$

where v is a wave speed depending on the physical parameters and defined by $v := 10\,\mathrm{d}$. If $x \in \mathbb{R}$ or $t \in \mathbb{R}$, then $\xi \in \mathbb{R}$. Substituting p and q in the two equations of (2.1), we obtain the following equivalent system of ordinary differential equations (ODEs):

$$
\begin{cases}
\mathrm{d}\psi_p''(\xi) + v\psi_p'(\xi) - \lambda_p\psi_p(\xi) - \mu_{pq}\psi_p(\xi)\psi_q(\xi) + \kappa_p = 0, & \xi \in \mathbb{R}, \\
\mathrm{d}\psi_q''(\xi) + v\psi_q'(\xi) - \lambda_q\psi_q(\xi) + \mu_{pq}\psi_p(\xi)\psi_q(\xi) = 0, & \xi \in \mathbb{R}.
\end{cases}
\tag{5.2}
$$

Under the additional assumptions $\lambda_q = \lambda_p$ and $\mathrm{d} = (\kappa_p\,\mu_{pq} - \lambda_p^2)/(24\lambda_p)$, it can be verified that system (5.2) admits the following solution:

$$\begin{aligned}
\psi_p(\xi) =& \frac{\lambda_p^2 + 3\kappa_p\mu_{pq} + (\lambda_p^2 - \kappa_p\mu_{pq})(\tanh(\xi)^2 - 2\tanh(\xi))}{4\lambda_p\mu_{pq}},\\
\psi_q(\xi) =& -\frac{(\lambda_p^2 - \kappa_p\mu_{pq})}{4\lambda_p\mu_{pq}}\,(1-\tanh(\xi))^2\,.
\end{aligned}$$

The functions ψ_p and ψ_q are positive for all $\xi \in \mathbb{R}$, under the assumption $\Upsilon_{pq} > 0$ already discussed in Section 2.1. They satisfy a homogeneous Neumann boundary condition at the limits $\xi \to \pm\infty$, which is equivalent to $x \to \pm\infty$ for each fixed value of $t \in (0,T)$. The homogeneous Neumann boundary condition is also satisfied in the y-direction, as p and q are both independent of y.

This solution respects the equilibria of system (2.1).[3] Indeed, considering the limit $t \to -\infty$ (or, equivalently, $\xi \to +\infty$) we find the *unstable* equilibrium solutions:

$$\lim_{\xi\to+\infty} \psi_p(\xi) = \frac{\kappa_p}{\lambda_p} = \mathcal{E}_p \qquad \text{and} \qquad \lim_{\xi\to+\infty} \psi_q(\xi) = 0.$$

Moreover, taking the limit $t \to +\infty$ (or, equivalently, $\xi \to -\infty$), we recover the *stable* equilibrium solutions:

$$\lim_{\xi\to-\infty} \psi_p(\xi) = \frac{\lambda_p}{\mu_{pq}} = \frac{\lambda_q}{\mu_{pq}} \qquad \text{and} \qquad \lim_{\xi\to-\infty} \psi_q(\xi) = \frac{\kappa_p\mu_{pq} - \lambda_p^2}{\lambda_p\mu_{pq}} = \frac{\kappa_p\mu_{pq} - \lambda_p\lambda_q}{\lambda_q\mu_{pq}} = \mathcal{E}_q.$$

For this test case, we consider a rectangular space domain $\Omega = (-10,10)\times(0,5)$, and the final time $T = 1$. We impose homogeneous Neumann boundary conditions not only at $y = 0$ and $y = 5$, but also at $x = -10$ and $x = 10$. Concerning the problem coefficients, we fix $\kappa_p = 0.1$, $\lambda_p = \lambda_q = 0.1$, and $\mu_{pq} = 1$, with corresponding diffusion coefficient $\mathrm{d} = 3.75 \times 10^{-2}$, velocity $v = 3.75 \times 10^{-1}$, and constant $C_f \approx 5.15$ for the bound in Proposition 3.1 on the reaction term.

Convergence with respect to the mesh size

We fix the penalty parameter $\varepsilon = 0$ again and analyze the convergence with respect to the mesh size h. For the space discretization, we adopt structured triangular meshes with $N_{\mathsf{el}} = 72, 288, 648, 1152$. We take as final time $T = 1$, and the step of the time discretization is set as $\tau \sim \mathcal{O}(h^{\ell+1})$, so as to equilibrate the errors in space and time.

In the first rows of Figures 3a and 3b, we report the numerical approximations $p_h^{(n)}$ and $q_h^{(n)}$, respectively, obtained with the mesh of 72 elements for different values of the polynomial degree $\ell = 1,...,5$. In the left column of both figures, we report the initial conditions $p_h^{(0)}$ and $q_h^{(0)}$ at time $t = 0$. In the second rows of Figures 3a and 3b, we report the associated approximation errors. We can observe that higher polynomial degrees result in a reduction of the projection error of the initial condition and of the approximation error at the final time. Moreover, we highlight that most of the error is spatially located near the wavefront, as expected. We recall that, in method (2.18), the initial conditions are imposed weakly, which slightly differs from the standard backward Euler time-stepping scheme.

To quantify the convergence properties of the discretization scheme, we perform an h-convergence analysis for $\ell = 1,...,4$. In Figures 4a and 4b, we report the errors E_p and E_q, respectively. Additionally, in Figures 4a and 4b, we report the errors $E_{\boldsymbol{\sigma}_p}$ and $E_{\boldsymbol{\sigma}_q}$. We can observe that the the errors $E_\star$ and $E_{\boldsymbol{\sigma}_\star}$ decrease with optimal convergence rates $\mathcal{O}(h^{\ell+1})$ and $\mathcal{O}(h^{\ell})$, respectively.

Comparison with an interior penalty DG method

As a final test, we compare the results obtained with our method against those of a non-structure-preserving method in the literature. In particular, we focus on the interior penalty DG (IPDG) method proposed in [3], which is able to approximate the analytical solution correctly only for a sufficiently refined space mesh or a high polynomial degree. To guarantee a fair comparison, we adopt an implicit Euler time-stepping scheme for the time discretization. In this simulation, we employ the structured mesh of 72 triangular elements of the previous test, and two time steps, $\tau = 0.10$ and $\tau = 0.25$.

[3]For $\Upsilon_{pq} > 0$, $(\mathcal{E}_p, 0)$ and $(\lambda_q/\mu_{pq}, \mathcal{E}_q)$ are admissible equilibria, the former unstable and the latter stable; see [15, §2.1].

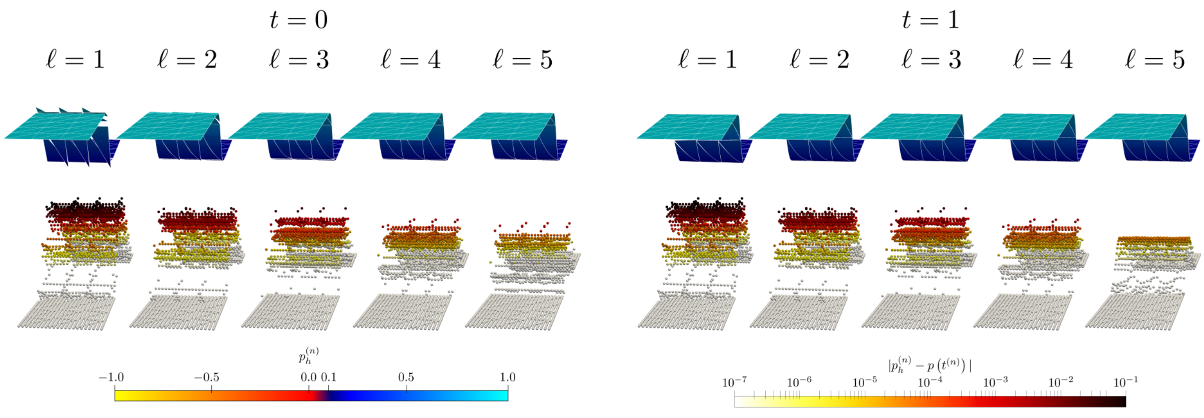

(a) Solutions (first row) with associated approximation errors (second row) for the variable p.

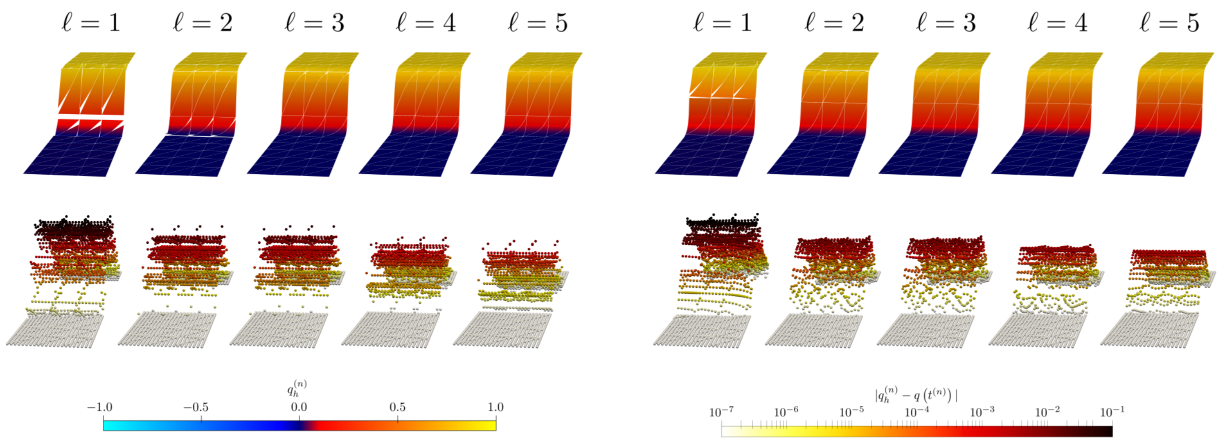

(b) Solutions (first row) with associated approximation errors (second row) for the variable q.

Figure 3: Test case 2: Initial conditions ($t = 0$) and solutions at $t = 1$ (first row) for different polynomial degrees $\ell = 1, ..., 5$ with associated approximation errors (second row) for the variables p (a) and q (b).

In Tables 1 and 2, we report the errors in the $L^2(\Omega)$ norm at the final time. The results obtained show that the method proposed in [3] approximates the exact solution accurately only for sufficiently high polynomial degrees. The two methods become comparable for higher-order approximations; however, our method can capture the solution more accurately and respect physical bounds, even with low polynomial degrees. Moreover, the IPDG method suffers from overshoots in the approximation of p, as well as undershoots in the approximation of q. Specifically, the numerical solution violates the bounds valid at the continuous level (see Equation (2.4)), whereas these bounds are enforced strongly in our LDG formulation. It can be noted that these undershoots can be reduced with a higher space resolution, while they are not monotonically decreasing with the time step τ, even if the $L^2(\Omega)$ errors are smaller.

5.3 Test case 3: simulations of different stable equilibrium behaviors

As discussed in [15], for $\Upsilon_{pq} > 0$, system (2.1) admits a stable equilibrium $(p_E, q_E) := (\lambda_q/\mu_{pq}, \mathcal{E}_q)$. Depending on the problem coefficients, the approach of the solution to the equilibrium (p_E, q_E) could be either monotonic (stable *node*) or oscillatory (stable *focus*). The goal of this section is to show the ability of our method to predict the correct asymptotic behavior of the equilibrium in both cases.

The analytical study of the bifurcation, which separates the two behaviors, is feasible only in the case of a one-dimensional propagating front and isotropic, constant diffusion $\boldsymbol{D} = \mathrm{d}\,\mathbb{I}_2$. This analysis for system (2.1) can be found in [24]. Following the steps used in [24, §6] for two populations with equal and constant isotropic diffusion

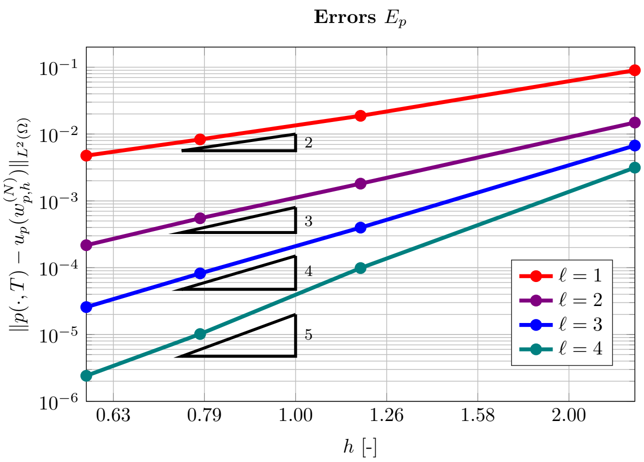

(a) Computed errors E_p w.r.t. the mesh size h.

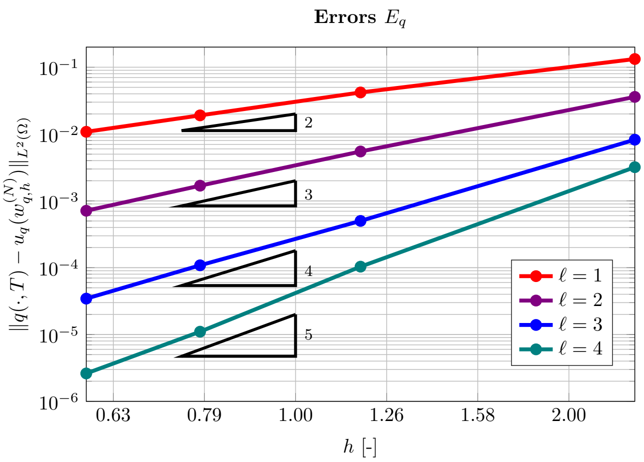

(b) Computed errors E_q w.r.t. the mesh size h.

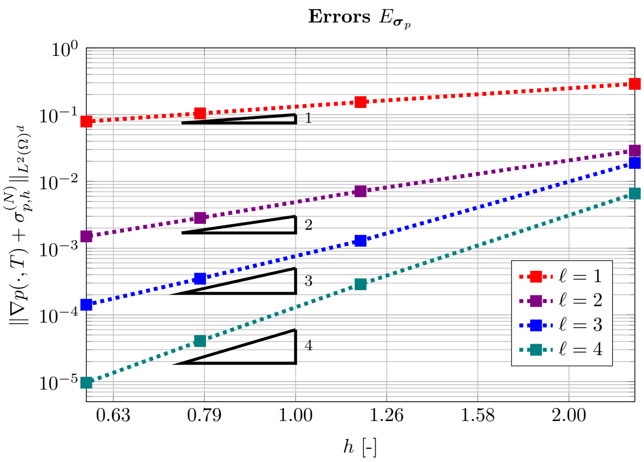

(c) Computed errors E_{σ_p} w.r.t. the mesh size h.

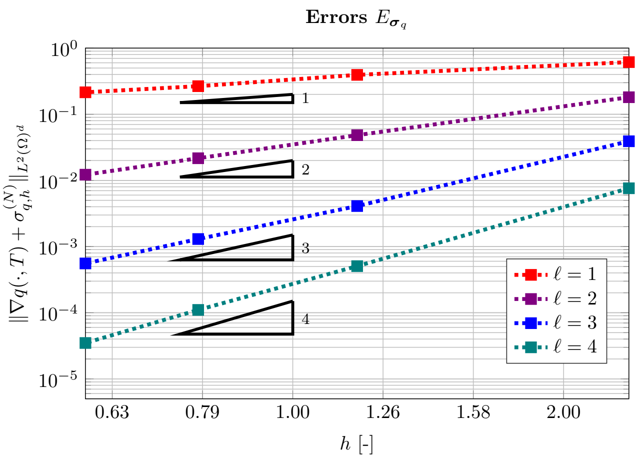

(d) Computed errors E_{σ_q} w.r.t. the mesh size h.

Figure 4: Test case 1: computed errors and convergence rates w.r.t. the polynomial degree ℓ.

d and imposing the absence of imaginary parts of the Fourier modes, we can observe that the equilibrium is a stable node if and only if

$$4\lambda_p\lambda_q^3 - 4\kappa_p\lambda_q^2\mu_{pq} + \kappa_p^2\mu_{pq}^2 \geq 0, \tag{5.3}$$

independently of the diffusion coefficients applied.

For both simulated tests, we consider a rectangular space domain $\Omega = (-10, 10) \times (0, 5)$, and the final time $T = 25$. We impose homogeneous Neumann boundary conditions on $\Gamma \times (0, T)$. Concerning the discretization, we fix the parameter $\varepsilon = 0$, and we adopt a structured triangular mesh with $N_{\text{el}} = 288$ and polynomial degree $\ell = 2$. The step of the time discretization is fixed as $\tau = 5 \times 10^{-3}$. As initial conditions, we consider the following analytical continuous functions:

$$p_0(x, y) = \frac{39}{40}\mathcal{E}_p, \qquad q_0(x, y) = \frac{\mathcal{E}_q}{2}\, e^{-x^2}.$$

To test the two distinct behaviors of the equilibrium, we vary the reaction parameters in the simulations. First, we fix $\kappa_p = 4$, $\lambda_p = 0.2$, $\lambda_q = 4.5$, and $\mu_{pq} = 1$ to obtain a stable focus. These parameters are associated with an unstable equilibrium $(\mathcal{E}_p, 0) = (20, 0)$ and a stable one $(\lambda_q/\mu_{pq}, \mathcal{E}_q) \simeq (4.5, 0.689)$. Moreover, we consider $\kappa_p = 0.1$, $\lambda_p = \lambda_q = 0.1$, and $\mu_{pq} = 1$ to simulate a stable node. With these parameters, the equilibrium $(\mathcal{E}_p, 0) = (1, 0)$ is unstable, whereas $(\lambda_q/\mu_{pq}, \mathcal{E}_q) = (0.1, 0.9)$ is stable.

In Figure 5, we report the results of the numerical simulation, together with the plane associated with the stable equilibrium constants. In the left panel, we report the results for the stable focus behavior, and it can be observed that the solution converges to the equilibrium at long times ($t = 25$), after exhibiting some damped oscillations around this value for both concentrations q and p. On the other hand, in the results on the right

Method	$\ell = 1$	$\ell = 2$	$\ell = 3$	$\ell = 4$	$\ell = 5$
$h \approx 2.3570$ and $\tau = 2.5 \times 10^{-1}$					
SP-LDG	2.66×10^{-1}	2.28×10^{-1}	2.35×10^{-1}	2.35×10^{-1}	2.35×10^{-1}
IPDG	9.71×10^{-1}	1.81×10^{-1}	1.80×10^{-1}	1.75×10^{-1}	1.74×10^{-1}
IPDG overshoot	$+1.34 \times 10^{-1}$	$+1.10 \times 10^{-3}$	$+5.01 \times 10^{-4}$	$+1.05 \times 10^{-4}$	$+2.03 \times 10^{-7}$
$h \approx 2.3570$ and $\tau = 1.0 \times 10^{-1}$					
Method	$\ell = 1$	$\ell = 2$	$\ell = 3$	$\ell = 4$	$\ell = 5$
SP-LDG	2.23×10^{-1}	8.01×10^{-2}	8.61×10^{-2}	8.66×10^{-2}	8.65×10^{-2}
IPDG	$1.13 \times 10^{+0}$	8.99×10^{-2}	8.30×10^{-2}	7.73×10^{-2}	7.70×10^{-2}
IPDG overshoot	$+6.89 \times 10^{-1}$	$+7.90 \times 10^{-3}$	$+6.01 \times 10^{-4}$	$+1.83 \times 10^{-4}$	$+2.20 \times 10^{-6}$

Table 1: Computed errors in the $L^2(\Omega)$ norm of solution p at final time $T = 5$ with the structure-preserving LDG (SP-LDG) and IPDG [3] methods.

Method	$\ell = 1$	$\ell = 2$	$\ell = 3$	$\ell = 4$	$\ell = 5$
$h \approx 2.3570$ and $\tau = 2.5 \times 10^{-1}$					
SP-LDG	2.98×10^{-1}	2.28×10^{-1}	2.35×10^{-1}	2.35×10^{-1}	2.35×10^{-1}
IPDG	$1.02 \times 10^{+0}$	4.64×10^{-1}	4.64×10^{-1}	4.61×10^{-1}	4.61×10^{-1}
IPDG undershoot	-1.23×10^{-1}	-1.44×10^{-3}	-5.01×10^{-4}	-1.15×10^{-4}	-2.97×10^{-7}
$h \approx 2.3570$ and $\tau = 1.0 \times 10^{-1}$					
Method	$\ell = 1$	$\ell = 2$	$\ell = 3$	$\ell = 4$	$\ell = 5$
SP-LDG	2.67×10^{-1}	8.45×10^{-2}	8.62×10^{-2}	8.66×10^{-2}	8.65×10^{-2}
IPDG	$1.11 \times 10^{+0}$	2.17×10^{-1}	2.14×10^{-1}	2.10×10^{-1}	2.10×10^{-1}
IPDG undershoot	-6.32×10^{-1}	-7.70×10^{-3}	-5.18×10^{-4}	-5.48×10^{-5}	-1.82×10^{-6}

Table 2: Computed errors in the $L^2(\Omega)$ norm of solution q at final time $T = 5$ with the structure-preserving LDG (SP-LDG) and IPDG [3] methods.

panel for the stable node, we observe that the concentrations reach equilibrium monotonically, and without large peak values in the solutions at intermediate times.

5.4 Test case 4: Impact of diffusion on population spatial distributions

In this section, we discuss the impact of the diffusion coefficient $\boldsymbol{D}$ on the spatial distribution of the solutions of system (2.1) and test the capabilities of our method to reproduce anisotropic dynamics of the system. Moreover, we will show that, also in the case of a stable node equilibrium, it is fundamental to apply an unbounded transformation for the variable q, because the solution can locally overcome the equilibrium value $\mathcal{E}_q$ and asymptotically approach it from above in a monotonic way. Namely, we cannot provide a bound on the maximum value reached by q.

We consider a square space domain $\Omega = (-2, 2)^2$, and the final time $T = 15$. Moreover, we introduce four subdomains of Ω (see Figure 6a), namely, $\Omega_1 = (-2, 0)^2$, $\Omega_2 = (0, 2) \times (-2, 0)$, $\Omega_3 = (-2, 0) \times (0, 2)$, and $\Omega_4 = (0, 2)^2$. We impose homogeneous Neumann boundary conditions, and we fix the reaction parameters $\kappa_p = 0.1$, $\lambda_p = \lambda_q = 0.1$, and $\mu_{pq} = 1$. These parameters are associated with an unstable equilibrium $(\mathcal{E}_p, 0) = (1, 0)$ and a stable one $(\lambda_q/\mu_{pq}, \mathcal{E}_q) = (0.1, 0.9)$. Analyzing the associated ODE with these parameter values, one can conclude that the stable equilibrium is a node, so the solution should monotonically approach the steady state. Concerning the diffusion coefficient, we consider four different cases:

(TC 4.1) constant isotropic diffusion tensor with high diffusion $\boldsymbol{D} = 5 \times 10^{-2}\mathbb{I}$;

(TC 4.2) constant isotropic diffusion tensor with low diffusion $\boldsymbol{D} = 10^{-2}\mathbb{I}$;

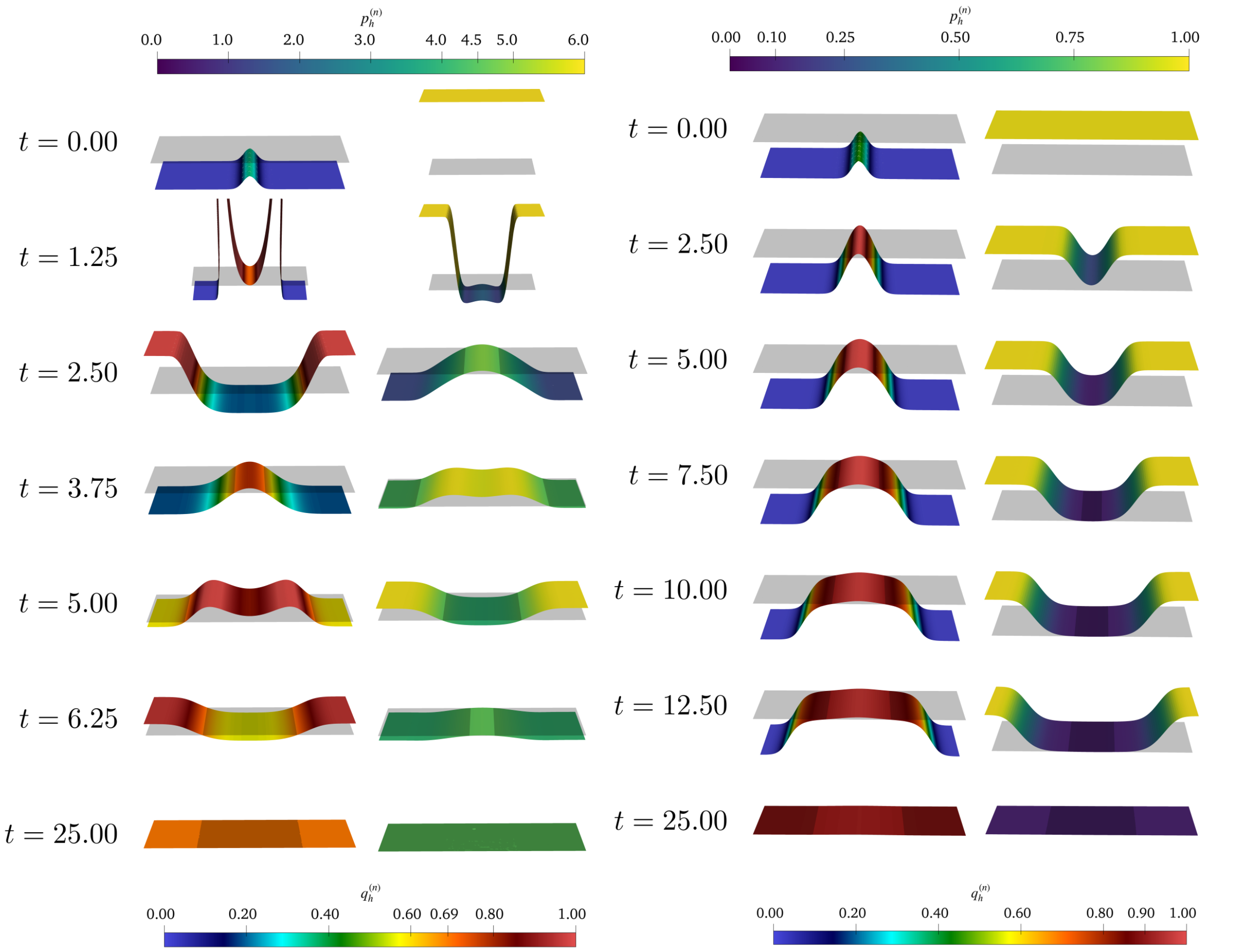

Figure 5: Test case 3: numerical solutions $q_h^{(n)}$ (first column of each panel) and $p_h^{(n)}$ (second column of each panel) at different times in the case of stable focus (left panel) and stable node equilibrium (right panel).

(TC 4.3) discontinuous isotropic diffusion tensor:

$$\boldsymbol{D} = \begin{cases} 10^{-3}\mathbb{I}, & \text{in}\,\Omega_1, \\ 10^{-2}\mathbb{I}, & \text{in}\,\Omega_2, \\ 5\times 10^{-3}\mathbb{I}, & \text{in}\,\Omega_3, \\ 5\times 10^{-2}\mathbb{I}, & \text{in}\,\Omega_4; \end{cases}$$

(TC 4.4) discontinuous anisotropic diffusion tensor (see Figure 6b):

$$\boldsymbol{D} = \begin{cases} 10^{-3}\mathbb{I}, & \text{in}\,\Omega_1, \\ 10^{-2}\mathbb{I}, & \text{in}\,\Omega_2, \\ 10^{-3}\mathbb{I} + 5\times 10^{-3}\boldsymbol{a}(x,y)\otimes\boldsymbol{a}(x,y), & \text{in}\,\Omega_3, \\ 10^{-2}\mathbb{I} + 5\times 10^{-3}\boldsymbol{a}(x,y)\otimes\boldsymbol{a}(x,y), & \text{in}\,\Omega_4, \end{cases} \quad \text{with } \boldsymbol{a}(\boldsymbol{x}) = \left((1-y)^2 + x^4\right)^{-1/2}\begin{pmatrix} 1-y \\ x^2 \end{pmatrix}.$$

Concerning the discretization, we fix the parameter $\varepsilon = 0$, and we adopt a structured triangular mesh with $N_{\text{el}} = 800$ ($h \approx 0.2828$) and polynomial degree $\ell = 2$. The step of the time discretization is fixed as $\tau = 5\times 10^{-3}$. As initial conditions, we consider the following analytical continuous functions:

$$p_0(x,y) = 1, \qquad q_0(x,y) = 0.5\,e^{-10(x^2+y^2)}.$$

We report the plot of the initial condition for the variable q in Figure 6c. In Figure 7, we report the numerical

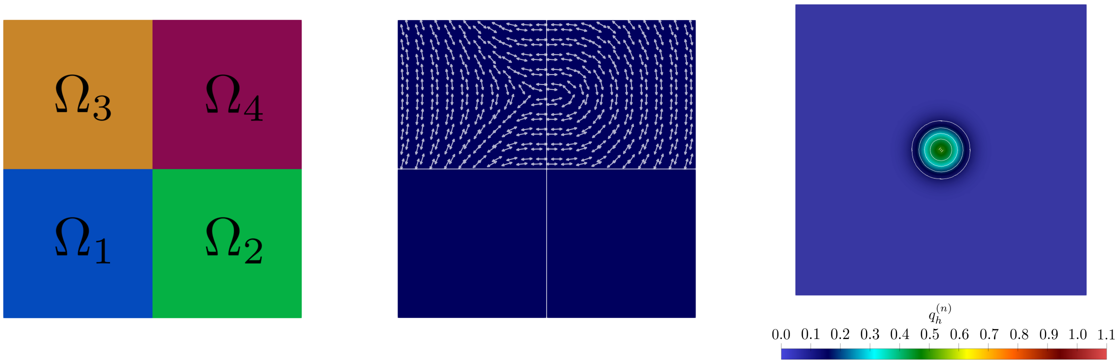

(a) Ω subdomains. **(b)** Anisotropic directions $\boldsymbol{a}$. **(c)** Initial condition $q_h^{(0)}$.

Figure 6: Test case 4: (a) subdomains of Ω, (b) anisotropic directions $\boldsymbol{a}(x, y)$ in subdomains Ω_3 and Ω_4, and (c) discrete initial condition $q_h^{(0)}$.

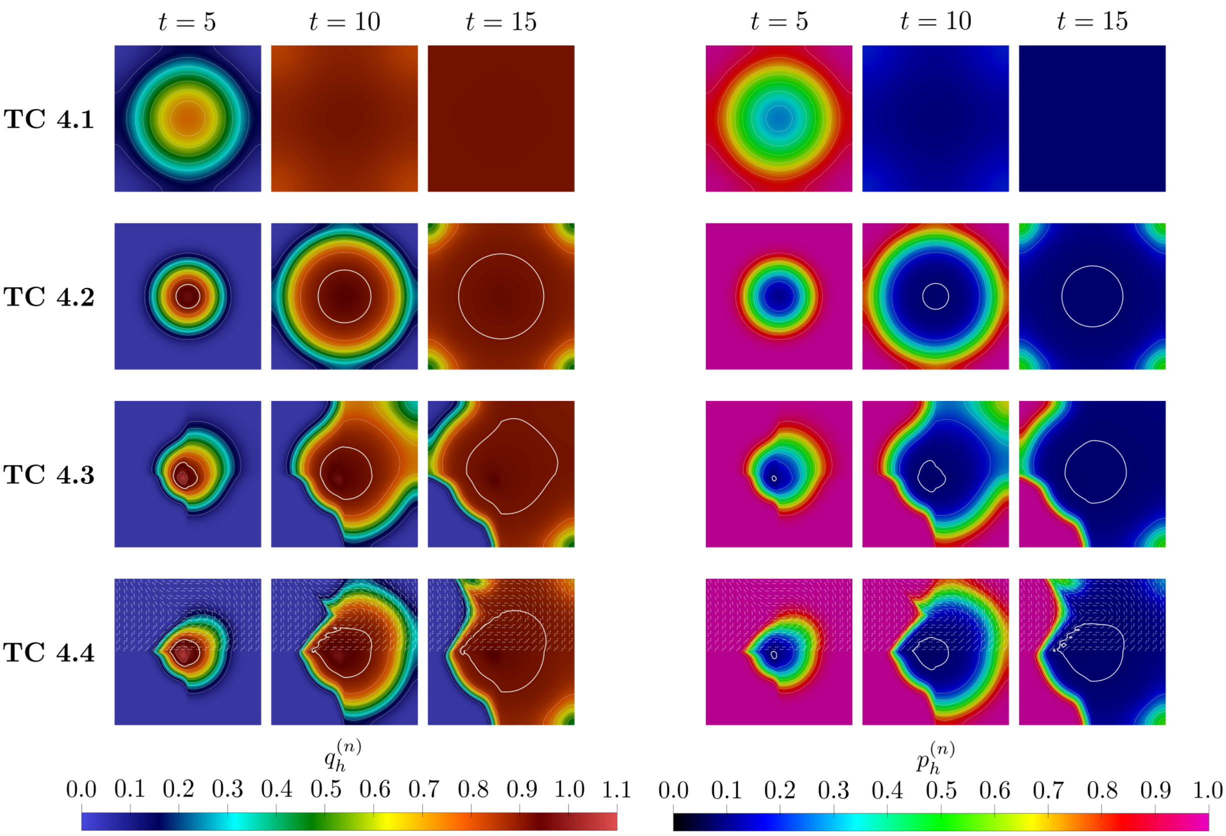

Figure 7: Test case 4: numerical solutions $p_h^{(n)}$ (first column) and $q_h^{(n)}$ (second column) at different times $t = 5, 10, 15$ considering four the different tested diffusion tensors.

solution computed for (TC 4.1) to (TC 4.4). The numerical solution is depicted at three different times $t = 5$, 10, 15, and the isolines of the solutions at levels $\{0.1, 0.2, ..., 1.0\}$ are also reported. In particular, the isolines associated with the stable equilibrium $(p, q) = (0.1, 0.9)$ are reported as thicker lines in the visualization. As we can observe, in the first case (TC 4.1), the solution approaches the equilibrium points monotonically from below and above for q and p, respectively. In contrast, a reduction of the diffusion value (TC 4.2) causes a change in the dynamics, and the solution exceeds the equilibrium values and then approaches them monotonically from above for q and from below for p.

In the latter cases (TC 4.3) and (TC 4.4), we have discontinuous diffusion tensors. These cases clearly demonstrate the impact of different diffusion regions on the solution. In areas with lower diffusion values, the wave fronts are sharper, and the solution spreads more slowly throughout the domain. We also notice that, in proximity to the diffusion tensor discontinuity, Ω_1 presents the highest peak of q (see $t = 5, 10$ in Figure 7). Finally, focusing on (TC 4.4), as a result of introducing a preferential direction of diffusion in the subdomain $\Omega_3 \cup \Omega_4$, we can observe that the propagating front moves fast along the direction $\boldsymbol{a}$. At the same time, it is significantly slower along the orthogonal direction. Consequently, the fronts are sharp in the orthogonal direction and soft in the $\boldsymbol{a}$ direction (see last row of Figure 7). This expected behavior confirms the method's ability to approximate the solution, even in the presence of anisotropic diffusion tensors.

6 Conclusions

In this work, we have analyzed a two-state conformational conversion system and proposed a novel structure-preserving numerical scheme that combines a local discontinuous Galerkin space discretization with a backward Euler time-integration method. The proposed approach guarantees essential physical and mathematical properties at the discrete level — namely, positivity, boundedness, and a discrete stability bound. We prove the convergence of the numerical solution (up to subsequences) under suitable regularity assumptions. As an additional outcome of the analysis presented, we show the existence of global weak solutions satisfying the problem's physical bounds. Numerical experiments validated the theoretical results and highlighted the practical performance of the proposed schemes. Possible further developments include the analysis of multi-state conformational systems, the introduction of high-order time integration schemes, and the development of adaptive strategies to enhance computational efficiency, while guaranteeing structural properties.

Acknowledgements

The first three authors were partially supported by the European Union (ERC Synergy, NEMESIS, project number 101115663). Views and opinions expressed are, however, those of the authors only and do not necessarily reflect those of the EU or the ERC Executive Agency. The first three authors are also members of the INdAM-GNCS group. This research was funded in part by the Austrian Science Fund (FWF) project 10.55776/F65. The present research is part of the activities of Dipartimento di Eccellenza 2023-2027 (Dipartimento di Matematica, Politecnico di Milano).

References

[1] A. Amiri, G. R. Barrenechea, and T. Pryer. A nodally bound-preserving finite element method for reaction-convection-diffusion equations. *Math. Models Methods Appl. Sci.*, 34(8):1533–1565, 2024.

[2] P. F. Antonietti, S. Bonetti, M. Botti, M. Corti, I. Fumagalli, and I. Mazzieri. `lymph`: discontinuous polytopal methods for multi-physics differential problems. *ACM Trans. Math. Software*, 51(1):Art. 3, 22, 2025.

[3] P. F. Antonietti, F. Bonizzoni, M. Corti, and A. Dall'Olio. Discontinuous Galerkin approximations of the heterodimer model for protein-protein interaction. *Comput. Methods Appl. Mech. Engrg.*, 431:Paper No. 117282, 17, 2024.

[4] P. F. Antonietti, M. Corti, S. Gómez, and I. Perugia. A structure-preserving LDG discretization of the Fisher-Kolmogorov equation for modeling neurodegenerative diseases. *Math. Comput. Simulation*, 241:351–366, 2026.

[5] G. R. Barrenechea, V. John, and P. Knobloch. Finite element methods respecting the discrete maximum principle for convection-diffusion equations. *SIAM Rev.*, 66(1):3–88, 2024.

[6] F. Bonizzoni, M. Braukhoff, A. Jüngel, and I. Perugia. A structure-preserving discontinuous Galerkin scheme for the Fisher-KPP equation. *Numer. Math.*, 146(1):119–157, 2020.

[7] M. Braukhoff, I. Perugia, and P. Stocker. An entropy structure preserving space-time formulation for cross-diffusion systems: analysis and Galerkin discretization. *SIAM J. Numer. Anal.*, 60(1):364–395, 2022.

[8] S. C. Brenner and L. R. Scott. *The mathematical theory of finite element methods*, volume 15 of *Texts in Applied Mathematics*. Springer-Verlag, New York, 1994.

[9] H. Brezis. *Functional analysis, Sobolev spaces and partial differential equations*. Universitext. Springer, New York, 2011.

[10] P. Castillo, B. Cockburn, I. Perugia, and D. Schötzau. An a priori error analysis of the local discontinuous Galerkin method for elliptic problems. *SIAM J. Numer. Anal.*, 38(5):1676–1706, 2000.

[11] P. Castillo, B. Cockburn, I. Perugia, and D. Schötzau. Local discontinuous Galerkin methods for elliptic problems. *Commun. Numer. Methods Eng.*, 18(1):69–75, 2002.

[12] L. Chen and A. Jüngel. Analysis of a parabolic cross-diffusion population model without self-diffusion. *J. Differential Equations*, 224(1):39–59, 2006.

[13] X. Chen, A. Jüngel, and L. Wang. The Shigesada-Kawasaki-Teramoto cross-diffusion system beyond detailed balance. *J. Differential Equations*, 360:260–286, 2023.

[14] B. Cockburn, G. Kanschat, D. Schötzau, and C. Schwab. Local discontinuous Galerkin methods for the Stokes system. *SIAM J. Numer. Anal.*, 40(1):319–343, 2002.

[15] M. Corti. Exploring tau protein and amyloid-beta propagation: a sensitivity analysis of mathematical models based on biological data. *Brain Multiphysics*, 7:100098, 2024.

[16] M. Corti, F. Bonizzoni, and P. F. Antonietti. Structure preserving polytopal discontinuous Galerkin methods for the numerical modeling of neurodegenerative diseases. *J. Sci. Comput.*, 100(2):Paper No. 39, 24, 2024.

[17] W. Cui, R. Marsland, and P. Mehta. Effect of resource dynamics on species packing in diverse ecosystems. *Phys. Rev. Lett.*, 125(4):048101, 6, 2020.

[18] M. Dreher and A. Jüngel. Compact families of piecewise constant functions in $L^p(0,T;B)$. *Nonlinear Anal.*, 75(6):3072–3077, 2012.

[19] A. Ern and J.-L. Guermond. *Finite elements I. Approximation and interpolation*, volume 72 of *Texts Appl. Math.* Cham: Springer, 2020.

[20] S. Fornari, A. Schäfer, M. Jucker, A. Goriely, and E. Kuhl. Prion-like spreading of Alzheimer's disease within the brain's connectome. *J. R. Soc. Interface*, 16(159):20190356, 2019.

[21] S. Fornari, A. Schäfer, E. Kuhl, and A. Goriely. Spatially-extended nucleation-aggregation-fragmentation models for the dynamics of prion-like neurodegenerative protein-spreading in the brain and its connectome. *J. Theoret. Biol.*, 486:110102, 17, 2020.

[22] S. Gómez, A. Jüngel, and I. Perugia. Structure-preserving Local Discontinuous Galerkin method for nonlinear cross-diffusion systems. arXiv:2406.17900, 2024.

[23] A. Jüngel. The boundedness-by-entropy method for cross-diffusion systems. *Nonlinearity*, 28(6):1963–2001, 2015.

[24] M. H. Kabir and M. O. Gani. Numerical bifurcation analysis and pattern formation in a minimal reaction-diffusion model for vegetation. *J. Theoret. Biol.*, 536:Paper No. 110997, 16, 2022.

[25] B. Keith, R. Masri, and M. Zeinhofer. A priori error analysis of the proximal Galerkin method. arXiv:2507.13516, 2025.

[26] B. Keith and T. M. Surowiec. Proximal Galerkin: A structure-preserving finite element method for pointwise bound constraints. *Found. Comput. Math.*, 2024.

[27] S. Lemaire and J. Moatti. Structure preservation in high-order hybrid discretisations of potential-driven advection-diffusion: linear and nonlinear approaches. *Math. Eng.*, 6(1):100–136, 2024.

[28] R. Marsland, W. Cui, and P. Mehta. The minimum environmental perturbation principle: A new perspective on Niche theory. *Am. Nat.*, 196(3):291–305, 2020.

[29] F. Matthäus. Diffusion versus network models as descriptions for the spread of prion diseases in the brain. *J. Theoret. Biol.*, 240(1):104–113, 2006.

[30] J. Moatti. A structure preserving hybrid finite volume scheme for semiconductor models with magnetic field on general meshes. *ESAIM Math. Model. Numer. Anal.*, 57(4):2557–2593, 2023.

[31] T. Roubíček. *Nonlinear partial differential equations with applications*, volume 153 of *ISNM, Int. Ser. Numer. Math.* Basel: Birkhäuser, 2005.

[32] J. Weickenmeier, M. Jucker, A. Goriely, and E. Kuhl. A physics-based model explains the prion-like features of neurodegeneration in Alzheimer's disease, Parkinson's disease, and amyotrophic lateral sclerosis. *J. Mech. Phys. Solids*, 124:264–281, 2019.

A Newton's iteration

In this section, we derive the linear systems resulting from Newton's iteration, thereby providing an implementable algorithm. The computational bottleneck in each Newton's iteration is the evaluation of the nonlinear terms within the multivariate function and its Jacobian matrix. As the nonlinearities in our approach do not affect the interface integrals, these terms can be computed separately for each mesh element. As a result, the Jacobians are block-diagonal, endowing the method with a naturally parallelizable structure.

We set, for convenience, $C := M_D M_I^{-1} B$ and, for $\star = p, q$,

$$
\begin{aligned}
\mathcal{G}_1^\star\big(\boldsymbol{\Sigma}_{\star,h}^{(n+1)}, \mathbf{W}_{\star,h}^{(n+1)}\big) &:= \mathcal{N}_\star\big(\mathbf{W}_{\star,h}^{(n+1)}\big)\boldsymbol{\Sigma}_{\star,h}^{(n+1)} + C\mathbf{W}_{\star,h}^{(n+1)},\\
\mathcal{G}_2^\star\big(\boldsymbol{\Sigma}_{\star,h}^{(n+1)}, \mathbf{W}_{p,h}^{(n+1)}, \mathbf{W}_{q,h}^{(n+1)}\big) &:= \varepsilon A_{\mathrm{LDG}}\mathbf{W}_{\star,h}^{(n+1)} + \frac{1}{\tau_{n+1}}\mathcal{U}_\star(\mathbf{W}_{\star,h}^{(n+1)}) - C^T\boldsymbol{\Sigma}_{\star,h}^{(n+1)} + J\mathbf{W}_{\star,h}^{(n+1)}\\
&\quad - \mathcal{F}_\star\big(\mathbf{W}_{p,h}^{(n+1)}, \mathbf{W}_{q,h}^{(n+1)}\big) - \frac{1}{\tau_{n+1}}\mathcal{U}_{\star,h}^{(n)}.
\end{aligned}
$$

Denote by $\mathcal{D}_{\boldsymbol{\Sigma}_\star}$ and $\mathcal{D}_{\mathbf{W}_\star}$ the Jacobian matrices with respect to $\boldsymbol{\Sigma}_\star$ and $\mathbf{W}_\star$, respectively. Omitting the temporal index $n+1$, the step $k \to k+1$ of Newton's iteration applied to system (2.23) reads as follows: for $\star = p, q$,

$$
\begin{aligned}
&\mathcal{D}_{\boldsymbol{\Sigma}_\star}\big(\mathcal{G}_1^\star\left(\boldsymbol{\Sigma}_{\star,h}^k, \mathbf{W}_{\star,h}^k\right)\big)\left(\boldsymbol{\Sigma}_{\star,h}^{k+1} - \boldsymbol{\Sigma}_{\star,h}^k\right) + \mathcal{D}_{\mathbf{W}_\star}\big(\mathcal{G}_1^\star\left(\boldsymbol{\Sigma}_{\star,h}^k, \mathbf{W}_{\star,h}^k\right)\big)\left(\mathbf{W}_{\star,h}^{k+1} - \mathbf{W}_{\star,h}^k\right) = -\mathcal{G}_1^\star\left(\boldsymbol{\Sigma}_{\star,h}^k, \mathbf{W}_{\star,h}^k\right),\\
&\mathcal{D}_{\boldsymbol{\Sigma}_\star}\big(\mathcal{G}_2^\star\left(\boldsymbol{\Sigma}_{\star,h}^k, \mathbf{W}_{p,h}^k, \mathbf{W}_{q,h}^k\right)\big)\left(\boldsymbol{\Sigma}_{\star,h}^{k+1} - \boldsymbol{\Sigma}_{\star,h}^k\right) + \mathcal{D}_{\mathbf{W}_p}\big(\mathcal{G}_2^\star\left(\boldsymbol{\Sigma}_{\star,h}^k, \mathbf{W}_{p,h}^k, \mathbf{W}_{q,h}^k\right)\big)\left(\mathbf{W}_{p,h}^{k+1} - \mathbf{W}_{p,h}^k\right)\\
&\qquad + \mathcal{D}_{\mathbf{W}_q}\big(\mathcal{G}_2^\star\left(\boldsymbol{\Sigma}_{\star,h}^k, \mathbf{W}_{p,h}^k, \mathbf{W}_{q,h}^k\right)\big)\left(\mathbf{W}_{q,h}^{k+1} - \mathbf{W}_{q,h}^k\right) = -\mathcal{G}_2^\star\left(\boldsymbol{\Sigma}_{\star,h}^k, \mathbf{W}_{p,h}^k, \mathbf{W}_{q,h}^k\right).
\end{aligned}
$$

We compute

$$
\begin{aligned}
\mathcal{D}_{\boldsymbol{\Sigma}_\star}\big(\mathcal{G}_1^\star\left(\boldsymbol{\Sigma}_{\star,h}^k, \mathbf{W}_{\star,h}^k\right)\big) &= \mathcal{N}_\star\big(\mathbf{W}_{\star,h}^k\big),\\
\mathcal{D}_{\mathbf{W}_\star}\big(\mathcal{G}_1^\star\left(\boldsymbol{\Sigma}_{\star,h}^k, \mathbf{W}_{\star,h}^k\right)\big) &= \mathcal{D}_{\mathbf{W}_\star}\big(\mathcal{N}_\star\big(\mathbf{W}_{\star,h}^k\big)\big)\,\boldsymbol{\Sigma}_{\star,h}^k + C,\\
\mathcal{D}_{\boldsymbol{\Sigma}_\star}\big(\mathcal{G}_2^\star\left(\boldsymbol{\Sigma}_{\star,h}^k, \mathbf{W}_{p,h}^k, \mathbf{W}_{q,h}^k\right)\big) &= -C^T,\\
\mathcal{D}_{\mathbf{W}_\star}\big(\mathcal{G}_2^\star\left(\boldsymbol{\Sigma}_{\star,h}^k, \mathbf{W}_{p,h}^k, \mathbf{W}_{q,h}^k\right)\big) &= \varepsilon A_{\mathrm{LDG}} + \frac{1}{\tau_{n+1}}\mathcal{D}_{\mathbf{W}_\star}\big(\mathcal{U}_\star(\mathbf{W}_{\star,h}^k)\big) + J - \mathcal{D}_{\mathbf{W}_\star}\big(\mathcal{F}_\star\big(\mathbf{W}_{p,h}^k, \mathbf{W}_{q,h}^k\big)\big),\\
\mathcal{D}_{\mathbf{W}_q}\big(\mathcal{G}_2^p\left(\boldsymbol{\Sigma}_{p,h}^k, \mathbf{W}_{p,h}^k, \mathbf{W}_{q,h}^k\right)\big) &= -\mathcal{D}_{\mathbf{W}_q}\big(\mathcal{F}_p\big(\mathbf{W}_{p,h}^k, \mathbf{W}_{q,h}^k\big)\big),\\
\mathcal{D}_{\mathbf{W}_p}\big(\mathcal{G}_2^q\left(\boldsymbol{\Sigma}_{q,h}^k, \mathbf{W}_{p,h}^k, \mathbf{W}_{q,h}^k\right)\big) &= -\mathcal{D}_{\mathbf{W}_p}\big(\mathcal{F}_q\big(\mathbf{W}_{p,h}^k, \mathbf{W}_{q,h}^k\big)\big).
\end{aligned}
$$

Therefore, the Newton iteration applied to system (2.23) is as follows: for $\star = p, q$,

$$
\begin{aligned}
\mathcal{N}_\star(\mathbf{W}^k_{\star,h})\boldsymbol{\Sigma}^{k+1}_{\star,h} &= -\Big[\mathcal{D}_{\mathbf{W}_\star}\big(\mathcal{N}_\star(\mathbf{W}^k_{\star,h})\big)\,\boldsymbol{\Sigma}^k_{\star,h} + C\Big]\mathbf{W}^{k+1}_{\star,h} + \big(\mathcal{D}_{\mathbf{W}_\star}\big(\mathcal{N}_\star(\mathbf{W}^k_{\star,h})\big)\,\boldsymbol{\Sigma}^k_{\star,h}\big)\,\mathbf{W}^k_{\star,h},\\
-\,C^T\boldsymbol{\Sigma}^{k+1}_{\star,h} &+ \Big[\varepsilon A_{\mathrm{LDG}} + \frac{1}{\tau_{n+1}}\mathcal{D}_{\mathbf{W}_\star}\big(\mathcal{U}_\star(\mathbf{W}^k_{\star,h})\big) + J\Big]\mathbf{W}^{k+1}_{\star,h}\\
&\quad - \mathcal{D}_{\mathbf{W}_p}\big(\mathcal{F}_\star(\mathbf{W}^k_{p,h},\mathbf{W}^k_{q,h})\big)\,\mathbf{W}^{k+1}_{p,h} - \mathcal{D}_{\mathbf{W}_q}\big(\mathcal{F}_\star(\mathbf{W}^k_{p,h},\mathbf{W}^k_{q,h})\big)\,\mathbf{W}^{k+1}_{q,h}\\
&= \frac{1}{\tau_{n+1}}\mathcal{D}_{\mathbf{W}_\star}\big(\mathcal{U}_\star(\mathbf{W}^k_{\star,h})\big)\,\mathbf{W}^k_{\star,h} - \mathcal{D}_{\mathbf{W}_p}\big(\mathcal{F}_\star(\mathbf{W}^k_{p,h},\mathbf{W}^k_{q,h})\big)\,\mathbf{W}^k_{p,h} - \mathcal{D}_{\mathbf{W}_q}\big(\mathcal{F}_\star(\mathbf{W}^k_{p,h},\mathbf{W}^k_{q,h})\big)\,\mathbf{W}^k_{q,h}\\
&\quad - \frac{1}{\tau_{n+1}}\Big[\mathcal{U}_\star(\mathbf{W}^k_{\star,h}) - \mathcal{U}^{(n)}_{\star,h}\Big] + \mathcal{F}_\star(\mathbf{W}^k_{p,h},\mathbf{W}^k_{q,h}).
\end{aligned}
\tag{A.1}
$$

Remark A.1 (Newton's iteration for (2.24))**.** *Using* (2.23a), *one can eliminate* $\boldsymbol{\Sigma}^k_{\star,h}$ *from* (A.1) *and obtain, for* $\star = p, q$,

$$
\begin{aligned}
&\Big[\varepsilon A_{\mathrm{LDG}} + \frac{1}{\tau_{n+1}}\mathcal{D}_{\mathbf{W}_\star}\big(\mathcal{U}_\star(\mathbf{W}^k_{\star,h})\big) + C^T\left(\mathcal{N}_\star(\mathbf{W}^k_{\star,h})\right)^{-1}C - \mathbb{M}_\star\mathbf{W}^k_{\star,h} + J\Big]\mathbf{W}^{k+1}_{\star,h}\\
&\qquad - \mathcal{D}_{\mathbf{W}_p}\big(\mathcal{F}_\star(\mathbf{W}^k_{p,h},\mathbf{W}^k_{q,h})\big)\,\mathbf{W}^{k+1}_{p,h} - \mathcal{D}_{\mathbf{W}_q}\big(\mathcal{F}_\star(\mathbf{W}^k_{p,h},\mathbf{W}^k_{q,h})\big)\,\mathbf{W}^{k+1}_{q,h}\\
&\quad= \frac{1}{\tau_{n+1}}\mathcal{D}_{\mathbf{W}_\star}\big(\mathcal{U}_\star(\mathbf{W}^k_{\star,h})\big)\,\mathbf{W}^k_{\star,h} - \mathcal{D}_{\mathbf{W}_p}\big(\mathcal{F}_\star(\mathbf{W}^k_{p,h},\mathbf{W}^k_{q,h})\big)\,\mathbf{W}^k_{p,h} - \mathcal{D}_{\mathbf{W}_q}\big(\mathcal{F}_\star(\mathbf{W}^k_{p,h},\mathbf{W}^k_{q,h})\big)\,\mathbf{W}^k_{q,h}\\
&\qquad - \left(\mathbb{M}_\star\mathbf{W}^k_{\star,h}\right)\mathbf{W}^k_{\star,h} - \frac{1}{\tau_{n+1}}\Big[\mathcal{U}_\star(\mathbf{W}^k_{\star,h}) - \mathcal{U}^{(n)}_{\star,h}\Big] + \mathcal{F}_\star(\mathbf{W}^k_{p,h},\mathbf{W}^k_{q,h}),
\end{aligned}
\tag{A.2}
$$

where $\mathbb{M}_\star$ *is the third-order tensor defined as*

$$
\mathbb{M}_\star := C^T\left(\mathcal{N}_\star(\mathbf{W}^k_{\star,h})\right)^{-1}\mathcal{D}_{\mathbf{W}_\star}\big(\mathcal{N}_\star(\mathbf{W}^k_{\star,h})\big)\left(\mathcal{N}_\star(\mathbf{W}^k_{\star,h})\right)^{-1}C.
$$

The expression in (A.2) *could also be obtained by applying Newton's iteration directly to the reformulation of system* (2.23) *given in* (2.24). ∎

MOX Technical Reports, last issues

Dipartimento di Matematica
Politecnico di Milano, Via Bonardi 9 - 20133 Milano (Italy)

66/2025 Speroni, G.; Mondini, N.; Ferro, N.; Perotto, S.
A topology optimization framework for scaffold design in soilless cultivation

65/2025 Pottier, A.; Gelardi, F.; Larcher, A.; Capitanio, U.; Rainone, P.; Moresco, R.M.; Tenace, N.; Colecchia, M.; Grassi, S.; Ponzoni, M.; Chiti, A.; Cavinato, L.
MOSAIK: A computational framework for theranostic digital twin in renal cell carcinoma

64/2025 Celora, S.; Tonini, A.; Regazzoni, F.; Dede', L. Parati, G.; Quarteroni, A.
Cardiocirculatory Computational Models for the Study of Hypertension

63/2025 Panzeri, S.; Clemente, A.; Arnone, E.; Mateu, J.; Sangalli, L.M.
Spatio-Temporal Intensity Estimation for Inhomogeneous Poisson Point Processes on Linear Networks: A Roughness Penalty Method

62/2025 Rigamonti, V.; Torri, V.; Morris, S. K.; Ieva, F.; Giaquinto, C.; Donà, D.; Di Chiara, C.; Cantarutti, A.; CARICE study group
Real-World Effectiveness of Influenza Vaccination in Preventing Influenza and Influenza-Like Illness in Children

61/2025 Coclite, A; Montanelli Eccher, R.; Possenti, L.; Vitullo, P.; Zunino, P.
Mathematical modeling and sensitivity analysis of hypoxia-activated drugs

60/2025 Antonietti, P. F.; Caldana, M.; Gentile, L.; Verani M.
Deep Learning Accelerated Algebraic Multigrid Methods for Polytopal Discretizations of Second-Order Differential Problems

59/2025 Wolf, F.; Botteghi, N.; Fasel, U.; Manzoni, A.
Interpretable and efficient data-driven discovery and control of distributed systems

58/2025 Pivato, C.A.; Cozzi, O.; Fontana, N.; Ieva, F., et al.
Clinical outcomes of percutaneous coronary interventions after transcatheter aortic valve replacement

57/2025 Guagliardi, O.; Masci, C,; Breschi, V; Paganoni A, ; Tanelli, M.
A Novel DNA-Inspired Framework to Study University Dropout: Insights from Politecnico di Milano